Effects of climate change on the power system:
a case study of the southeast U.S.

Submitted in partial fulfillment of the requirements for

the degree of

Doctor of Philosophy

in

Engineering and Public Policy

Francisco Ralston Fonseca

B.S., Electrical Engineering, Pontifical Catholic University of Rio de Janeiro
M.S., Electrical Engineering, Pontifical Catholic University of Rio de Janeiro
M.S., Industrial Engineering and Operations Research, Columbia University

Carnegie Mellon University
Pittsburgh, PA

May, 2020

Acknowledgements

This work was supported by the National Science Foundation (NSF) as part of the Resilient Interdependent Infrastructure Processes and Systems (RIPS) program via Grant Number EFRI-1441131. It used the Extreme Science and Engineering Discovery Environment (XSEDE), which is supported by National Science Foundation grant number ACI-1548562. Specifically, it used the Bridges system, which is supported by NSF award number ACI-1445606, at the Pittsburgh Supercomputing Center (PSC). I thank Roberto Gomez for his assistance accessing the appropriate resources in the Bridges system, which was made possible through the XSEDE Extended Collaborative Support Service (ECSS) program.

I would like to express my sincere gratitude to my advisors Dr. Paulina Jaramillo (chair), Dr. Mario Bergés, and Dr. Edson Severnini for their continuous support of my graduate study and related research. I would not have been able to complete this work without their patience, motivation, friendship, and knowledge. Their guidance helped me in all the time of research and writing of this thesis.

Besides my advisors, I would like to thank the rest of my thesis committee: Dr. Haibo Zhai, and Dr. Bart Nijssen. Their support, comments, and encouragement greatly contributed to expand my research.

I would also like to thank all other members of the team involved in the RIPS project for

their support and stimulating discussions: Michael Craig, Aviva Loew, Yifan Cheng, Julia Chelen, Jorge Izar Tenorio, Nathalie Voissin, and John Yearsley.

I thank all my colleagues in the Inferlab and Green Design Institute research groups for their friendship, feedback, and thoughtful conversations which have enriched my graduate work.

I would also like to thank the staff at the Engineering and Public Policy department for all their assistance during my graduate studies.

Last but not the least, I would like to thank my family. My parents, Denise and Odemiro, and siblings, Isabel and Diogo, for their unconditional support. My uncles, Liane and Roberto, who have helped to make this personal project possible. Above all I thank my wife Bianca and my two daughters, Cora and Antonia, for enduring this journey by my side.

Abstract

The U.S. power sector faces several vulnerabilities due to climate change. On the demand side, increasing temperatures may result in shifting electricity consumption patterns and increase need for energy. On the supply side, changes in air temperatures, water availability, and water temperatures could reduce the capacity and efficiency of thermal units, which currently represent 85% of generating capacity. Previous studies that analyze climate change effects in the power sector have mostly focused on analyzing these risks separately. Further, studies in the supply side risks usually looked only at effects of climate change only in existing thermal generators. However, such studies fail to capture how these demand and supply risks interact with each other and with the operation of the power grid in general. In order to analyze these risks in more detail, it is important to integrate them into system-wide assessments. Such assessments should take into account the economic dispatch of the complete generator fleet and future economic decisions to expand this fleet.

This dissertation attempts to understand how climate change will affect the power sector in the U.S. We implemented an integrated framework where we use different modeling methods to represent the different risks the power sector faces due to climate change. We used our modeling framework in a case study of the SERC Reliability Corporation (SERC), one of eight regional electric reliability councils under North American Electric Reliability Corporation authority (NERC).

Firstly, we used an econometric model to estimate changes in hourly electricity demand due to climate change. We used this model to analyze changes hourly electricity demand patterns in the Tennessee Valley Authority (TVA) region for different seasons of the year. Our results suggest that climate change could result in an average increase in annual electricity consumption in the TVA region. However, this increase was not uniformly distributed throughout the year. During summer, total electricity consumption could increase on average by 20% while during winter it may decrease on average by 6% by the end of the century.

Secondly, we combined the estimates of future hourly electricity demand described in Chapter 2 with simulations of decreases in available capacity of thermal generators due to climate change. We integrated these simulations in a capacity expansion (CE) model. This CE model is a mixed integer linear programming (MILP) model that we adapted and developed for this study. It finds the composition of the future generator fleet that minimizes costs subject to the estimated effects of climate change. We ran this model under different climate change scenarios from 2020 to 2050. Our results showed that by including these effects due to climate change in the decision making process, the estimated participation of renewables in the generator fleet in 2050 increased from 24% to over 37–40%. Solar power plants could become more economically attractive. As they have higher energy output during the summertime, they could help to offset the climate-induced loss of thermal capacity during this season because of higher air and water temperatures.

Thirdly, we simulated the operation of SERC's power system assuming the different scenarios and generator fleets presented in Chapter 3. To accomplish this, we used a unit commitment and economic dispatch (UCED) model. The UECD model is a mixed integer linear programming (MILP) model that we adapted and developed for this study. We used this model to investigate the tradeoffs between investing or not in the generator fleet assuming different climate change scenarios. Our results suggest that by not including cli-

mate change effects in the planning stage, SERC's power system could experience loss of load levels of 12% and overall energy costs could be 260% higher if climate change conditions do materialize by 2050.

Contents

List of Tables

List of Figures

Chapter 1

Introduction

1.1 Background

In 2018, the Intergovernmental Panel on Climate Change (IPCC) published the Special Report on Global Warming of 1.5 °C (SR15). According to the SR15, average global temperatures are likely to rise 1.5° C above pre-industrial levels by 2052 [45]. The IPCC also projects a likely increase in meteorological variability, climatic extremes, and droughts. These projected changes in climate pose a serious threat to different human and natural systems.

As the impacts of climate change become more widespread, society must decide how to address this issue. The amount of future climate change will be determined by the responses society makes about carbon emissions. Response actions can be categorized into two broad classes: *mitigation* and *adaptation* [68]. Mitigation usually refers to actions taken to reduce the amount and speed of future climate change by reducing emissions of heat-trapping gases or removing carbon dioxide from the atmosphere. On the other hand, adaptation stands for actions that can be taken to prepare and adjust to the new climate

conditions. Mitigation and adaptation actions are interconnected in multiple ways. For example, effective mitigation may reduce the need for future adaptation. Also, some adaptation measures could result in activities that have lower carbon emissions. Because of the long-lived nature of many of the gases emitted in the past, some additional climate change and related impacts are considered unavoidable at this time. Therefore, both mitigation and adaptation actions are considered essential parts of a comprehensive climate change response strategy [68].

The U.S. power sector, considered one of the largest contributors to the emissions of greenhouse gases (GHG) in the country [107], faces several vulnerabilities related to climate change [100, 99]. On the demand side, increasing temperatures may result in shifting demand patterns. Higher temperatures can result in higher cooling demand in the summer and lower heating demand in the winter [5]. The magnitude of these variations, however, will be highly dependent on different local factors, such as electricity consumption behaviors. These changes in demand could by themselves result on challenges to the operation of the power sector. However, these threats are compounded by vulnerabilities on the generation side as well. In the U.S., thermoelectric power plants generate roughly 85% of the electricity in the U.S. [102] and could be affected by climate change through several pathways. Decreased water availability and increased water temperatures could reduce the capacity and efficiency of thermal units that use once-through cooling. Additionally, increased air temperature and humidity could reduce the capacity and efficiency of thermal units that use re-circulating cooling. Increased air temperature could also reduce the capacity and efficiency of gas turbines. Finally, all the aforementioned threats become even more critical because of the nature of energy infrastructure planning and investment. Planning horizons can span several decades – the typical service life of most energy assets – and associated investments can extend into the billions of dollars. Because of all these vulnerabilities, adaptation responses to climate change could be an important factor in the design of the future U.S. electricity grid. Planning agents in the power sector should take

into account the risks imposed by climate change into their decision making process in order to ensure a reliable and affordable electricity supply.

Recent events in the U.S. and European power systems have already underscored the vulnerabilities of the power sector to weather extremes. In the summer of 2007, acute drought conditions in the southeast U.S. resulted in the curtailment and shutdown of some nuclear and coal-fired plants within the Tennessee Valley Authority (TVA) system. In France, many nuclear power plants had to reduce operations during a serious drought in 2003 [48]. With climate change, such hazards may become even more serious and frequent. There will likely be more frequent hot temperature extremes on daily and seasonal timescales. It is also anticipated that heat waves will occur with a higher frequency and longer duration [44].

The analysis of climate-induced hazards in energy systems is not a new topic. In recent years, many studies have looked at the impacts of climate change on global systems, including energy systems. One important class of such studies are those that use Integrated Assessment Models (IAMs). IAMs typically include a representation of agriculture, energy, economic, water, and climate systems. These models have different types of spatial and temporal coverage. Most IAMs are developed for more general scenario analyses, providing output at coarse spatial and temporal resolutions and do not include detailed processes that incorporate more detailed impacts on electricity supply and demand [111]. To capture the spatial and temporal heterogeneity of the power system, models usually used for capacity planning and system operations require data in higher resolution. Therefore, coupled hydrological-electricity modelling approaches are considered more suitable to analyze climate impacts on the power system [111].

Several studies have looked at the impacts of climate change in electricity demand and generation [23, 19, 85]. On the demand side, most of the studies that have assessed the impacts of climate change on electricity demand used historical data to fit multiple linear

regression models relating regional electricity consumption and weather variables. Many of such models used data in a monthly time-frame [12, 84, 83, 42, 4, 82, 70] and typically employ cooling degree-day (CDD) and heating degree-day (HDD) metrics as the weather regressors. For example, Sailor and Muñoz [84] used multivariate linear regression models to analyze the sensitivity of electricity demand to climate in eight U.S. states. The authors used, among others, CDD and HDD as regressors. They found that climate variables are statistically significant and the magnitude of the sensitivity coefficients varied substantially between the different states (which indicates the importance of performing regional analysis). Amato et al. [4] explored regional energy demand responses to climate change in the Commonwealth of Massachusetts. The authors found that climate change scenarios resulted in 2.1% increase in per capita residential electricity consumption by 2020. More recently some studies have started looking at higher temporal resolution in order to represent inter-day or intra-day variability in demand [95, 75, 34, 6]. For example, Franco and Sanstad [34] used detailed data to estimate the relationships between temperature and both electricity consumption and peak demand at a sample of locations around California. The authors found that climate change could result in an increase in annual electricity and peak load demands of up to 18% by the end of the century. Auffhammer, Baylis, and Hausman [6] used daily data at the level of load balancing authorities in the continental U.S. to analyze the relationship between average or peak electricity demand and temperature. The authors found moderate and heterogeneous changes in consumption due to climate change, with an average increase of 2.8% by end of century.

On the supply side, studies have analyzed how climate change can affect the production of electricity by thermoelectric power plants. Usually, these studies have focused on assessing reductions in capacity and efficiency of existing individual generators. Koch and Vögele [49] estimated available capacity reduction for nuclear power plants in Germany by 2050. Koch et al. [50] used a similar approach to analyze the effects of climate change on power plants and adaptation options at the city of Berlin, Germany. Van Vliet et al.

[112] estimated that the average useable capacities of 61 thermal plants in the eastern U.S. could decrease by up to 16% by 2060. Furthermore, the frequency of significant (>50%) and extreme (>90%) capacity reductions could increase significantly. Bartos and Chester [10] found similar results for generating capacity in the Western United States. Miara et al. [69] analyzed capacity shortfalls of individual U.S. power plants due to climate–water impacts in a regional electric grid context. They found that reserve margins (a measure of systems-level reliability) could drop by 2.3–6.9% in the Eastern Connection, and 1.9–4.3% in the Western Interconnection. Payet-Burin et al. [76] developed an integrated water-power model and performed a system-wide analysis of climate change impacts at the Iberian Peninsula's power system. They found that average available capacity of freshwater-cooled thermal power plants is reduced by 16 – 30% while production is reduced by 5–12% in summer. Tobin et al. [96] assessed the impacts of climate change on wind, solar photovoltaic, hydro, and thermoelectric power generation in Europe. Their results showed that climate change has negative impacts on electricity production in most countries and for most technologies. Henry and Pratson [39] investigated the separate effects of temperature-induced efficiency loss (TIEL), drought-induced capacity loss (DICL), and regulation-induced capacity loss (RICL) on usable capacity of power plants with once-through cooling. They found that if surface waters warm 3 °C and river discharges drop 20%, droughts would account for up to 20% of total capacity reduction, warming surface waters $\leq$2.3%, and environmental regulations as most as 80%. Peter [77] did an assessment of power system planning under pre-defined climate change scenarios. However, this study used exogenous climate change assumptions, instead of estimating them endogenously in their analysis. For example, the author used average thermal capacity reduction values calculated in other studies [96]. He found that climate change impacts increase system costs of a system designed without climate change anticipation. Turner et al. [97] analyzed how combined climate change impacts on loads and hydropower generation could influence the nature and seasonality of power shortfall risk in the U.S. Pacific Northwest. They found

that potential shortfall events in the Northwest could occur more frequently, but with less severity.

While this previous work helps to shed light on risk to individual components of the power system, most of them fail to capture how these effects interact with the operation of the power grid and with changes in electricity demand patterns. Few of these studies have integrated their findings into a comprehensive system level analysis, a necessary step to understand how climate change may affect cost and reliability of the power system as a whole. For instance, large reductions in generators' capacities in a region would pose a greater threat to system reliability if they were coincidental across the fleet than if they were not. Moreover, as mentioned previously, periods of high air and water temperatures could result on curtailment of thermal power generation at the same time that demand for electricity could be peaking. Also, the few studies that have performed system level analysis, have done so either using a present time system configuration or have used exogenous assumptions of future expansions of the generator fleet. In order to have a better understanding of the vulnerabilities of the power system to climate change, it is important to integrate these different aspects into a more complete system-wide analysis.

1.2 Research Questions and Scope

In this thesis I propose and implement an integrated framework for analyzing the potential effects of climate change on three different parts of the power sector: electricity demand, planning of the expansion of the generator fleet, and operation of the system. I plan to do so by addressing the following research questions, divided into three chapters:

1. Seasonal effects of climate change on intra-day electricity demand
    - How will climate change affect the intra-day demand profile?

- How will this estimated effect differ between different seasons?

2. Effects of climate change on power system planning

    - How will climate change affect the decisions to expand the generation fleet?
    - How will these effects translate in terms of the compositions of the generation fleet?
    - How sensitive are these results to different projections of climate change?

3. Effects of climate change on power system operation

    - How could climate change affect power system cost and reliability through generator capacity and efficiency reductions?
    - What tradeoffs exist between power system planning and operations under climate change?

I apply this integrated framework on a study case of the entire SERC Reliability Corporation (Figure 1.1), one of eight regional authorities within the North American Electric Reliability Council. According to the National Climate Assessment, the Southeast U.S. is a region particularly vulnerable to some of the expected impacts of climate change [68].

The proposed modeling configuration uses a combination of different quantitative methods. In Chapter 2, I use multivariate linear regression to model the relationship between weather variables and hourly electricity demand and estimate future electricity demand under climate change. In Chapter 3, I combine these projections of hourly electricity demand with simulations of thermal power plant curtailments into a Mixed Integer Linear Programming (MILP) model in order to simulate the least-cost capacity expansion (CE) policy considering different scenarios of climate change. Finally, I combine the results from previous chapters into a unit commitment and economic dispatch (UCED) model to look

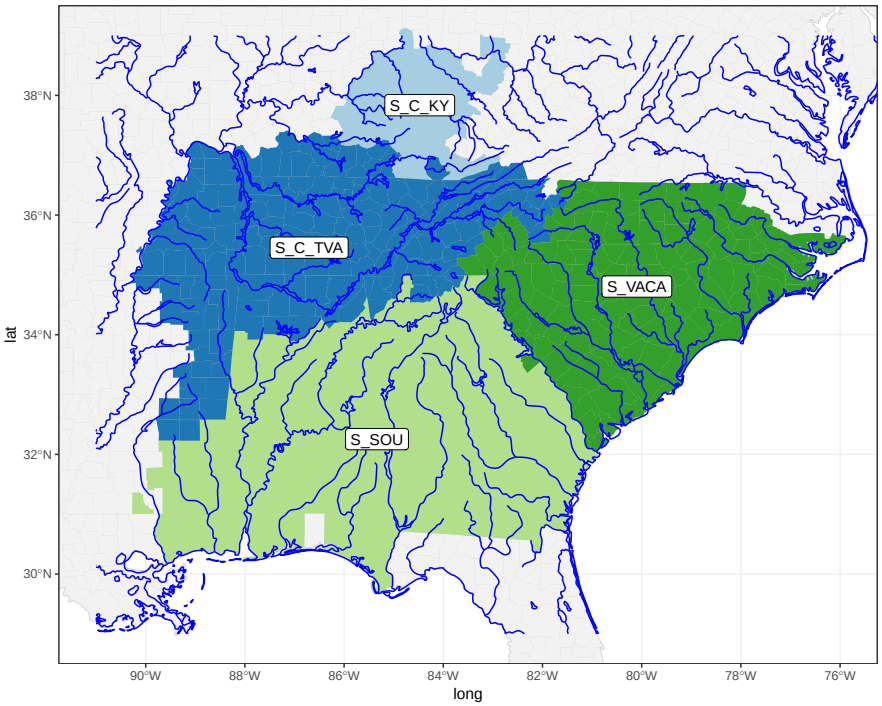

.

Figure 1.1: Illustration of the area included in the study case in this thesis (SERC Reliability Corporation)

at how these climate induced impacts in the power sector can impact different measures of efficiency and reliability in the power sector. Figure 1.2 presents a complete view of the methodological framework used in this thesis and how the results from each chapter relate to the other ones.

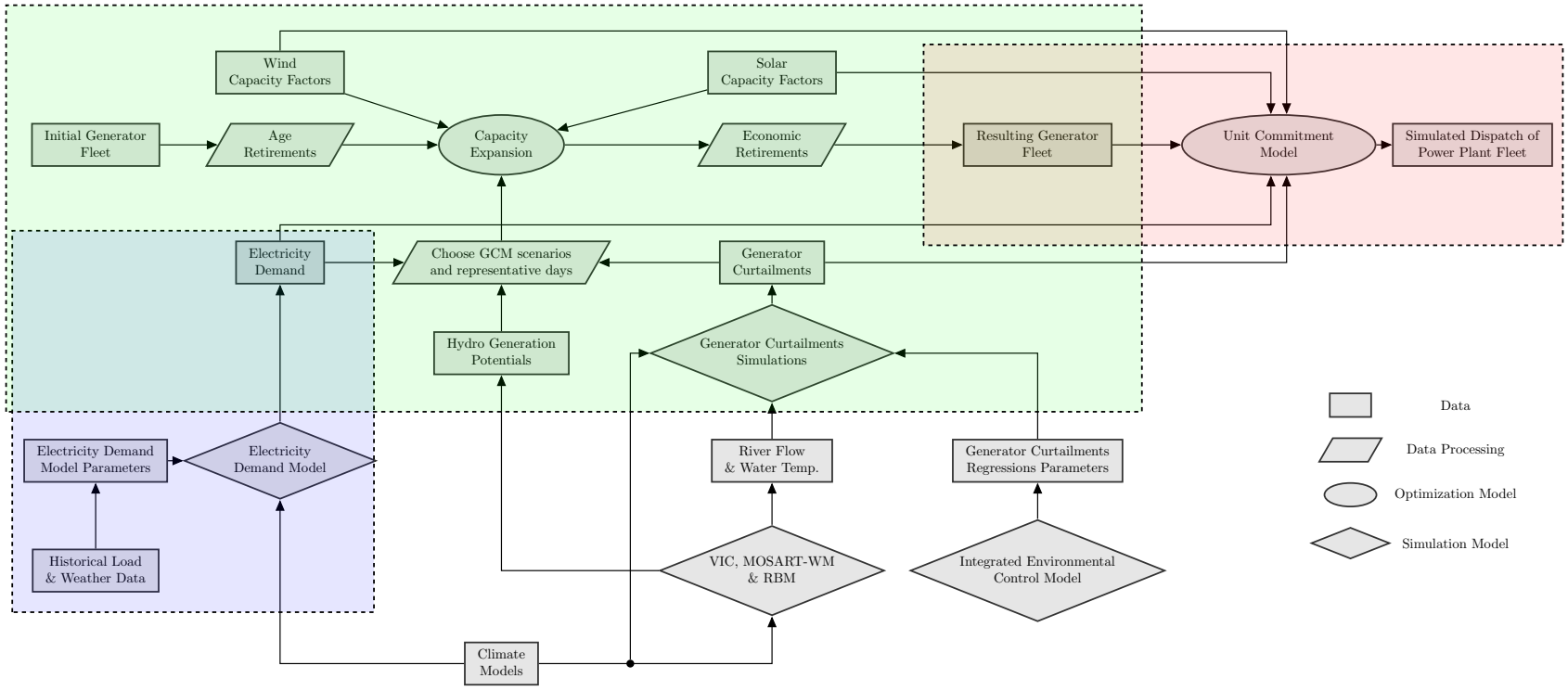

Figure 1.2: Diagram illustrating the complete methodological framework presented in this thesis. The blue rectangle represents the electricity demand model used in the analysis of Chapter 2. The green rectangle includes the capacity expansion model used in the analysis of Chapter 3. The red rectangle includes the unit commitment model used in the analysis of Chapter 4

Chapter 2

Seasonal effects of climate change on intra-day electricity demand patterns

2.1 Background

While significant efforts are being made to mitigate emissions of greenhouse gases that contribute to climate change, there is increasing interest in using Integrated Assessment Models (IAM) to understand the social costs of climate change and possible adaptation strategies across the world and across economic sectors [90, 47]. An important component of these costs is the impact climate change can have in the power sector [99]. A straightforward – but important – example of this impact is that higher temperatures can result in higher cooling demand and lower heating demand [5]. However, the actual costs due to these changes are highly dependent on local factors. Regions where natural gas is the primary source of electricity will have different impacts than those that rely more heavily on hydroelectricity. Also, electricity consumption patterns differ by geography. For instance, peak electricity demand (the maximum quantity of electricity demanded during an hour)

in the United States typically occurs in the summer. However, some areas in the southeastern U.S. experience winter peak demand due to their use of electricity for ambient heating. This heterogeneity in the characteristics of electricity demand across the country underscores the importance of regional impact analysis that captures important local factors.

In recent years many studies have looked at the impacts of climate change on global systems, including energy systems. Integrated Assessment Models include a representation of global agriculture, energy, economic, water, and climate systems. Prior work with IAM has included analyses of energy demand implication of climate change [37, 46, 32, 52, 120, 117, 20, 67, 29, 3, 21]. However, IAMs typically have a coarse spatial and temporal representation. Power system models used for capacity planning and system operations require hourly data, which are not usually available in IAMs.

Other work on climate impacts on electricity demand has relied on historical data to fit multiple linear regression models relating regional electricity consumption and weather variables. Many of such models use data in a monthly time-frame [12, 84, 83, 42, 4, 82, 70]. These monthly models typically employ cooling degree-day (CDD) and heating degree-day (HDD) metrics as the weather regressors. Models also differ on the type of demand they represent. While some examine only residential or commercial electricity demand, others aim to represent overall electricity demand for the entire system. Moreover, these models also differ in the way they represent long-term, non-climate trends in electricity demand. The most common practice[1] has been to explicitly include variables associated with these trends (such as population growth, economic activity, and changes in energy efficiency) in parametric models.

[1]The inclusion of additional time-varying explanatory variables may absorb residual variation, hence producing more precise estimates. However, adding more controls will not necessarily produce an estimate of the coefficient of interest that is closer to the true parameter. If the additional controls are themselves outcomes of changes in climatic variables, which may well be the case for controls such as GDP, institutional measures, population, and socioeconomic variables, including them will induce an "over-controlling problem." (see [27]). For example, suppose that poorer counties in the U.S. tend to be both hot and have

Recently, some studies have argued that using data averaged over large temporal or spatial ranges instead of higher resolution data can result in different conclusions when estimating some of the social costs of climate change [87, 88, 92, 40]. For example, the actual decision to dispatch power plants occurs at an hourly or sub-hourly resolution. Different types of power plants have specific operational and economic properties that affect their ability to be turned up or down quickly. Because of these characteristics, some types of power plants (such as nuclear) are better suited for base load generation, while other types (such as natural gas) are typically used to meet hourly changes in electricity demand. Therefore, planning studies that focus on changes in demand on monthly (or even daily) temporal resolutions may miss important constraints that occur in the actual operation of the power system. Some studies have started to work with data with higher temporal resolution in order to represent inter-day or hourly variability in demand [95, 75, 34, 6]. Our study expands on this previous work to improve our understanding of how climate change can affect the hourly patterns of demand using hourly demand data. We also focus on the seasonal aspects of these changes and how this in turn could affect the operations of the power system. For this analysis, we use a linear regression model that combines a piecewise linear function with fixed effects coefficients in order to capture unobserved factors that distinctively affect hourly electricity demand. Additionally, we use a simplified economic dispatch model to analyze how these changes in demand can alter some of the dispatch patterns of power plants at the level of the local balancing authority. The high resolution of our dataset makes it possible to perform different analysis of the resulting simulations, such as analyzing changes in the simulated hourly demand profile and constructing probability distributions of the changes in demand. We can also analyze how the climate-induced changes in demand profiles could affect the capacity factors of different types of power plants and how these impacts are different in each season of the year. We apply our

low-quality institutions. If hot climates were to cause low-quality institutions, which in turn cause low income, then controlling for institutions can have the effect of partially eliminating the explanatory power of climatic variables, even if climate is the underlying fundamental cause.

method to analyze the potential effects of climate change on the electricity demand patterns of the Tennessee Valley Authority (TVA) area as a case study. TVA is a corporate agency of the United States that provides electricity to customers in the southeast United States. TVA has a diverse generation portfolio (that includes fossil-based power plants and a significant contribution of hydroelectricity), and a demand profile with peaks in both summer and winter. According to the National Climate Assessment, it is a region that is particularly vulnerable to some of the expected impacts of climate change [68].

2.2 Data & Methods

2.2.1 Electricity Demand Data

Hourly electricity demand data for the TVA service area came from the Federal Energy Regulatory Commission (FERC) Form 714 [33] for the years 2006–2015. Figure 2.1 shows the time series plot of TVA's hourly electricity demand. The gray line shows the observed hourly demand and the black line represents the annual moving average of the hourly data. The light gray shaded areas in the background represent summer periods. From this figure we can observe that TVA's average annual electricity consumption has experienced a consistent downward trend in the last decade, after peaking around 2007/2008. Between 2007 and 2015, TVA's annual electricity consumption has decreased by approximately 13%. This downward trend in TVA's electricity demand is credited to a combination of an increase in energy efficiency, economic changes, and distributed energy generation [41, 81]. Additionally, TVA regularly faces events of high peak demand during the winter months. For example, in 2014 and 2015 the annual peak demand values occurred during the winter.

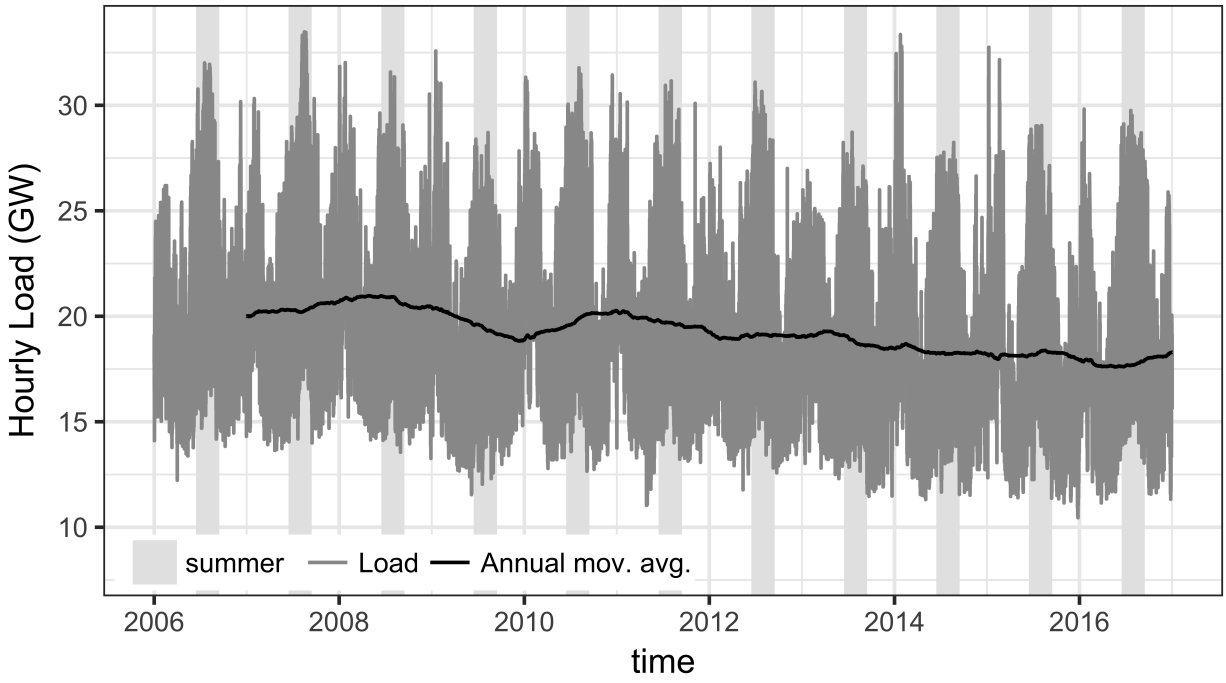

Figure 2.1: Hourly electricity demand for the TVA area, January 1, 2006 to December 31, 2015. The gray line represents the observed hourly demand. The black line shows the annual moving average of the hourly data. The light gray shaded areas in the background represent summer periods.

2.2.2 Weather Data

To fit our regression model, we use weather data from the University of Idaho Gridded Surface Meteorological Data (UofI METDATA) dataset [1]. This dataset combines desirable spatial attributes of gridded climate data from the PRISM dataset [78, 26] with desirable temporal attributes from the regional reanalysis dataset NLDAS-2 [71] to derive a high-resolution (1/24th degree, ∼4 km) gridded dataset of daily surface meteorological variables. This dataset has been validated by its authors against an extensive network of weather stations. The daily data is then disaggregated to hourly values using the Mountain Microclimate Simulation Model (MTCLIM) [15]. We use the air temperature data of the grid cell in Nashville, TN to represent the typical weather patterns in the TVA service area. We tested using data from other locations inside the TVA area, but because of the high spatial correlation between different grid cells, the results of our model did not

change. Figure 2.2 shows the observed relationship between hourly demand and hourly air temperature in our historical data set. We can observe the nonlinear relationship between demand and temperature. The main reason for this "U-shaped" relationship is that electricity can be used for both ambient heating and cooling [103]. In winter months, higher temperatures will result in decreased electricity demand for space heating. On the other hand, higher temperatures during the summer lead to increased electricity demand for space cooling.

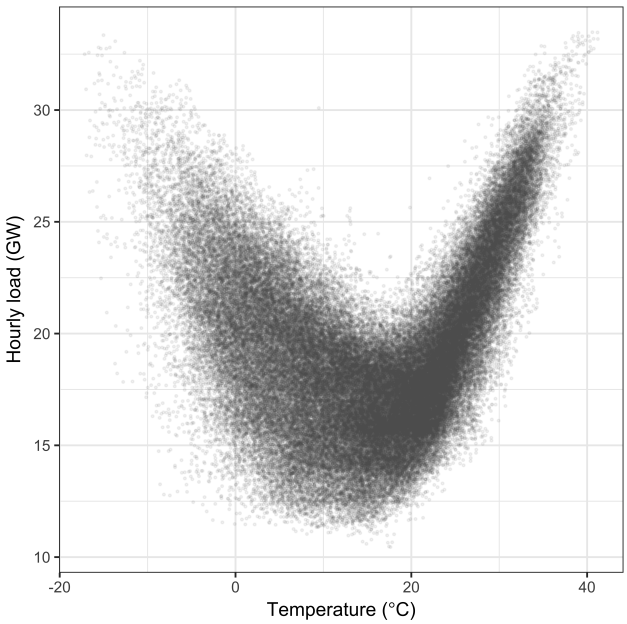

Figure 2.2: TVA's hourly electricity demand plotted against temperature (degrees Celsius) for the period January 1, 2006 to December 31, 2015.

To simulate the changes in electricity demand induced by climate change, we first need projections of our explanatory weather variables (air temperature and air humidity). We obtained the output of twenty different Global Circulation Models (GCM) from the Coupled Model Intercomparison Project 5 [93], spatially downscaled using the Multivariate Adaptive Constructed Analogs (MACA) method [2]. In addition, these projections were also disaggregated to hourly values using the Mountain Microclimate Simulation Model (MTCLIM).

Note that we use the UofI METDATA dataset for climate data between 2006 and 2015 to fit our regression model because this is the same dataset used in the training phase of the MACA method used to downscale projections of future climate. Therefore, our baseline meteorological data will be coherent with our projected weather variables from the downscaled GCMs. This way we avoid potential biases between the data generated by the climate model and the historical data used as a baseline to fit the regression model [7, 6]. We focus on the projections of air temperature and air humidity simulated by the 20 GCMs under the Representative Concentration Pathway (RCP) 8.5, which is usually called the "business as usual" scenario, since it assumes that concentrations will keep increasing in the same rate as in the present. We focus on the projections for two different periods: 2055-2065 and 2089-2099.

2.2.3 Electricity Demand Model

To estimate the typical response function of hourly electricity demand to weather changes, we use the historical data described above to fit a multiple regression model. We used a piece-wise linear function to represent the non-linear relationship between electricity consumption and temperature [65] (more details about this formulation are available in the Appendix). This formulation also enforces continuity on the breakpoints of the piece-wise linear curve. To control for unobserved factors affecting electricity demand in each hour of the day, our model includes fixed effects coefficients for each hour of the day in different seasons and different types of day (workday or weekend). The annual long-term trends are modeled using fixed-effects for each year in the historical data set. This way our model is capable of controlling for changes in the demand in electricity caused by economic and technological shifts in our historical dataset.

We also experimented with using air humidity as an explanatory variable. We used in-

teractions between air temperature and air humidity in each temperature bin of our estimated piece-wise linear function to capture the heterogeneity of how changes in air humidity affect demand for different air temperature levels [86]. However, the resulting fit of the model did not improve significantly, while the interpretability of the resulting model was considerably compromised. Therefore, we chose the more parsimonious model (without air humidity as an explanatory variable).

Equation 2.1 shows the regression model.

$$y_t = \beta_0 + \alpha_{hds} + \gamma_a + \sum_{j=1}^{N} \delta_j T_{jt}^c + \epsilon_t \tag{2.1}$$

where t denotes hourly data, h hour of the day ($h \in [1, 24]$), d type of day (workday vs. non-workday), s season of the year, and a calendar year. y_t represents hourly demand at t (in MW). T_{jt}^c is the j-th piecewise linear component of the temperature at hour t. Finally, α_{hds} and γ_a are, respectively, the fixed effects for hour of the day by different seasons and types of day, and year fixed effects.

All coefficients in our model are estimated by Ordinary Least Squares (OLS). The different fixed effects coefficients estimated by our model aim to capture unobserved factors in our dataset that influence hourly electricity demand and may be related to changes in temperature. The annual fixed effects (γ_a) capture all observed and unobserved variables that change on an annual basis such as economic activity, energy efficiency gains, and population changes. The hourly fixed effects (α_{hds}) capture hourly patterns of electricity demand in different seasons, controlling for unobservable behavioral responses regarding consumers' utilization electric appliances, and other time-varying decisions not easily observable. This way, the estimated coefficients of our response curve of electricity demand to temperature will not be biased because of the omission of these unobserved hourly, seasonal, or annual effects.

2.2.4 Dispatch Model

In order to simulate dispatch patterns due to changes in electricity demand resulting from climate change, we use a similar approach outlined in previous studies [14, 113]. A reduced-form economic dispatch model simulates the order in which power plants would be dispatched to meet hourly electricity demand. For each 24-hour day in the complete simulation period, a linear programming (LP) optimization model finds the dispatch schedule that minimizes the total generation cost. To define the short-run marginal costs of each power plant we compile data from different sources. Heat rates of thermal power plants come from the Emissions & Generation Resource Integrated Database (eGRID) [106] from the United States Environmental Protection Agency (EPA). Fuel costs for each power plant come from the Energy Information Agency (EIA) Form 923 [31], which collects detailed electric power data on electricity generation, fuel consumption, fossil fuel stocks, and receipts at the power plant level. In the cases of specific power plants for which this type of data is missing, we use regionally appropriate fuel costs and national average heat rates reported by the EIA. Combining all these data sources, we compute the short-run marginal costs of each individual power plant in our study. These costs are used in the linear programming problem to define the optimal daily dispatch policy.

Figure 2.3 plots the estimated short-run marginal costs of TVA's individual plants. Following the methods outlined in previous studies [14, 113], we represent planned maintenance and forced outages in thermal power plants by using an availability factor as an upper bound of the plant's generation. This availability factor was computed as a percentage of nameplate capacity as reported by EPA's Integrated Planning Model (IPM). Also, in the case of wind and solar power plants we use capacity factors instead of availability factors, since the former better represent the constraints these type of power plants face [113]. One difference in our model is that, for hydroelectric power plants, we impose a restriction that at a specific hour the power plant may generate up to its available power. However,

its total daily energy generated cannot be above its capacity factor (as reported in the eGRID data base). This flexibility is needed in order to meet peaks of demand throughout the day in areas that had a significant share of hydroelectric power. Turndown constraints are represented as a 50% minimum-operation limit for coal steam and nuclear units. These constraints ensure that these plants – which typically are operated as base load generators – are not cycled.

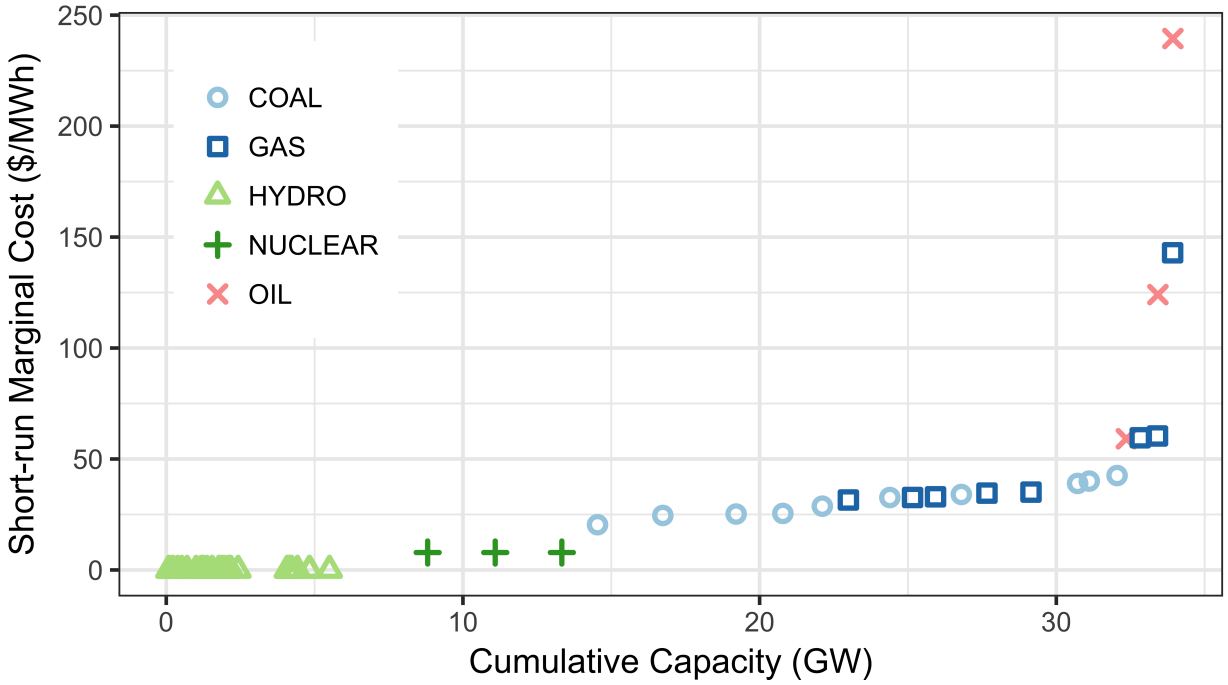

Figure 2.3: Estimated short-run marginal cost curve (supply curve) for Tennessee Valley Authority (TVA)

Equation 2.2 shows the formulation of the linear programming problem. Table 2.1 presents the variables used in the formulation and a brief description of each of them.

Table 2.1: Variables used in the definition of the dispatch problem

$\mathcal{P}$	Set with all the power plants in TVA
$\mathcal{P}_{min}$	Set with the power plants in TVA with minimum generation constraints ($\mathcal{P}_{min} \subset \mathcal{P}$)
$\mathcal{P}_{hyd}$	Set with all the hydro power plants in TVA ($\mathcal{P}_{hyd} \subset \mathcal{P}$)
$\mathcal{H}$	Period of simulation (24-hour day)
$x_{p,h}$	hourly generation (MWh) in hour $h \in \mathcal{H}$ of power plant $p \in \mathcal{P}$
c_p	generation cost (\$/MWh) of power plant $p \in \mathcal{P}$
y_h	total demand (in MWh) at hour $h \in \mathcal{H}$
C_p	maximum capacity power plant $p \in \mathcal{P}$ (in MW)
CF_p	capacity factor of power plant $p \in \mathcal{P}$ (in %). Used only for hydro plants.
G_p^{min}	minimum dispatch value of power plant $p \in \mathcal{P}$ (in MW)

$$
\begin{aligned}
&\min_{\forall x_{p,h}} \sum_{h\in\mathcal{H}} \sum_{p\in\mathcal{P}} c_p x_{p,h} \\
&\text{s.t.} \\
&\quad \sum_{p\in\mathcal{P}} x_{p,h} \geq y_h && \forall h \in \mathcal{H} \\
&\quad x_{p,h} \leq C_p && \forall h \in \mathcal{H}\,,\ \forall p \in \mathcal{P} \\
&\quad x_{p,h} \geq G_p^{min} && \forall h \in \mathcal{H}\,,\ \forall p \in \mathcal{P}_{min} \\
&\quad \sum_{h\in\mathcal{H}} x_{p,h} \leq |\mathcal{H}| * CF_p * C_p && \forall p \in P_{hyd} \\
&\quad x_{p,h} \geq 0 && \forall h \in \mathcal{H}\,,\ \forall p \in \mathcal{P}
\end{aligned}
\tag{2.2}
$$

The objective function represents the total generation cost over the period $\mathcal{H}$ (in this case, a 24-hour day). This total cost is the sum of the hourly costs of each power plant p in the set of all the power plants owned by TVA ($\mathcal{P}$). The first constraint states that for each hour h, total generation must be greater than the demand (y_h). The second constraint represents the capacity upper bound: in each hour, generation of each power plant ($x_{p,h}$) must be smaller than its capacity (C_p). The third constraint applies to thermal generators that have turn-down restrictions such as coal plants. To emulate these restrictions, we use lower bound on their dispatch (G_p^{min}). The fourth constraint is an energy restriction that applies to hydro generators. Generators of this type cannot generate more than their av-

erage capacity factor (CF_p) over the period $\mathcal{H}$. This constraint assures that the simulated dispatch of hydro generators will not be unrealistically large. Finally, the fifth constraint is the non negativity constraint, to ensure that the solution will not have negative generation values.

Validating the results of the dispatch simulations can be difficult task as the dispatch model does not include many factors that affect real-time power plant dispatch. For example, system operators have to consider real world constraints such as transmission limits and ramping constraints in thermal power plants. The constraints on the operation of dams would also affect the amount of hydro generation available. For the purpose of this paper, the objective was to make a comparison between the results in a baseline (or present) scenario without the effects of climate change, and a scenario with the estimated effects of climate change. Using the same model formulation and basic assumptions ensures that the biases that result from the model specification are constant in all the simulations. The relevant results relate to the comparison between the scenarios and the implications of such differences.

2.3 Results

We use our complete historical data set (years 2006 – 2015) to estimate the coefficients of our regression model by Ordinary Least Squares (OLS). The specified model results in $R^2 = 0.853$ and $R^2_{adj} = 0.853$, meaning that 85.3 percent of the variation in hourly electricity demand in the TVA area is explained by our model. Figure 2.4 presents the TVA's estimated response function of electricity demand to changes in temperature according to our model. The Supplemental Material includes the estimated values of the slopes in each temperature bin . The gray points in the background in Figure 2.4 represent the observed values of hourly temperature and residualized electricity demand in our historical

data set. The histograms at the top and at the right of the panel display the observed distribution of the variable on the respective axis. To compute the residualized electricity demand we subtract our estimated values of α_{hds} and γ_a (but not β_0) from the observed values of hourly demand. This way we are left with our estimated values of hourly electricity demand that are temperature dependent and are not influenced by non-observed hourly, seasonal, or annual effects. We can observe that the estimated response function appears to be capturing the overall shape of the relationship between air temperature and electricity demand. One interesting aspect that we can observe from this scatter plot is that the response curve appears to have a more symmetrical shape when compared to similar response functions in other load regions, e.g., PJM [61]. This can be explained by the larger use of electricity for ambient heating in the southeastern U.S. than other regions [103]. As a result, increased winter temperatures lead to decreased electricity demand for heating, while increased summer temperatures lead to an increase in demand for cooling.

After specifying the electricity demand model, we use it to simulate future electricity demand given the scenarios of climate change from the different GCMs. We run the simulation for two future periods: 2055-2065 and 2089-2099. Throughout this document we will refer to these two simulation periods as 2060 and 2099, respectively. This way we aim to account for normal inter annual variability in the weather data in each of these future periods being simulated. Also we avoid potential biases in our results due to the selection of a single future year for our analysis. Since our goal is to study the impacts that predicted changes in climate trends can have on electricity demand, we create our simulations of future electricity demand under the assumption that all other estimated factors will remain constant. For example, we use the estimated value of the annual fixed effect for 2015 (γ_{2015}) in our simulations of demand in 2060 and at the end of the century. Additionally, in order to create a comparable base case of present demand (i.e., without the effect of climate change), we use our model with historical air temperature data from 2005 to 2015 to backtrack hourly electricity demand in this period (also using the value of γ_{2015} for the

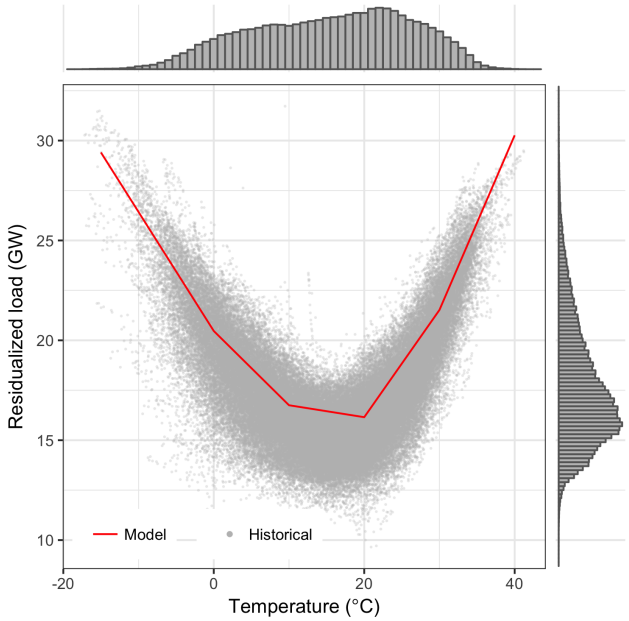

Figure 2.4: Estimated hourly electricity demand temperature response function. The gray dots represent the historical values (2006-2015) of hourly temperature and residualized electricity demand (temperature dependent). The red solid line is the average response curve according to our estimated model. To compute the residualized electricity demand we subtract our estimated values of α_{hds} and γ_a (but not β_0) from the observed values of hourly demand. The histograms at the top and at the right of the panel display the observed distribution of the variable on the respective axis.

whole period).

Figure 2.5 presents the simulated average annual load duration curves (LDC) for the present and each of the two future periods. The LDCs show the percentage of time in the year that the hourly demand is above a certain value. The solid line is the average present load curve (the average is taken over the 2005–2015 period). The dashed lines represent the average load curves simulated for the periods 2060 and end-of-century (averages are taken over the 11 year period and over all 20 GCMs). The gray shaded areas show the range of these future simulated averages LDCs over the 20 GCMs. The plot shows a significant increase in the occurrence of peak demand values through the year in 2060 and 2099 when compared with the present. Overall, the simulations indicate that annual consumption of electricity in TVA increases by 2.5% by 2060 and 6% by the end of the century as a result

of climate change. However, this increase is not uniformly distributed throughout the year. Most of it occurs on approximately 25% of the year (2,500 hours). Additionally, if we focus on the highest 1,000 hourly values in each curve, the total consumption of electricity during these hours increases by 11% by 2060 and 21% by the end of the century. Also, we can see by the gray shaded area that the trend observed in the average curve is consistent across all the 20 GCMs simulated.

The LDCs in Figure 2.5 do not show how changes in demand due to climate change may be chronologically distributed throughout the year. Figure 2.6 shows the simulated average hourly load curves for each season in the present and each of the future periods. As with the LDCs, the solid curves represent the average hourly load curve according to present weather conditions (the average is taken over the 2005–2015 period). The dashed lines represent the simulated average hourly load curves according to projected weather conditions in 2060 and 2099 (averages are taken over each 11 year period and over all twenty GCMs). The gray shaded areas show the range of these future simulated hourly load curves over the twenty GCMs used in our simulations of electricity demand.

In winter time, electricity consumption decreases on average by 4% by 2060 and by 6% using the simulated data for 2099. On the other hand, summer electricity consumption increases on average by 11% by 2060 and by 20% using the simulated data for 2099. Figure 2.6 shows that there is a large spread on the potential increases in the hourly electricity demand during summer time depending on which GCM is used to simulate future electricity demand. However, this uncertainty in the simulations results does not show up on other seasons. Figure 2.4 shows a non-linearity in the response of hourly demand to temperature. This suggest that a 1°C change in summer temperature has a larger effect on demand than a 1°C change in winter. As a result, the variability in temperatures represented in the different GCMs result in a wider spread in the summer demand values.

The results of the demand simulations under climate change highlight that electricity con-

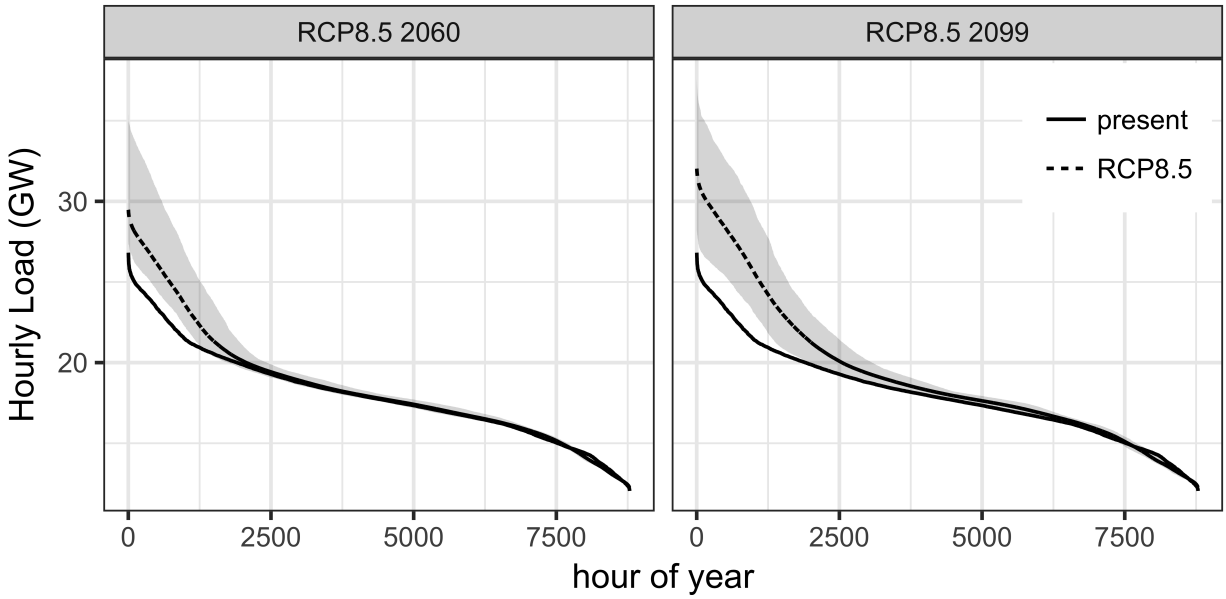

Figure 2.5: Present and future simulated average load duration curves (LDC). The solid curves represent the average LDC according to present weather conditions. The dashed lines represent the simulated average LDCs according to projected weather conditions in 2060 and end of century. The gray shaded areas show the range of these future simulated averages LDCs over the 20 GCMs.

sumption during the summer will account for a larger proportion of the total annual consumption under climate change in TVA. Furthermore, TVA will see changes in the distribution of daily peak demand. Figure 2.7 shows simulated kernel density plots of daily peak demand. This figure suggests that there will be an increase in the probability of larger values of peak demand, illustrated by the increase in the right tail of the distribution. The 95th percentile of these curves increases by 10% by 2060 and 19% by the end of the century. These values are comparable to the ones found by previous studies such as [6]. In that work, the authors found an increase between 15% and 21% of 95th percentile of daily peak demand by the end of the century for different load zones in the US.

The changes in the seasonal distribution of electricity consumption and the distribution of peak demand hours could affect the operations of the power system. Increased peak demands in the summer require increased available generation capacity, which will not be used in the winter, when increased temperatures will lead to decreased demand. To evalu-

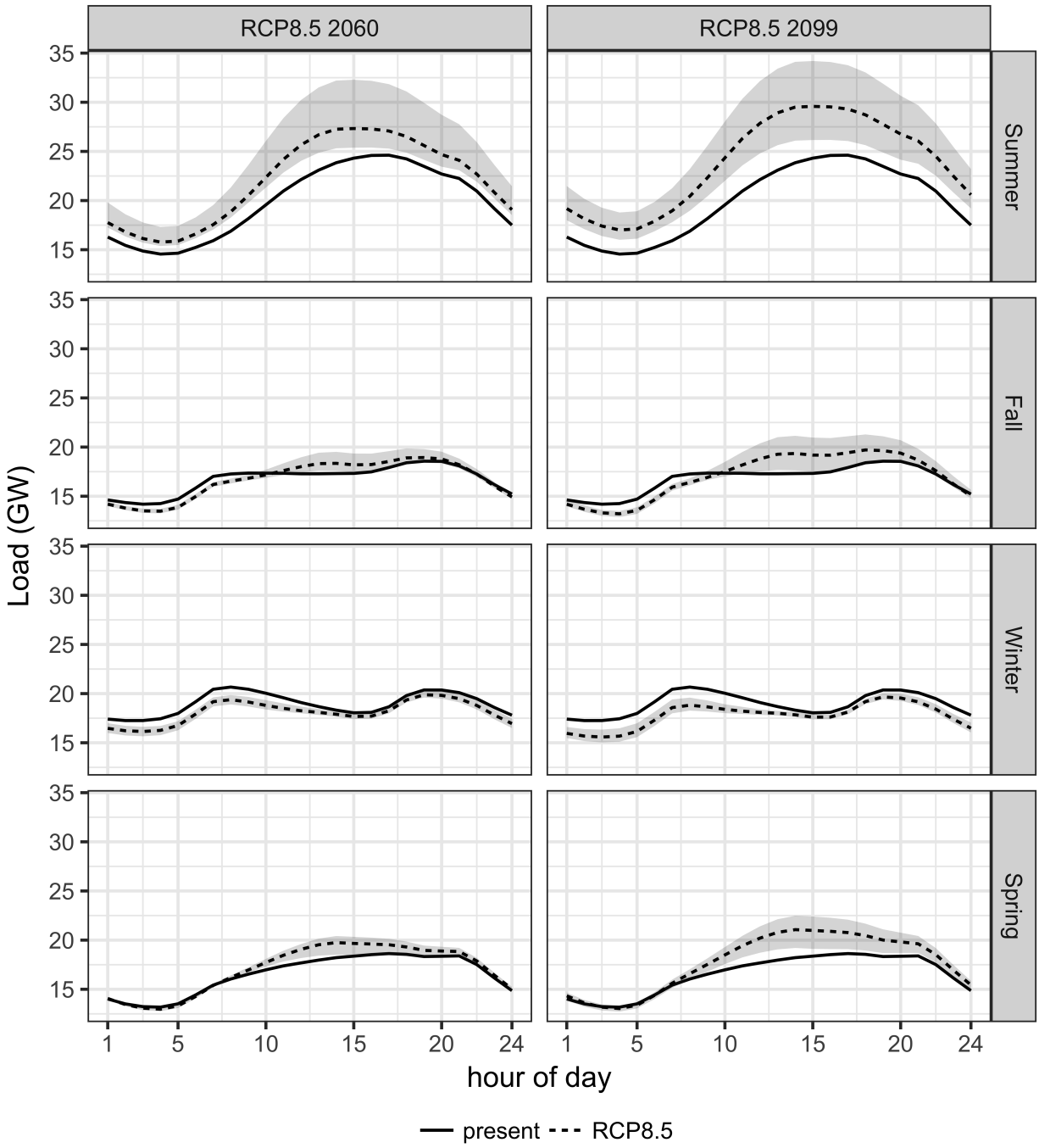

Figure 2.6: Present and future simulated average hourly load curves for each season. The solid curves represent the average hourly load curve according to present weather conditions. The dashed lines represent the simulated average hourly load curves according to projected weather conditions in 2060 and end of century. The gray shaded areas show the range of these future average hourly load curves over the 20 GCMs.

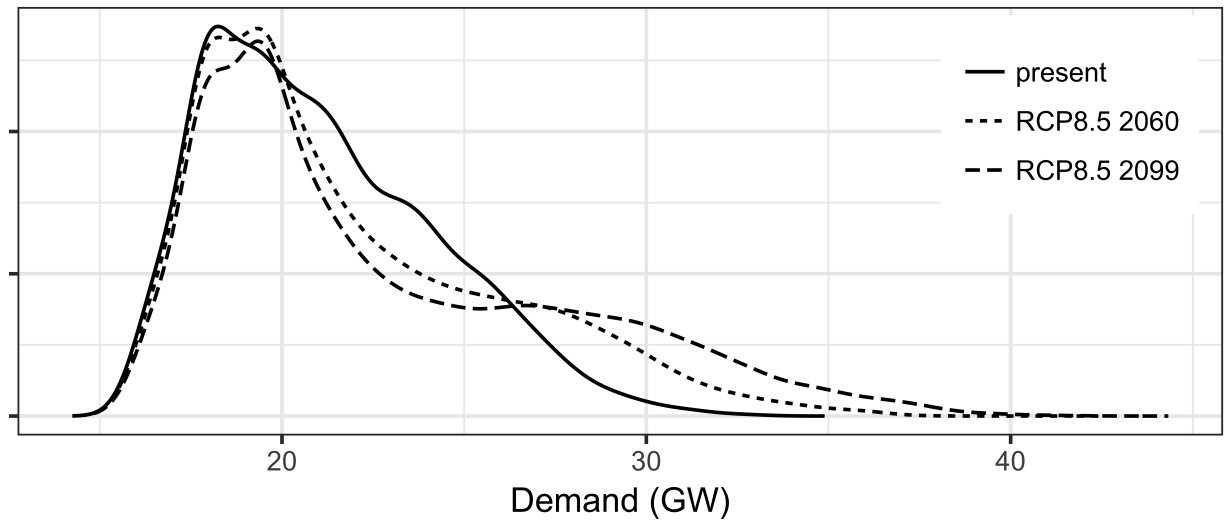

Figure 2.7: Comparison of simulated kernel density plots of daily peak demand. The solid curves represent daily peak demand values under present weather conditions. The dashed and dotted lines represent daily peak demand values according to projected weather conditions in 2060 and end of century, respectively.

ate these operational impacts, we used the projected values of electricity demand to simulate the generation dispatch using a linear programming model (see section 2.2.4).

Different types of power plants have different marginal costs of generation and different operational properties that affect their ability to be turned up or down quickly. Nuclear power plants, for example, have a low marginal cost of generation and have a limited ability to respond to rapid changes in demand for electricity. As result, nuclear power plants are better suited for based load generation. Natural gas power plants, on the other hand, have a higher marginal cost of generation but can very quickly respond to demand changes. Therefore, natural gas plants have historically been used to "follow load." The costs and constraints of different power plants will affect how they are scheduled to meet hourly demand under climate change. Figure 2.8 shows the simulated average capacity factors of different plant types in TVA. The capacity factor for a power plant is the ratio between annual generation (from the dispatch model) and the maximum amount of electricity the plant can generate in a year given its rated power (assuming the plant operates at its rated

capacity 24 hours a day, 7 days a week). Figure 2.8 does not include results for hydro and nuclear power plants because the magnitude of the change in their capacity factors was not substantial. In our simulation the variable operating cost of these types of plants is zero or close to zero, therefore they are typically the first ones to be dispatched in every season (with or without climate change). We display one plot for each season in the year in order to be able to understand how the changes in demand affect the dispatch of the different types of power plants in each season. The darkest bars show the average capacity factor for each plant type resulting from the dispatch simulations using current demand (without climate change). The bars of lighter colors show the simulated capacity factors for each plant type in 2060 and 2099. The error bars represent the 90% uncertainty range computed over each simulation period (11 years) and over all the 20 GCMs used in our simulations. As expected, we observe a large increase on the average capacity factor in the summer and a decrease in the winter using climate simulations for 2060. Furthermore, we find coal, natural gas, and oil-based power plants experience most of the changes in their average capacity factors, since the changes in demand by 2060 are within the range in the supply curve in which these plants provide the marginal supply.

In the simulations for the end of the century we find that average peak demand values during the summer can increase by more than 10% as a result of climate change. These shifts move the peak demand values closer to the right region of the supply curve, resulting in an increase of the dispatch of the more expensive power plants, such as oil. According to our results, capacity factors of natural gas power plants in the summer would increase from 8% in the present to more than 37% using end of the century temperatures. On the other hand, during the winter they would decrease from 3% to virtually zero. The capacity factor of coal power plants in the summer would increase from 71% to 84%, while in the winter it would decrease from 67% to 60%. Oil plants would experience an increase on their average capacity factors from approximately 0% to approximately 14% during the summer.

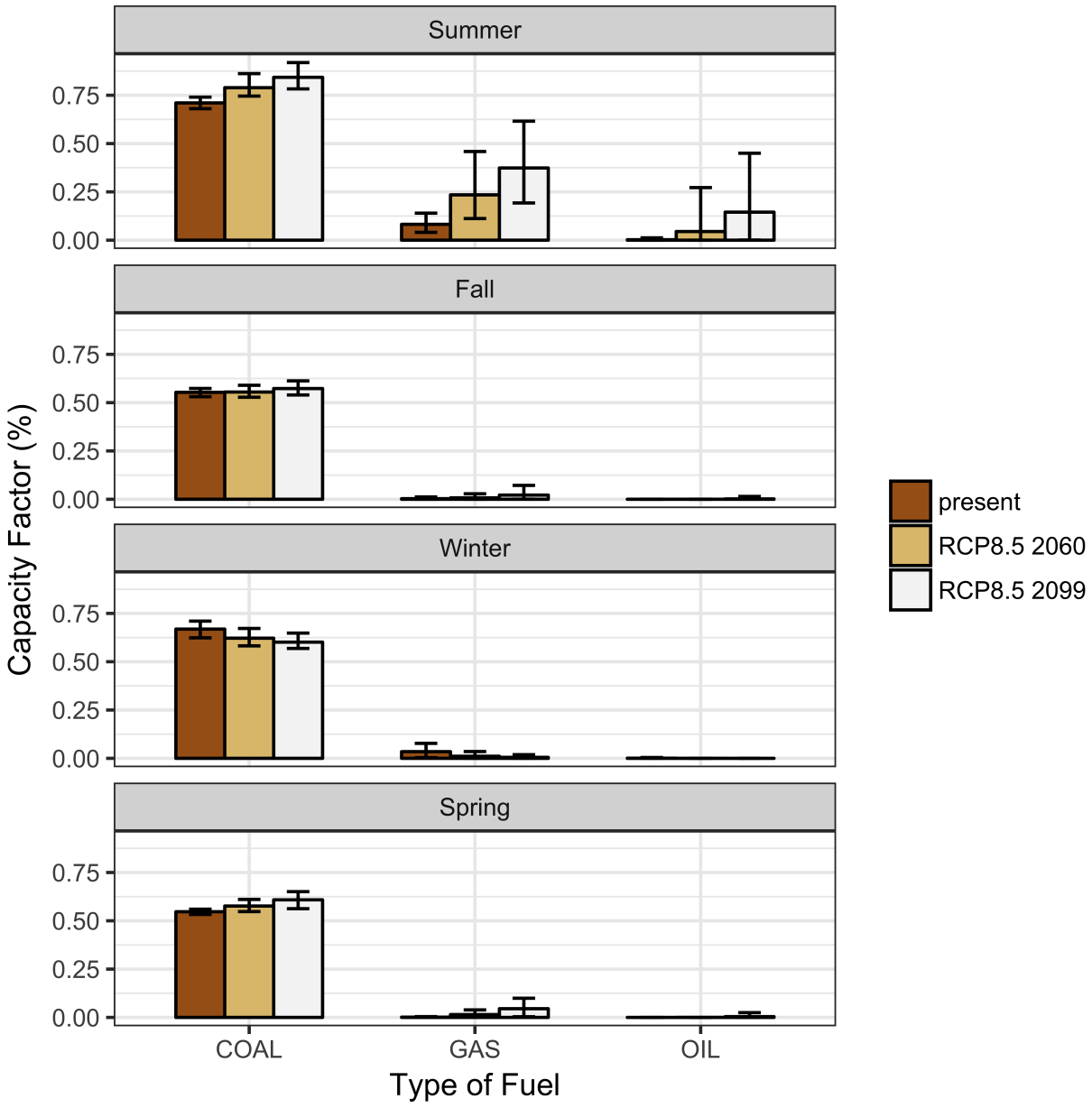

Figure 2.8: Barplots with average simulated capacity factors by generation fuel in each season of the year. The error bars represent the 90% uncertainty range computed over each simulation period and over all the 20 GCMs. We did not include hydro and nuclear in this figure because the change in their capacity factors was not substantial.

These results can have important implications for TVA's planning agents. The projected increase in electricity consumption in the summer and the decrease in consumption in the winter may imply two effects. On the one hand, the decreased consumption in the winter may offset part of the increased consumption in the summer. On the other hand, the changes in seasonal peak demands might mean that more power plant capacity would remain idle in the winter, just waiting to be dispatched during the months of higher demand in the summer. This could have implications for cost recovery and electricity tariffs in vertically integrated utilities. In de-regulated regions that operate wholesale electricity markets, the shifts in seasonal capacity factors could have implications for spot prices, capacity markets, and market design. While this analysis relies on the existing fleet of power plants, which will not be the same by mid-century (much less by the end of the century), these results highlight why the analysis of the climate-induced impacts on hourly load curves is relevant for system planning and operations.

A related consequence of increased summer peak demand would be the need for additional reserve margins, in order to cope with the increased probability of higher values of peak demand. Currently, the "rule-of-thumb" in the power sector is that utilities should have a reserve margin (i.e., amount of capacity above average peak demand) of 15% in order to cope with values of peak demand higher than the expected ones. As peak demand increase, so will the amount of capacity (in GW) needed to maintain appropriate reserve margins, which would likely affect costs.

There are some caveats in our analysis. First, we assume that the only variable that affects demand for electricity is temperature. This is a deliberate assumption, since our goal is to estimate how the changes in climate projected by the GCMs will affect the demand for electricity. However, changes in weather patterns will certainly not be the only factor that will affect electricity demand. Even in our regression analysis, the amount of variability in the historical data of electricity demand that was explained by the estimated

temperature function was smaller than, for example, the variability explained by the annual fixed effect terms. This suggests the non-observed socioeconomic variables that these annual fixed effects are meant to represent (such as economic growth, population changes and efficiency gains) have a larger effect on electricity demand than changes in temperature, as suggested by previous studies [82].

Incorporating alternative socioeconomic assumptions in our study would result in evaluating their mitigating or compounding effects on the climate-induced impacts. However, the direction of those effects can be ambiguous. Economic growth is usually related to increases in electricity consumption. However, it may also result on greater investment on energy efficiency technologies that could offset demand growth. As illustrated in Figure 2.1, TVA's electricity demand has decreased in recent years despite positive population and economic growth in the region in the same period, which is arguably a result of recent energy efficiency gains [41]. Additionally, other changes in technology and infrastructure could affect our estimated hourly fixed effects. For example, the possible increase in the penetration of plug-in hybrid electric vehicles (PHEVs) could shift electricity demand patterns [36] in ways that are not yet clear. Analyzing such effects could be the subject of future studies.

These modeling limitations not-withstanding, the results in this paper suggest that temperature changes as a result of climate change could, by themselves, affect demand profiles in important ways. These results suggest that total electricity consumption during the summer in TVA under climate change could increase by up to 20% by the end of the century, while overall winter electricity consumption could decrease by up to 6%. Such effects are significant enough to suggest that power system planner and operators should account for climate change-induced effects in electricity consumption when making decisions.

2.4 Conclusion

In this chapter we analyzed the impacts of climate change on hourly electricity demand and how these can affect the dispatch of power plants. We used a linear regression model capable of representing hourly electricity demand and its non-linear relationship to air temperature. This high resolution analysis can be important when trying to estimate the social costs of climate change in the power sector, because it better approximates how the system is operated (as opposed to using averaged/aggregated data). We focused our analysis on a case study of the TVA service area. However, the framework presented in this study can be directly applied to other load areas where data are available. As observed previously, these results are dependent on location-specific parameters, such as electricity consumption behavior (for example, the higher share of electricity usage as a source of energy for space heating) and the characteristics of the power plant fleet that supplies electricity for this region. Future work could expand this analysis to other regions of the U.S. to compare how these regional issues affect our results. Additionally, it could also combine the effects of climate change with scenarios of changes of other variables that affect electricity demand, such as economic activity and population growth.

In order to evaluate the system-effects of changes in demand patterns, we use a reduced-form economic dispatch model. Dispatch decisions account for more constraints and variables than we included in our model [23]. Furthermore, climate may also affect the technical operations of power plants, and the hydrological conditions which may result in new constraints. In future work, we will analyze potential interactions of climate impacts on different components of the power system using more complex power system models than the one used in this paper. It is clear from our results, however, that climate change could have an important effect on the shape of the hourly load curve as well as on the differences between seasons, and that these effects could have implications for the dispatch of power plants, which in turn would affect the costs of power supply.

Chapter 3

Capacity expansion of an electricity generation fleet under climate change

3.1 Background

According to the Intergovernmental Panel on Climate Change (IPCC), average global temperatures are likely to rise 1.5° C above pre-industrial levels by 2052 [45]. The IPCC also projects a likely increase in meteorological variability, climatic extremes, and droughts. Such changes will likely result in climate-related risks for natural and human systems. Among the human systems that may be affected is the energy sector. In the United States, the electric power sector faces many climate related challenges [100, 99]. On the demand side, increasing air temperatures may result in shifting demand patterns [100], higher cooling demand in the summer, and lower heating demand in the winter [100]. These changes in demand could, by themselves, result in challenges to the operation of the power sector. However, these threats are compounded by vulnerabilities on the generation side. In the U.S., thermoelectric power plants, which account for roughly 85% of power genera-

tion [102], could be affected by climate change through several pathways. For example, decreased water availability and increased water temperature could reduce the capacity and efficiency of thermal units that use once-through cooling [100]. Additionally, increased air temperature and humidity could reduce the capacity and efficiency of thermal units that use recirculating cooling [100].

Previous studies have mostly focused on analyzing these risks separately [24]. For example, studies that focus on electricity demand [34, 38, 6, 79] have shown that by the end of the century climate change could increase U.S. electricity consumption and daily peak demand by 2.8% and 3.8% on average, respectively [6]. Recent assessments have also analyzed the vulnerabilities of thermoelectric power plants to climate change in the U.S. and Europe [112, 10, 114]. These studies have shown that thermoelectric power plants could experience a summer average decrease in their available capacity of 6%–19% in Europe and 4%–16% in the United States [112, 114]. Peter [77] assessed power system planning in Europe using average climate change impacts exogenously derived from other studies. He found that climate change impacts increase system costs of a system designed without climate change anticipation. While this previous work helps to shed light on risks to individual power system components, it usually fails to capture systemic risks caused by interactions between demand-side and supply-side impacts on the operation of the power grid. These systemic risks become even more critical because of the nature of energy infrastructure planning and investment. Planning horizons can span several decades – the typical service life of most energy assets – and associated investments can extend into the billions of dollars. Therefore, it is imperative to evaluate how climate-induced risks could affect capacity expansion planning and operations of the U.S. power system.

Here, we developed an integrated, multi-model framework to examine how climate-related risks in the power sector can potentially affect power system planning decisions, which would, in turn, change the composition of the future power plant fleet. Through this work,

we simulated the different climate-change risks in a consistent way [96], by considering the same ensemble of climate models, emission scenarios, and time horizons. At the center of the multi-model approach, we implemented a deterministic capacity expansion (CE) model that chooses future generator additions that minimize the sum of annualized fixed investment costs and variable generation costs subject to user-defined constraints (such as meeting electricity demand). Our analysis focused on the SERC Reliability Corporation (SERC), one of the North American Electric Reliability Corporation (NERC) subregions. This region has a diverse generation portfolio (that includes fossil-based power plants and a significant contribution of hydroelectricity) and a demand profile with peaks in both summer and winter. According to the National Climate Assessment, the SERC region is particularly vulnerable to some of the expected impacts of climate change [68]. To simulate the effect of climate on investment decisions, our model used spatially- and temporally-differentiated estimates of weather-induced constraints to the system's supply and demand. Figure 3.1 summarizes our modeling framework. We used the downscaled output from twenty different General Circulation Models (GCMs) [93, 2] to generate projections of hourly electricity demand [79]. We also used the output from these climate models as inputs into a chain of hydrological models [56, 55, 115, 73, 116] to generate series of daily river flows and water temperatures, which we then used to estimate hydropower potential under climate change. In addition, we used climate forcings and hydrological variables to estimate capacity deratings for existing and potential thermoelectric power plants under climate change [57, 17, 119]. Moreover, we used U.S. National Renewable Energy Laboratory (NREL) data sets of simulated wind and solar generation profile [109, 30] as upper bounds on wind and solar hourly generation. Finally, we combined all the aforementioned simulations into our capacity expansion model.

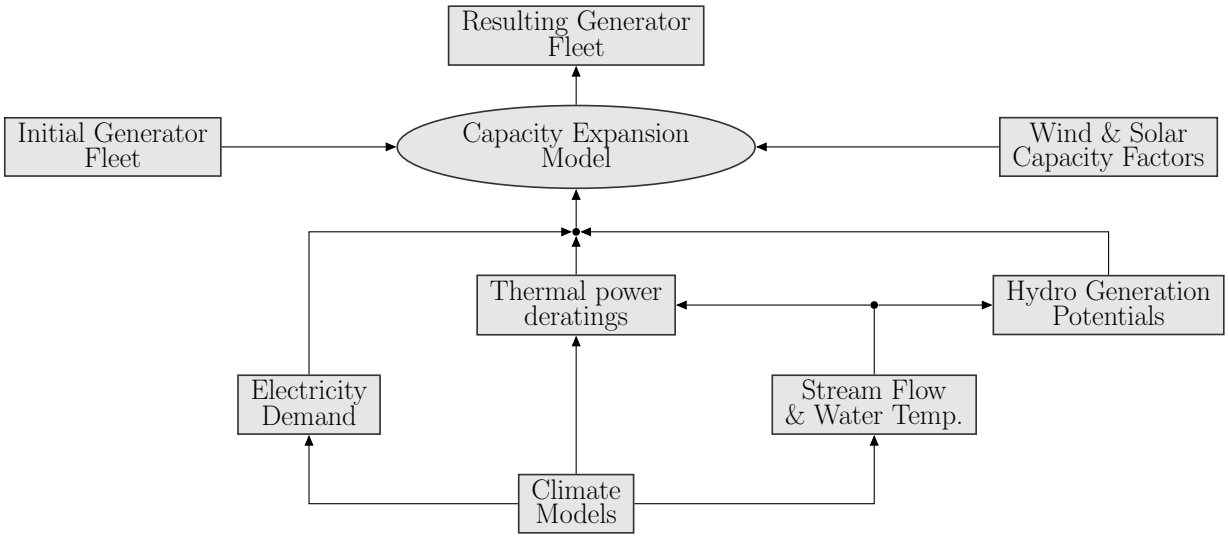

Figure 3.1: Diagram showing the modeling framework of our analysis.

3.2 Data & Methods

3.2.1 Configuration of study area

We focused our analysis in the SERC Reliability Corporation (SERC). To define the geographical domain of our study, we used the definitions of the Integrated Planning Model (IPM) developed by the United States Environmental Protection Agency (EPA) [105]. In IPM, there are 67 IPM model regions covering the 48 states in the contiguous U.S. and District of Columbia. The IPM model regions are approximately consistent with the configuration of the NERC assessment regions in the NERC Long-Term Reliability Assessments. Further disaggregation of the NERC assessment regions and RTOs allows a more accurate characterization of the operation of the U.S. power markets by providing the ability to represent transmission bottlenecks across RTOs and ISOs, as well as key transmission limits within them. The NERC assessment region SERC is divided into Kentucky (S_C_KY), TVA (S_C_TVA), AECI (S_D_AECI), the Southeast (S_SOU), and the Carolinas (S_VACA). In order to simplify the hydrological simulations needed for our analysis, we did not include areas west of the Mississippi river[1]. Therefore, the IPM region AECI

(S_D_AECI) was not included in our description of the SERC region.

The IPM model includes data on transmission limits between the different zones. Our capacity expansion model is capable of considering transmission limits between each region in the analysis. However, for this study we did not set upper bounds on the electricity exchanged between the four IPM zones.

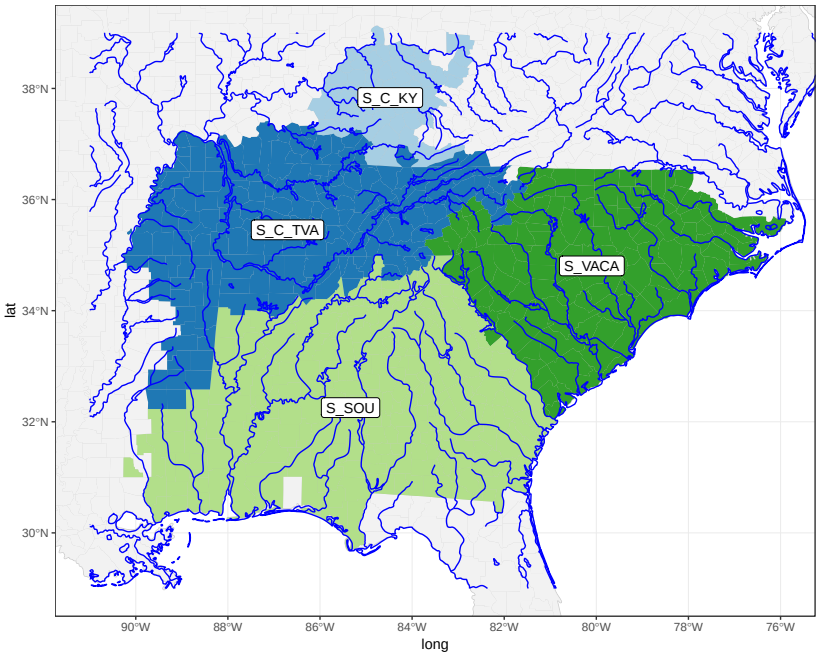

Figure 3.2: Area of study

3.2.2 Existing generator fleet data

We imported the list of existing generator units in the SERC area from the National Electric Energy Data System (NEEDS) database [108]. NEEDS is a database that contains the generation unit records used that represent existing and planned/committed units in EPA modeling applications of the IPM model. It includes basic geographic, operating, air

[1] Adding areas west of the Mississippi river to our analysis would require simulating flows from the river basins that feed into the Mississippi. This would result in a major increase of the simulation area of the hydrological models, which would then include the whole northwestern region of the continental U.S. Since the S_D_AECI IPM region represents a small fraction of the SERC area in IPM, we chose to exclude it from our analysis.

emissions, and other data on these generating units. It is compiled by EPA using different sources such as surveys and reports from the Energy Information Administration (EIA), and comments from utilities and regional EPA offices.

Emission rates for each power plant were imported from EPA's Emissions & Generation Resource Integrated Database (eGRID) [106]. eGrid is a comprehensive source of data on the environmental characteristics of almost all electric power generated in the United States.

Finally, cooling technologies for each power plant were imported from Form EIA-860 [104]. This survey collects generator-level specific information about existing and planned generators and associated environmental equipment at electric power plants.

This resulted in a current (as in 2015) fleet of 172 GW of installed capacity. Approximately 85% (149 GW) of this capacity was composed by thermoelectric power plants, including nuclear (17%), coal (32%) and natural gas (37%). Hydroelectric power plants represented approximately 12% of SERC's installed capacity. Other renewables, such as wind and solar, represented around 1% of the generator fleet. Figure 3.3 shows the composition of SERC's generator fleet. Regarding cooling technologies of thermoelectric power plants, once through cooling systems represented approximately 38.2 GW (around 25% of thermoelectric capacity). Recirculating cooling systems represented 77 GW (51% of thermoelectric capacity). According to the data disclosed by form EIA-860, dry cooling systems represented just a small fraction of the total thermoelectric capacity in SERC.

Figure 3.4 shows the remaining capacity of the existing fleet over time after considering the retirements of existing generators due to estimated age limits. According to this data, around 50% of the installed capacity available in 2020 could retire by 2050 due to age limits.

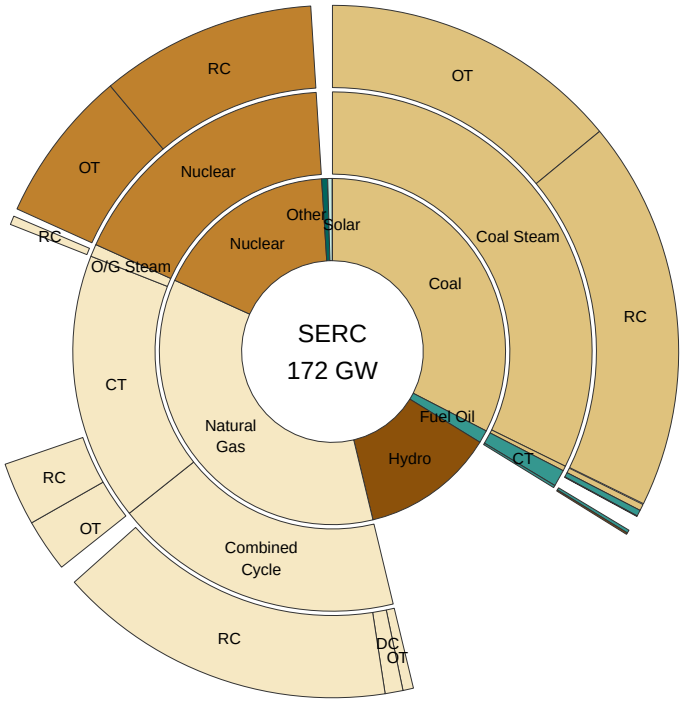

Figure 3.3: Composition of SERC's power plant fleet. The first level of the pie chart shows the breakdown into the different fuel sources used by the power plants in SERC. The second level shows the types of generating technologies – where applicable – used for each type of fuel source. The code "CT" stands for Combustion Turbine. The third level presents the cooling technologies used in for the respective thermoelectric generators. The codes "OT", "RC", and "DC" stand for, respectively: once-through cooling, recirculating cooling, and dry cooling.

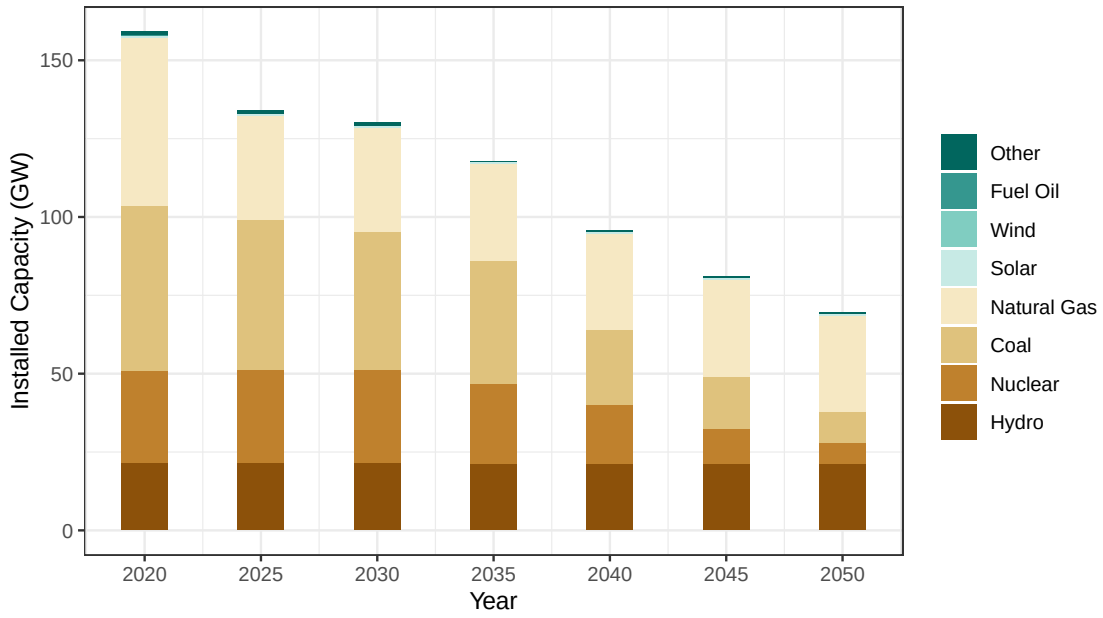

Figure 3.4: Remaining capacity from those generators online in 2015. Around 50% the installed capacity available in 2020 could retire by 2050 due to age limits.

3.2.3 Climate and hydrology data

We used gridded projections of daily air temperature, air humidity, and air pressure from the Global Circulation Models (GCM). We obtained the output of twenty different GCMs (Table A.1) from the Coupled Model Intercomparison Project 5 [93], spatially downscaled using the Multivariate Adaptive Constructed Analogs (MACA) method [2]. In addition, these projections were also disaggregated to hourly values using METSIM (Meteorology Simulator) [13].

To simulate regulated daily river flows and water temperatures in the study region we used a physically based modeling framework. This process-based modeling approach consists of three separate models. First, we used a macroscale, spatially distributed hydrological model, the Variable Infiltration Capacity (VIC) model [56], to simulate runoff. Second, the runoff was used as an input into a river routing model, the Model for Scale Adaptive River Transport (MOSART) [55], dynamically coupled to a spatially distributed water management model (WM) [115], to simulate reservoir storage and regulated streamflow. Third, surface meteorological data and simulated hydrologic conditions are used to simulate regulated river temperatures, using a one-dimensional stream temperature model, the River Basin Model (RBM) [116], coupled with a two-layer reservoir thermal stratification module [73]. We ran these models at a grid resolution of 1/8 degree ($\sim$ 12 km) using the climate forcing data from twenty different GCMs from the Coupled Model Intercomparison Project 5 [93], spatially downscaled using the MACA method [2].

3.2.4 Electricity demand

We used an econometric model to estimate the projections of SERC's electricity hourly demand in future years under different climate change scenarios [79]. To fit this model, we used historical hourly electricity demand data of the utilities within our study area im-

ported from the Federal Energy Regulatory Commission (FERC) Form 714 [33] for the years 2006–2015. We also used weather data from the University of Idaho Gridded Surface Meteorological Data (gridMET) dataset [1]. This dataset combines desirable spatial attributes of gridded climate data from the PRISM dataset [78, 26] with desirable temporal attributes from the regional reanalysis dataset NLDAS-2 [71] to derive a high-resolution (1/24th degree, ∼4 km) gridded dataset of daily surface meteorological variables. This dataset has been validated by its authors against an extensive network of weather stations. Then, we disaggregate the daily data to hourly values using METSIM (Meteorology Simulator) [13]. After the parameters of the model were defined, we used projections of daily air temperature of twenty different Global Circulation Models (GCM) from the Coupled Model Intercomparison Project 5 [93], spatially downscaled using the Multivariate Adaptive Constructed Analogs (MACA) method [2]. In addition, we again disaggregated these daily projections to hourly values using METSIM [13]. For each of the four subregions in SERC considered in this study, we used hourly air temperature from the two most populous cities and compute their mean.

Note that we used the gridMET dataset for climate data between 2006 and 2015 to fit our regression model because this is the same dataset used in the training phase of the MACA method used to downscale projections of future climate. Therefore, our baseline meteorological data was coherent with our projected weather variables from the downscaled GCMs. This way we avoided potential biases between the data generated by the climate model and the historical data used as a baseline to fit the regression model [7, 6].

The econometric model used a piece-wise linear function to represent the non-linear relationship between electricity consumption and temperature [65]. This formulation enforced continuity on the breakpoints of the piece-wise linear curve. To control for unobserved factors affecting electricity demand in each hour of the day, the model included fixed effects coefficients for each hour of the day in different seasons and different types of day (work-

day or weekend). Annual long-term trends were modeled using fixed-effects for each year in the historical data set. This way the model was capable of controlling for changes in the demand in electricity caused by economic and technological shifts in our historical dataset. Since our goal was to study the impacts that predicted changes in climate trends can have on electricity demand, we created our simulations of future electricity demand under the assumption that other factors that could influence electricity demand (such as economic activity and population growth) would remain constant. For example, we used the estimated value of the annual fixed-effect for 2015 (γ_{2015}) in our simulations of future electricity demand.

Figure 3.5 shows the estimated response functions of hourly electricity demand to temperature. Each plot presents the response function of one of the load zones considered in this study. These response functions and the other fixed-affects parameters of our regression models are used to simulate future values of electricity demand under the climate change conditions simulated by the twenty different climate models.

3.2.5 Technical and economic parameters of candidates technologies

In order to be able to analyze how climate change can impact the decisions to expand the generator fleet, we need economic and technical specifications of different types of candidate power plants. These details were used by the optimization model to choose the configuration of the power plant fleet that minimizes the sum of fixed and variables costs while satisfying the operating and system constraints included in our model.

We used the technical and economic parameters detailed on the NREL Annual Technology Baseline (ATB) [51]. ATB is a freely available database compiled by NREL that provides technology-specific cost and performance parameters such as capital expenditures

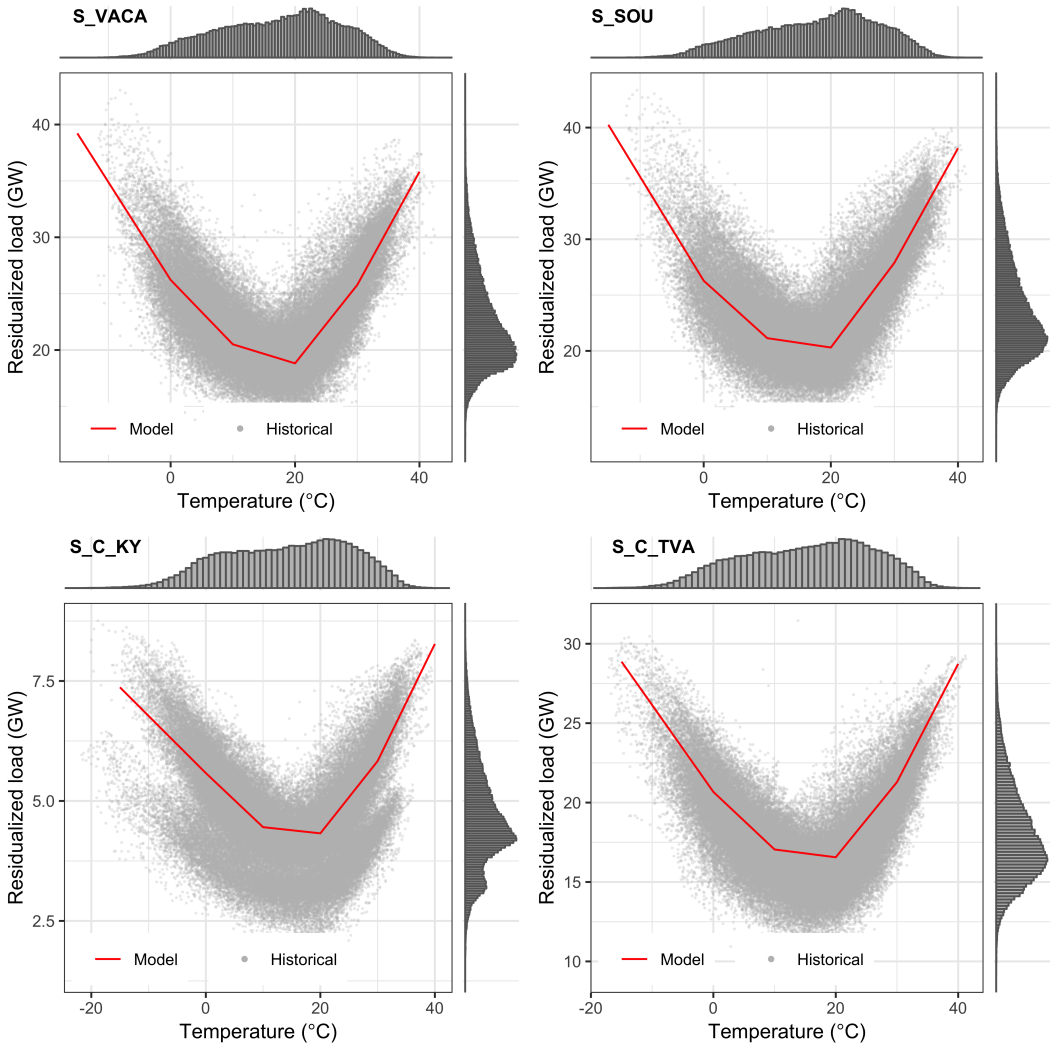

Figure 3.5: Estimated hourly electricity demand temperature response function. The gray dots represent the historical values (2006-2015) of hourly temperature and residualized electricity demand (temperature dependent). The red solid line is the average response curve according to our estimated model. To compute the residualized electricity demand we subtract our estimated values of the fixed-effects α_{hds} and γ_a (but not the intercept β_0) from the observed values of hourly demand. The histograms at the top and at the right of the panel display the observed distribution of the variable on the respective axis.

(CAPEX), operations and maintenance (O&M) costs, and capacity factor estimates. These estimates are put together for a range of resource characteristics, sites, or fuel price assumptions for electricity generation technologies both at present and with projections through 2050. Capex values include estimated overnight capital costs and financing costs, and thus account for construction duration of different technologies.

Table 3.1: Technical and economic parameters of candidate plants (Source: ATB)

Type	CAPEX ($/kW)	Fixed O&M ($/kW-year)	Fuel Costs ($/MWh)	Var. O&M ($/MWh)
Coal-CCS 90%	5,941	78.99	25.00	9.33
Coal	3,882	31.95	18.62	4.58
Gas-CC	1,036	10.20	18.24	2.67
Gas-CC-CCS	2,162	32.47	21.24	6.93
Nuclear	6,049	97.44	6.50	2.23
Wind	1,532	50.42	0.00	0.00
Solar PV	1,746	13.78	0.00	0.00

The capex values in Table 3.1 do not take into account potential tax credits and other financial incentives. In our model we included the financial incentives given to renewable technologies under the Business Energy Investment Tax Credit (ITC) [89]. The ITC offers different levels of tax credits over capital expenditures for several types of renewable generation such as wind and solar generators. For wind generators, the tax credit expires in 2020. Values of the tax credit between 2016 and 2019 average around approximately 21% of investment values. For solar generators, the tax credits decreases to 10% after 2020, but do not expire. In our model, we updated the investment costs of new solar and wind generators in order to take into account these financial incentives.

The values shown in Table 3.1 are specifically for investments in these types of generators in 2016. The ATB also projects how these costs evolve over future years (in constant monetary values). These changes in future investment costs try to capture typical cost reductions resulting from expected improvements in the technology. Figures 3.6 – 3.9 show the projected change in values of capex, fixed O&M, variable O&M, and fuel costs for each of the technologies considered in this work, according the ATB database. Note that capex values do not account for the ITC tax credits discussed above.

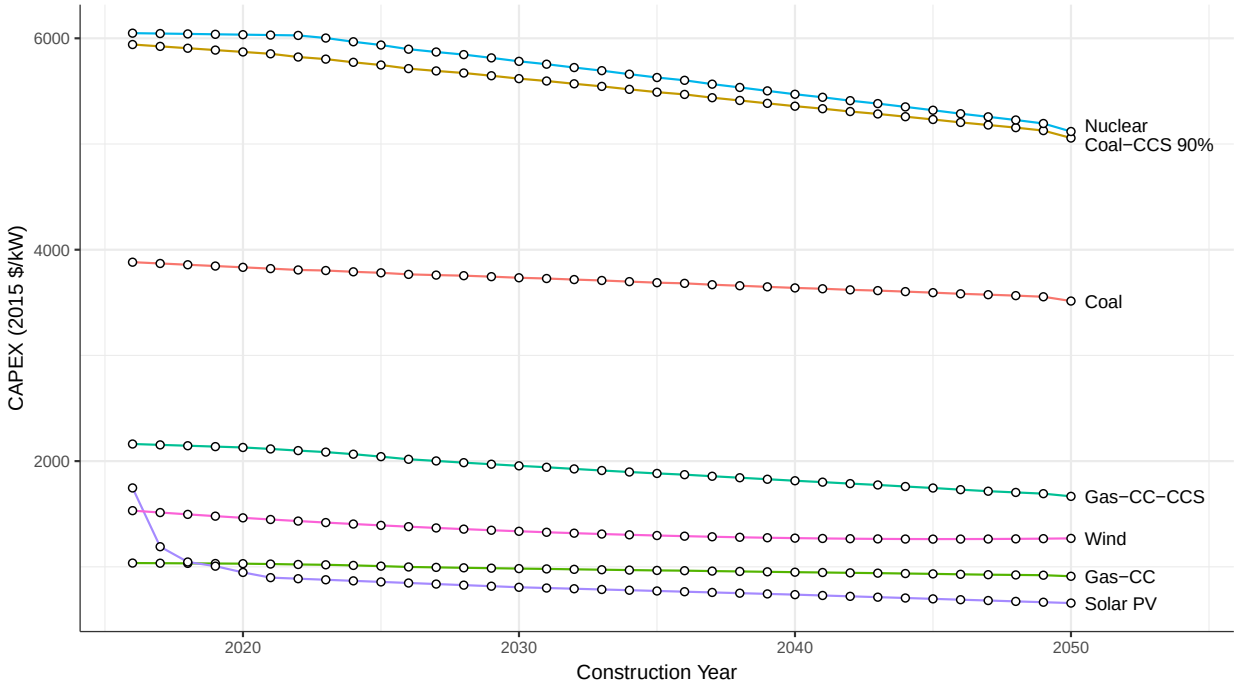

Figure 3.6: Projection of CAPEX values (in 2015 $/kW) for different candidate technologies. The values in this plot do not take into account ITC tax credits. (Source: ATB)

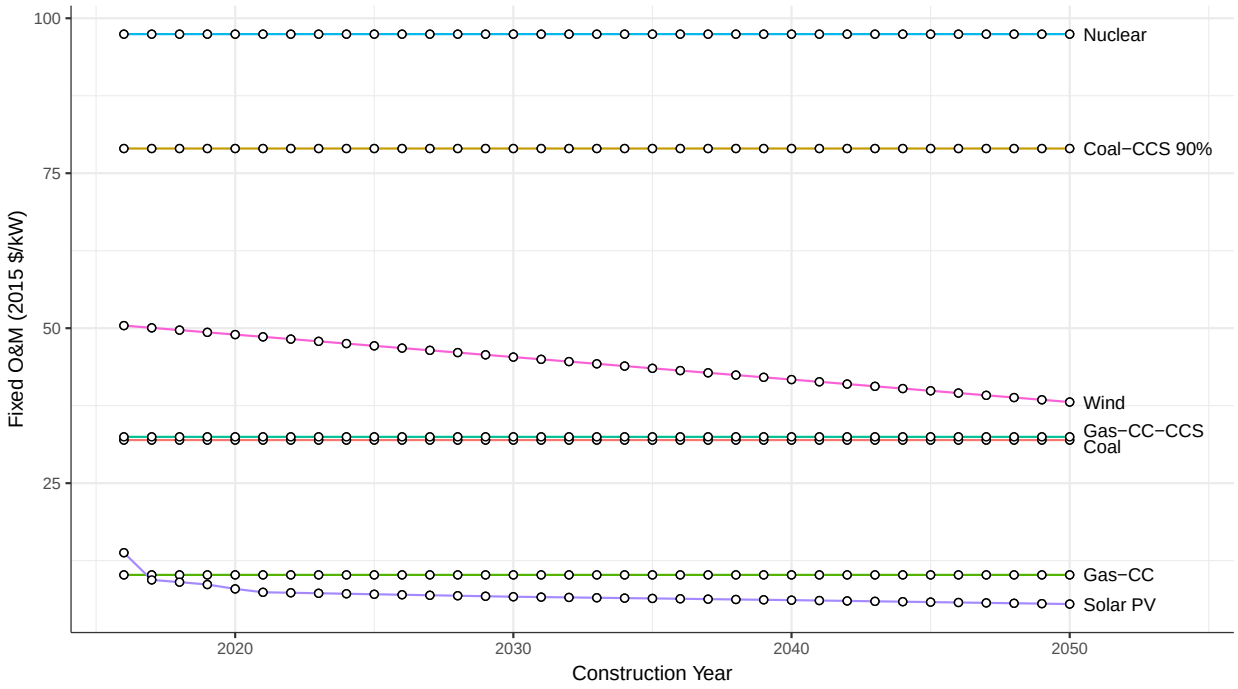

Figure 3.7: Projection of fixed O&M values (in 2015 $/kW-year) for different candidate technologies. (Source: ATB)

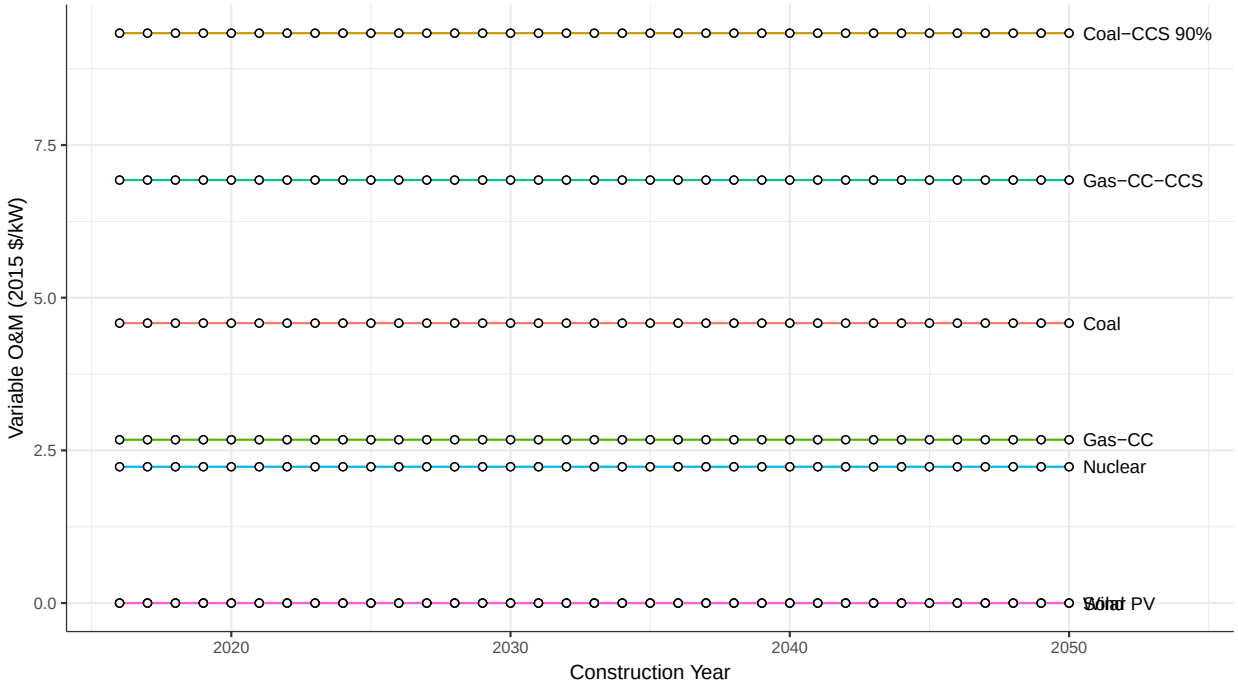

Figure 3.8: Projection of variable O&M values (in 2015 $/MWh) for different candidate technologies. (Source: ATB)

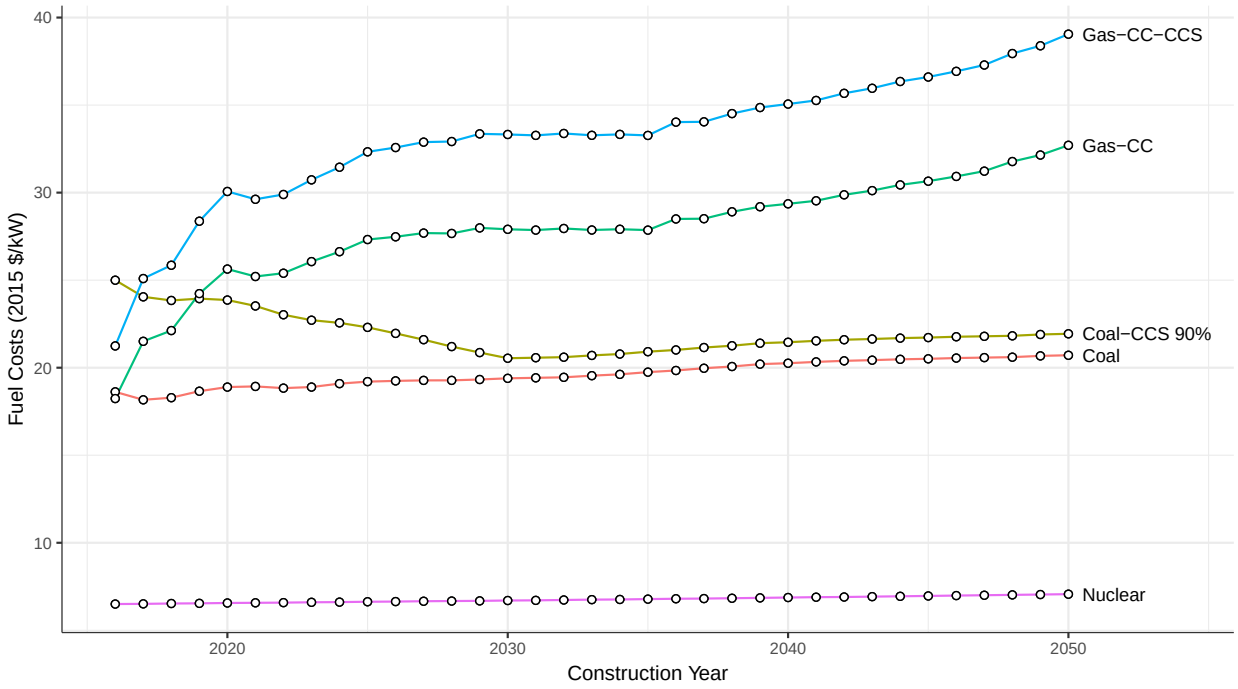

Figure 3.9: Projection of fuel costs values (in 2015 $/MWh) for different candidate technologies. (Source: ATB)

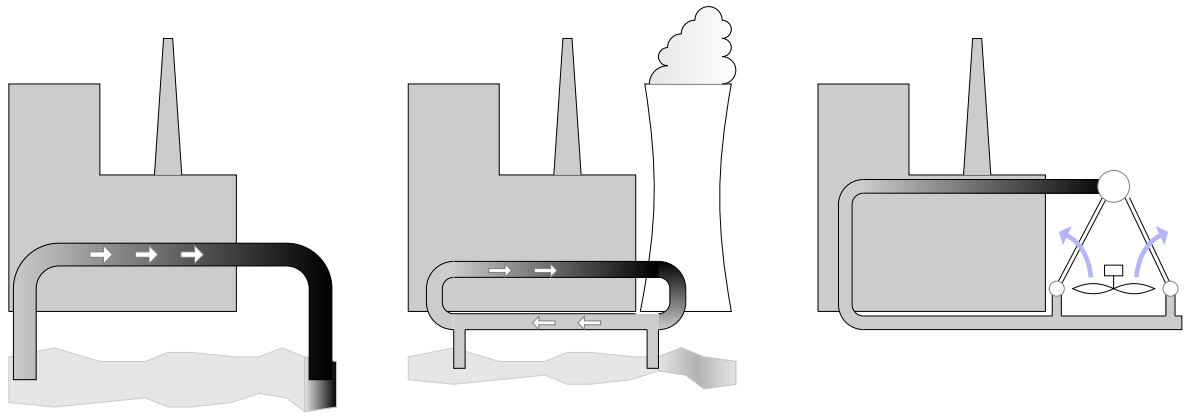

(a) Once through cooling (b) Recirculating cooling (c) Dry cooling

Figure 3.10: Types of cooling technologies (adapted from Koch and Vögele [49])

Another dimension of our analysis were the different cooling technologies that can be used by thermal generators. In our work we focused on three types of cooling technologies: once-through cooling, recirculating cooling, and dry cooling, as illustrated in Figure 3.10. Once-through cooling systems (Figure 3.10a) operate by continuously withdrawing large quantities of water from a (usually) large water source (such as a river or a lake), use this water to absorb heat from exhaust steam, and subsequently discharge this higher temperature water to the environment. The net consumption of water is considered negligible. In recirculating cooling systems (Figure 3.10b), the water is recirculated to the condenser after it has been cooled in a cooling tower that lowers the water temperature mainly due to evaporation of water in contact with ambient air. This type of cooling system minimizes the withdrawal of water from the water bodies and avoids discharges of highly heated water back into them. Finally, dry-cooling systems (Figure 3.10c) use the sensible heating of atmospheric air passed across finned-tube heat exchangers to reject the heat from condensing steam [118, 119, 58].

The choice of the different cooling systems can have important consequences for the operation of power plants. Once-through systems need large volumes of water withdrawls to operate their cooling systems. In times of drought or high water temperature, these sys-

tems may not have enough resources in order to properly lower the temperature of the exhaust heat. This could result in loss of efficiency. Moreover, because once-through cooling systems typically discharge large volumes of high temperature water back into the environment, they could have negative impacts on aquatic ecosystems, including fish kills in certain ecosystems and impacts on species diversity. The U.S. Environmental Protection Agency (EPA) and a majority of states in the U.S. have environmental regulations regarding water temperature standards that apply to the operation of thermal power plants. If the operation of a power plant results in a violation of these standards, the plant may be required to curtail its generation.

Recirculating and dry-cooling plants can suffer from unfavorable ambient conditions. High air temperatures and high humidity could reduce the capacity of the evaporation process, which could result in efficiency losses. Moreover, compared to once through systems, these recirculating and dry-cooling typically have higher capacity and operating expenses, and lower efficiency rates [66].

To represent the additional costs of different cooling systems we used the Integrated Environmental Control Model (IECM), previously developed at Carnegie Mellon University [17, 119, 57]. This model outputs plant performance characteristics and costs for different combinations of power plant technologies and cooling systems. Since the ATB data does not have cooling technologies specifications, we made the assumption that those values are associated with once-through cooling systems (which is the least expensive one). For the other two cooling systems, we computed the differences in the IECM's output with respect to the once-trough system and applied this difference to the ATB values. We did this for Coal Steam and Combined Cycle Natural Gas (with and without CCS), since these are the power plant technologies currently modeled in IECM.

Table 3.2: Summary of IECM outputs for Coal Steam and CCNG power plants. The values shown in this table are the differences in the IECM outputs of each variable with respect to a power plant of the same type using once-through cooling. Values were compiled using IECM Version 11.2.

Performance and costs	Coal	Coal CCS	NGCC	NGCC CCS
Δ Total capital requirement (2015 $/kW)				
Recirculating	87.82	143.82	47.83	79.26
Dry-cooling	295.76	243.12	138.41	92.59
Δ Fixed O&M (2015 M$/yr)				
Recirculating	1.57	2.03	1.07	1.30
Dry-cooling	3.70	2.97	2.21	1.70
Δ net plant efficiency (%)				
Recirculating	0.91	2.95	0.62	1.38
Dry-cooling	4.91	5.56	2.10	1.91

3.2.6 Wind & solar generation data

In order to capture spatial and temporal variability in output among wind and solar farms, we set upper bounds to the hourly generation of wind and solar power plants equal to simulated wind and solar generation profiles from the U.S. National Renewable Energy Laboratory (NREL) [109, 30]. These wind and solar generation databases provide simulated generation profiles for hypothetical plants in the SERC area at 5-minute increments, for 2007–2012 and 2006, respectively. We used 2009 wind generation data, since the overall simulated capacity factor (CF) in this year was closer to the average over the complete dataset. We aggregated generation data to hourly increments by calculating the average generation values for all time steps in each hour. After excluding several solar plants with no generation data, hourly capacity factors for hypothetical wind and solar plants in SERC in the NREL dataset ranged from 17%–55% and 12%–19%, respectively.

For existing wind units in the CE model, we calculated the installed capacity of wind in our initial fleet, and added wind farms from the NREL dataset to our fleet in order of decreasing capacity factor. Note that existing wind units in each CE model run included wind units added in previous CE runs. For instance, a wind unit added in the 2020 CE run is considered an existing wind unit in the 2025 CE simulation. We performed the same process for existing solar units. Since we did not account for transmission within each of the four SERC subregions in our CE model, each existing wind and solar unit varied only by capacity and hourly generation profile within each subregion. As such, in order to improve the computational efficiency of the model, we combined existing wind and solar units into single equivalent wind and solar units by summing up their capacities and hourly generation profiles.

Similarly, in order to maintain computational tractability, rather than inputting numerous small potential new wind and solar units with unique generation profiles to the CE model, we instead determined capacity additions for blocks of size 1 GW of representative wind units and representative solar units in the CE model. These blocks of representative units each had an hourly generation profile. To determine the generation profiles, we estimated capacity-weighted generation profiles for assumed capacities of wind and solar incremental to the existing capacities of wind and solar.

We set these assumed capacities equal to 1 GW in order to balance two competing factors: first, the generation profile should represent marginal investment in wind and solar, i.e. the next MW of additional wind and solar, but second, the CE model runs in 5-year intervals, so wind and solar investment in each period will be on the order of gigawatts. To calculate the generation profiles for 1 GW of incremental wind and solar capacities, first we temporarily removed wind and solar farms from the NREL datasets with a combined capacity equal to the existing fleet capacity in order of decreasing capacity factor. From the remaining wind and solar farms in the NREL datasets, we obtained hourly generation

profiles for 1 GW of wind and solar in order of decreasing capacity factor, then calculated the capacity-weighted average hourly generation profile for those generators. As discussed above, once wind or solar capacity were added by an annual step of the CE model, that wind and solar capacity was treated as "existing" capacity in subsequent CE simulations. Consequently, that added wind and solar capacity was assigned a generation profile in future CE runs following the process described previously in this paragraph.

Note that it is possible that in some scenarios, installed wind and/or solar capacities ultimately exceeded total capacity in the NREL databases. In those cases, we could not obtain generation profiles for additional wind and/or solar capacity for the CE model from the NREL databases, as no wind and/or solar capacities incremental to existing wind and solar capacities exists in the NREL databases. Therefore, in these cases, we estimated generation profiles for additional wind and/or solar capacities as the capacity-weighted generation profiles of the least efficient (lowest annual CF) block of wind and/or solar units.

Figure 3.11 illustrates some characteristics of our dataset of solar sites in SERC. Figure 3.11a shows the distribution of annual capacity factors over the complete dataset of solar sites. The best solar sites have an annual capacity factor close to 20%, while the worst sites have one around 13%. The average capacity factor of the solar dataset is approximately 16%. Figure 3.11b presents the average hourly capacity factors of the solar sites. We plot the average hourly capacity factors for both the complete year and the summer period. The summer capacity factors are relevant because in our simulations, thermal power plants experience a reduction in their available capacity mainly during summertime. In other seasons, the reduction in the capacity to generate electricity is not significant. Therefore it is important to understand how other energy sources are able to complement the scaling down of thermal capacity. As expected, the hourly generation profile of solar sites in summertime is greater than during the rest of the year.

Figure 3.12 illustrates some characteristics of our dataset of wind sites in SERC. Figure

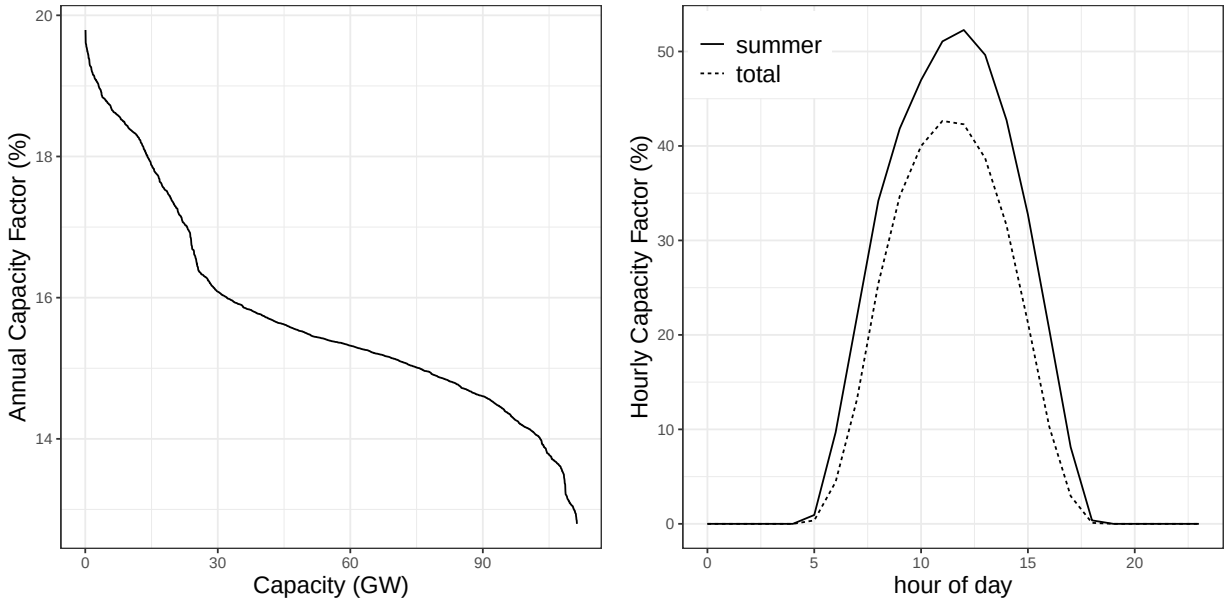

(a) (b)

Figure 3.11: Characteristics of SERC's solar sites dataset. (a) shows the distribution of annual capacity factors over the complete dataset of solar sites (b) presents the average hourly capacity factors of the solar sites

3.12a shows the distribution of annual capacity factors over the complete dataset of wind sites. The best wind sites have an annual capacity factor close to 55%, while the worst sites have one around 17%. The average capacity factor of the solar dataset is approximately 16%. Figure 3.12b presents the average hourly capacity factors of the wind sites. Again, we plot the average hourly capacity factors for both the complete year and the summer period in order to understand how new wind energy power plants are able to complement the summertime scaling down of thermal capacity due to climate change. In opposition to the behavior of solar sites, the hourly generation profile of wind sites during summertime is lower than the rest of the year.

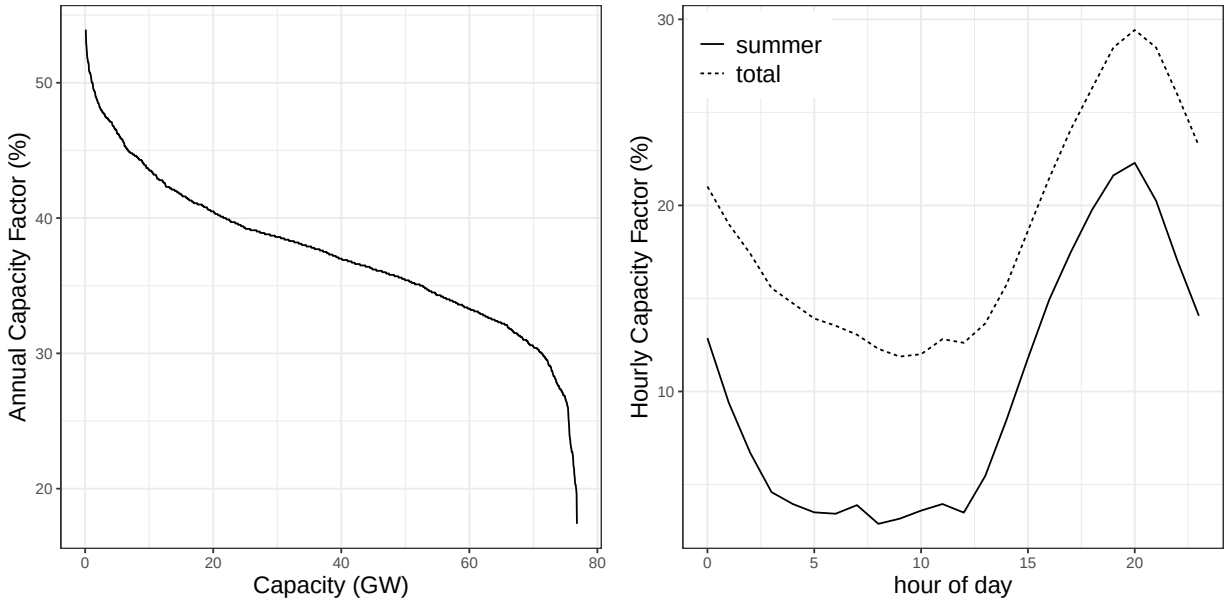

(a) (b)

Figure 3.12: Characteristics of SERC's wind sites dataset. (a) shows the distribution of annual capacity factors over the complete dataset of wind sites (b) presents the average hourly capacity factors of the wind sites

3.2.7 Capacity deratings of thermal generators

To simulate the effect of climate conditions on the operation of thermal power plants, we used results from the Integrated Environmental Control Model (IECM) to estimate operating curves for a variety of thermal power plant configurations under different meteorological and hydrological conditions [17]. IECM allows the user to configure power plants according to a variety of characteristics, including plant type, cooling technologies, boiler type, and coal ranks. IECM was ran with a set of weather conditions and configurations to observe the resulting operation characteristics including power plant efficiency, available power capacity, and water use intensities [57]. Then, linear regression models were used to fit response surfaces to this simulated data [57]. This way we obtained operating curves that represented how changes in meteorological and hydrological conditions due to climate change could affect the operating conditions of existing and future thermal power plants. In this analysis we included pulverized coal plants and natural gas combined cycle

(NGCC) plants with different types of cooling systems (once-through, recirculating cooling, and dry cooling). Because the IECM does not model nuclear power plants, we did not have response curves for this type of technology. Therefore, for nuclear power plants we did not simulate any weather related capacity reductions. However, we did simulate capacity reductions due to environmental regulations that control water quality in the rivers that feed cooling water to these nuclear power plants.

Figure 3.13 presents the estimated response functions of the available capacity of coal steam and NGCC power plants under different meteorological conditions. The three plots in the top row (a–c) show the response functions for coal steam with once-through cooling, coal steam with recirculating cooling, and coal steam with dry cooling. The three plots in the bottom row (d–f) show the response functions for NGCC with once-through cooling, NGCC with recirculating cooling, and NGCC with dry cooling.

Figure 3.14 presents the estimated response functions of the water withdrawal rate (in kgal/MWh) of coal steam and NGCC power plants under different meteorological conditions. The two plots in the top row (a–b) show the response functions for coal steam with once-through cooling, and coal steam with recirculating cooling. The two plots in the bottom row (c–d) show the response functions for NGCC with once-through cooling, and NGCC with recirculating cooling. As mentioned previously, the IECM does not model nuclear power plants. For these types of power plants we used a fixed water withdrawal rate according to figures reported in the literature [62]. This way we were able to simulate potential capacity reductions related to environmental regulations that control water quality.

In our simulation, we combined these response curves with the spatially gridded hourly projections of meteorological and hydrological variables mentioned in section 3.2.3. This resulted in time series of hourly projections of available capacity and water withdrawal rates for each existing and candidate power plant. We used the available capacities as upper bounds on the electricity generation of individual power plants in our capacity expan-

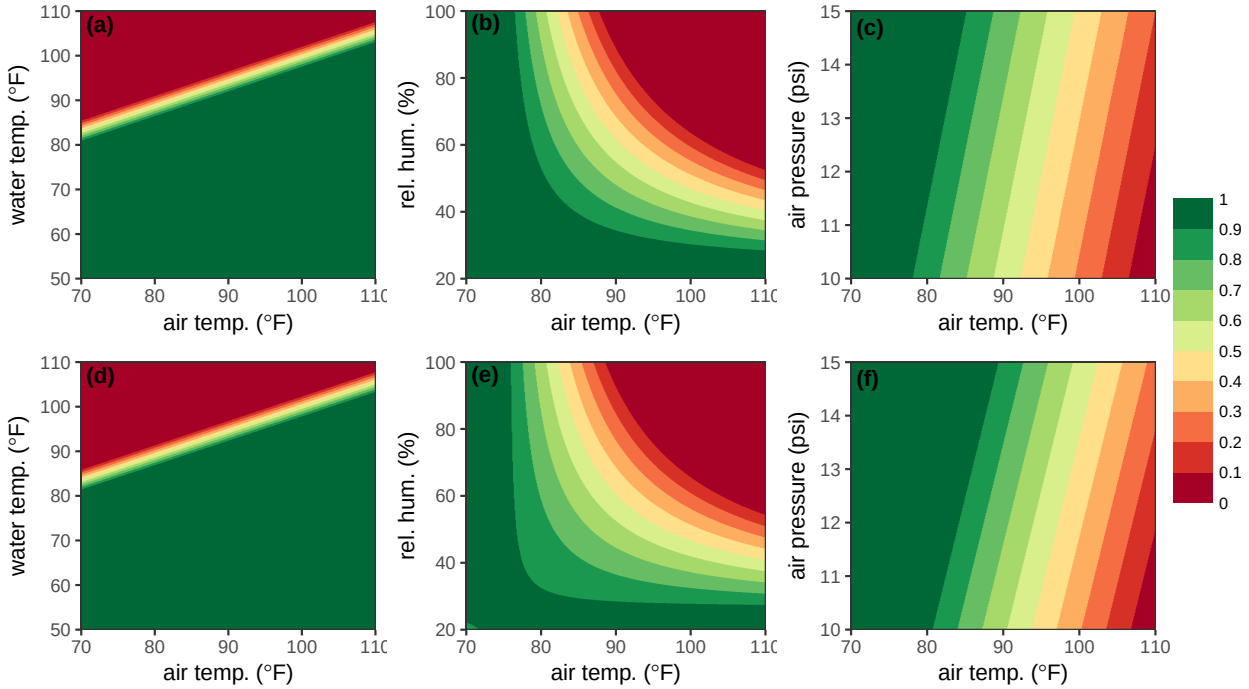

Figure 3.13: Estimated effect of meteorological conditions on the fraction of available capacity of different types of thermal power plants. (a) coal steam with once-through cooling (b) coal steam with recirculating cooling (c) coal steam with dry cooling (d) natural gas combined cycle with once-through cooling (e) natural gas combined cycle with recirculating cooling (f) natural gas combined cycle with dry cooling. (Adapted from Loew [57])

sion model.

For power plants using once-through cooling, we also simulated the effects of water quality regulations that govern the cooling water sources. Once-through cooling systems withdraw from a nearby large water body (such as rivers or lakes) and discharge the heated cooling water downstream in the same water body, after it leaves the condenser. This water discharged at high temperatures can result in negative impacts on aquatic ecosystems, including fish kills in certain ecosystems and impacts on species diversity [8, 28]. To minimize these environmental hazards, the U.S. Environmental Protection Agency (EPA) and state environmental agencies regulate cooling water systems and thermal discharges under the Clean Water Act [66]. Water quality standards differ by state, but they normally require surface water to remain under 32 °C [63]. If the water discharged by a power plant

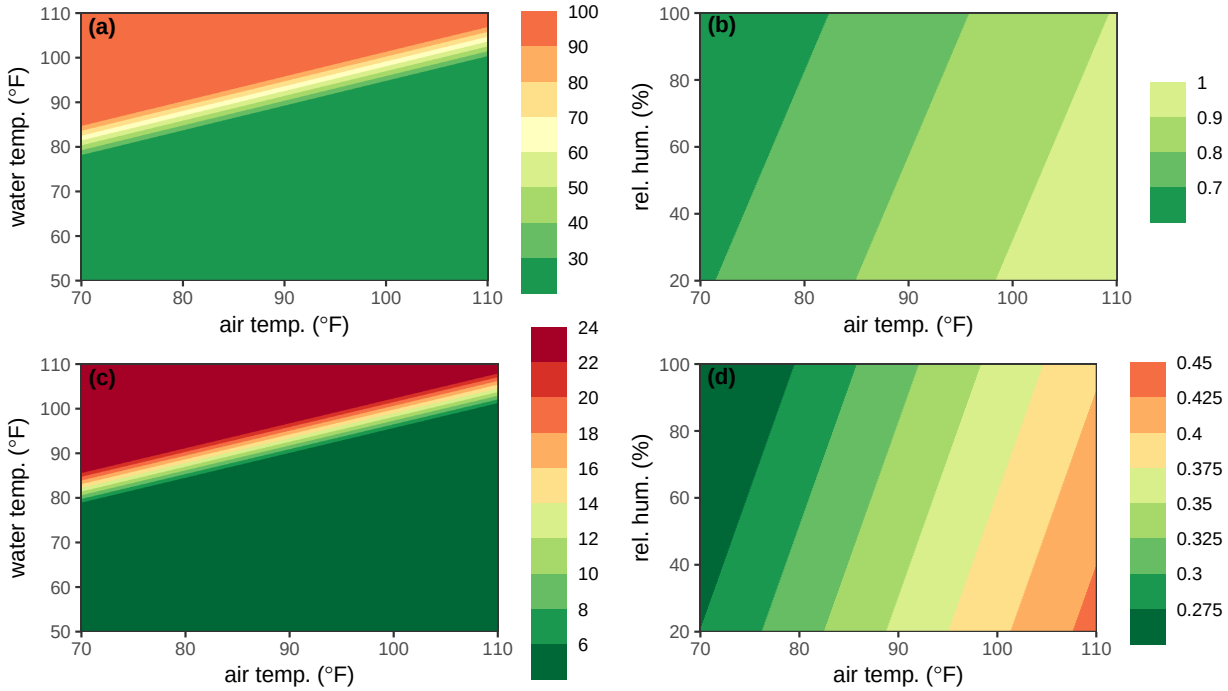

Figure 3.14: Estimated effect of meteorological conditions on the water withdrawal rate (in kgal/MWh) of different types of thermal power plants. (a) coal steam with once-through cooling (b) coal steam with once-through cooling (c) natural gas combined cycle with once-through cooling (d) natural gas combined cycle with recirculating cooling (Adapted from Loew [57])

causes stream temperatures to rise above this threshold, power plants could be forced to shut down or curtail their power generation[2].

We simulated operating constraints due to such environmental regulations on power plants using once-through cooling. We used a thermal balance equation to compute the final stream temperature after the mixing of the water from the river and the water discharged from the power plant.

$$T_x = \frac{\frac{m_g}{m_r} T_g + T_r}{\frac{m_g}{m_r} + 1} = T_r + \frac{\frac{m_g}{m_r}}{\frac{m_g}{m_r} + 1} \cdot \Delta T_g = T_r + \frac{m_g}{m_g + m_r} \cdot \Delta T_g \tag{3.1}$$

[2]According to McCall, Macknick, and Hillman [66], in practice the enforcing of the Clean Water Act varies on a case-to-case basis, and limits are not always adequately set or enforced to protect aquatic life. State regulators can issue thermal variances to individual power plants that allow these plants to exceed water quality limits.

where T_x is the final mixed stream temperature, m_g is the water flow of the power plant discharge, m_r is the upstream flow of the river, and T_r is the upstream stream temperature (before mixing, i.e. stream temperature in that cell). T_g is the temperature of the power plant discharge (which equals $T_r + \Delta T_g$). ΔT_g is the increase in temperature of cooling water through the condenser, which we assumed is a fixed value that depends on the condenser design.

To estimate the withdrawal/discharge flow from a power plant (m_g) we used the following equation:

$$m_g = \min\left(\gamma \cdot m_r, p \cdot f^{(i,\Delta T_g)}(\mathbf{x})\right) \tag{3.2}$$

where i indicates the type of power plant. $\mathbf{x}$ represents a vector with a values for a set of meteorological variables at the location of the power plant. $f^{(i,\Delta T_g)}(\mathbf{x})$ is the estimated regression function mapping the values of $\mathbf{x}$ to water intensity estimates (in gal/MWh) for a power plant of type i and design parameter ΔT_g (see Figure 3.14). p is the power output of the power plant (in MWh). γ indicates the maximum fraction of the river flow that can be extracted for cooling purposes.

Combining the two equations, we get:

$$T_x = T_r + \left(\frac{\min\left(\gamma \cdot m_r, p \cdot f^{(i,\Delta T_g)}(\mathbf{x})\right)}{\min\left(\gamma \cdot m_r, p \cdot f^{(i,\Delta T_g)}(\mathbf{x})\right) + m_r}\right) \cdot \Delta T_g \tag{3.3}$$

Our objective was to find the maximum value of p such that T_x is still less than the environmental limit. However, we can't analytically solve the above equation for p . Also, it does not explicitly account for environmental limits. However, given a mixed stream temperature T_x, we can compare that to the regulatory limit and determine whether the output of the power plant p needs to be curtailed.

Specifically, for each power plant, we iteratively tested a range of power output values be-

tween 0 and its maximum capacity and determined the maximum potential power output before mixed stream temperatures exceed regulatory limits. Using the same approach, we also simulated the environmental limit on the maximum fraction of the river flow that can be extracted for cooling purposes. If sufficient water was not available, then the available capacity of the plant was reduced accordingly.

3.2.8 Hydro potential data

To simulate the potential effects of climate change in the available hydro energy at power plants we combined historical data of hydro energy produced by the hydro power plants in the SERC region with the simulations of river flows from the VIC and MOSART-WM models. We assumed that the energy generated at each power plant is proportional to the water released by the hydro dam simulated by the hydrological models.

We used monthly historical hydro generation for the hydro power plants in our data set from 2003 to 2011 as reported by the Energy Information Agency (EIA). We used these values to compute twelve monthly reference average generation values ($\bar{g}_{i,m}$) for each hydro power plant i (where m is the month of the year, i.e. $m \in [1, 12]$).

Next we used the outputs from the VIC and MOSART-VM models to compute the adjustments in hydro power potential in the future. We used the period 1982 to 2011 as our control period. For each power plant i, we computed a factor $\lambda_{y,i}$ representing the ratio between the total annual water flow in year y ($w_{y,i}$) and the total average annual water flow in the complete control period (1982 to 2011) at the location of the power plant i, i.e.,

$$\lambda_{y,i} = \frac{w_{y,i}}{\sum_{y' \in [1982,2011]} w_{y',i}} \qquad y \in [2012, 2050] \tag{3.4}$$

Then, the estimated potential of hydro energy generation at power plant i in future month

m and year y is defined as

$$P^{(H)}_{i,m,y} = \eta_{y,i} \times \bar{g}_{i,m} \qquad m \in [1,12], y \in [2012, 2050] \tag{3.5}$$

The values of $P^{(H)}_{i,m,y}$ represent hydro energy *potential* at the site of power plant i, and not estimated hydro generation by this power plant. Within the optimization model, the actual generation decision for each hydro generator is limited by both this potential and the installed capacity of the power plant.

3.2.9 Cap on CO_2 emissions

We analyzed how the implementation of CO_2 emission caps on the power sector would affect the investment decisions of our model. These limits on emissions were represented in our optimization model as constraints that could be considered or not in our simulations (see Appendix E). To simulate the scenarios with CO_2 limits, we used a carbon emission target of 50% reduction by 2050. This target would be consistent with 2 °C stabilization pathway, as reported by the IPCC [45]. We used the reference year in our study (2015) and the final year (2050) to derive the reduction goals. To define the reference emissions in 2015 in our simulation, we ran the economic dispatch simulation in our CE model in 2015 to compute estimated generation of the existing fleet. To define electricity demand values for this simulation, we used the reference case (no climate change). Next we used emission factors for each generator in the fleet (imported from the eGrid model – see section 3.2.2) to compute a reference carbon pollution value in 2015. This resulted in a total carbon emissions amount of approximately 390 million metric tons of CO_2. We used this as our reference emissions value for 2015. Finally, we applied the 50% reduction level over this estimated 2015 reference emission level. We applied a linear interpolation to define emission limit values for the years between 2015 and 2050.

3.3 Results

We ran the CE model in five year increments between 2015 and 2050. In each iteration, the model selected what plant types to build to minimize total annualized system cost. Specifically, the model had the choice to build wind, solar, coal steam, coal steam with carbon capture and sequestration (CCS), combined cycle natural gas, combined cycle natural gas with CCS, and nuclear power plants. New coal and natural gas plants could use recirculating or dry cooling systems. Although we account for existing hydropower facilities, our analysis did not include hydropower plants as a candidate technology. Investment in hydropower plants has been minimal in the last few decades [98] and available resources for new hydro plants in our study area (the southeast U.S.) are limited [101].

To evaluate the effect of climate on investment decisions, we simulated three different future scenarios: a reference scenario (where climate conditions are assumed to be the same as historical until 2050), a scenario where climate conditions follow Representative Concentration Pathway (RCP) 4.5, and a scenario where climate conditions follow RCP 8.5. In the reference scenario, we included simulations of electricity demand created using historical meteorological conditions. However, we did not account for capacity deratings for thermal power plants. For the two future scenarios assuming climate change (RCP 4.5 and RCP 8.5), we used our estimates of electricity demand, hydro generation potential, and thermoelectric available capacity estimated using projections of meteorological variables from the GCMs. To account for the intrinsic inter-annual variability among the twenty different GCMs and mantain computational tractability, we included three different climate simulations in the optimization step of our model. We sampled the output of three among the twenty GCMs that represented the 20%, 50%, and 80% quantile values from the distribution of system-wide peak demand. We selected peak demand as a descriptive metric because the electricity grid tends to be designed for maximum load days [6]. In the reference scenario we sampled the three quantile values from the distribution of system-wide

peak demand estimated using our historical dataset (more details in appendixes D and E).

Figures 3.15a – 3.15b present the projected distributions of electricity consumption and peak demand, respectively. In this analysis, we assumed that other factors that could affect our projections of demand (such as changes in economic activity and population) remained constant at their estimated 2015 levels. This way, we were able to isolate the impacts of climate change on electricity demand. Figures 3.15a – 3.15b show that, by 2050, annual electricity consumption and annual peak demand could increase by 3% and 16%,respectively, when compared to the reference case. These values are comparable to results found by previous studies [6, 79].

Figure 3.16 displays the distributions during summertime of the simulated daily available capacity of four different existing thermal power plants using RCP 8.5. We show the results for these four power plants to exemplify the simulated impacts on different types of thermal generators. These four power plants include coal steam with once-through cooling (Hammond), coal steam with recirculating cooling (Ghent), natural gas combined cycle with recirculating cooling (Richmond), and natural gas combined cycle with dry cooling (Choctaw). The figure shows an overall trend of decreasing available capacity for thermal power plants with once-through cooling and recirculating cooling. According to these results, natural gas combined cycle power plants with dry cooling experienced no climate-induced capacity deratings. Figure 3.6 plots the projected values of capacity investment costs for the different technologies considered in our study as potential candidates for adding new capacity to the system in the future.

Figure 3.17 presents the results of the capacity expansion simulations without enforcing carbon emission limits in the generator fleet. Figures 3.17a – 3.17c plot the resulting generator fleet in 2050 for the three scenarios (reference, RCP 4.5, and RCP 8.5). These figures show that including climate constraints in the planning process would result in capacity investments that are roughly 40% higher than in the reference scenario. Increased peak

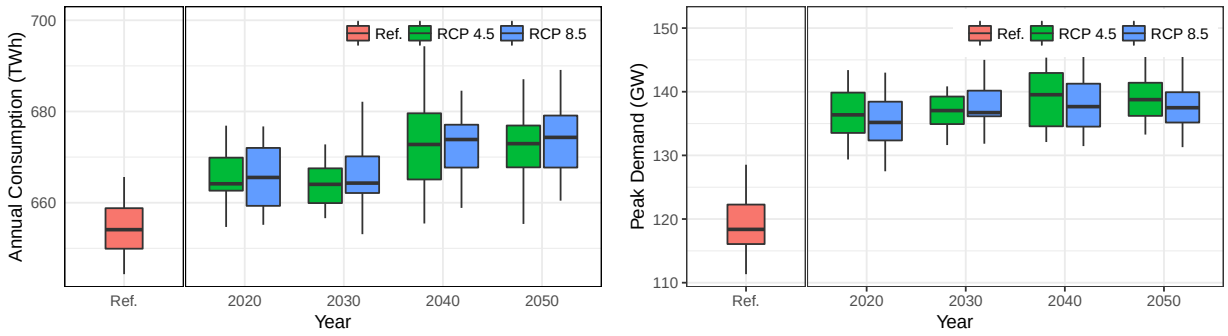

(a) (b)

Figure 3.15: Distributions of simulated future electricity demand under climate change (a) shows the distribution of simulated annual electricity consumption in (TWh/year) using all twenty GCMs for RCP 4.5 and RCP 8.5. (b) shows the distribution of simulated annual peak electricity demand using all twenty GCMs for RCP 4.5 and RCP 8.5. Values of future electricity demand are simulated under the assumption that other factors that could influence electricity demand (such as economic activity and population growth) remain constant.

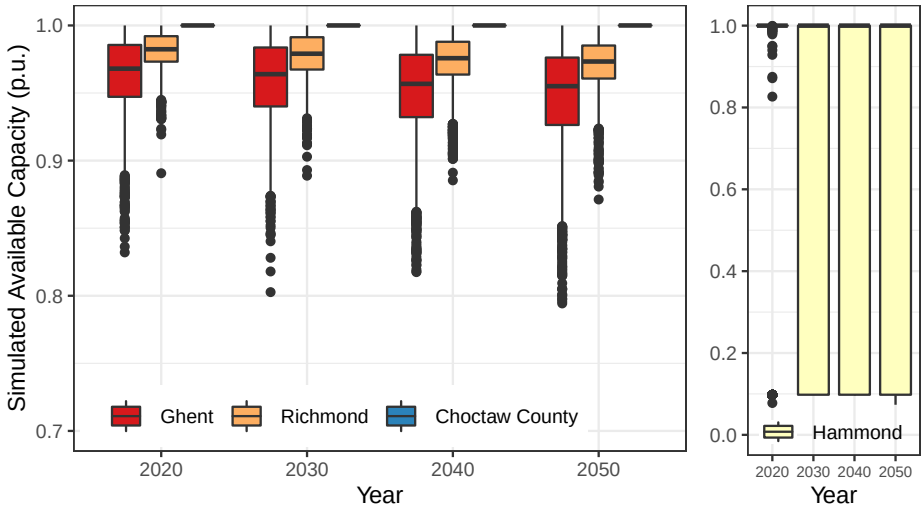

Figure 3.16: Distribution of the simulated summer time daily available capacity of four different existing thermal power plants. The types of power plants include coal steam with once-through cooling (Hammond), coal steam with recirculating cooling (Ghent), natural gas with recirculating cooling (Richmond), and natural gas with dry cooling (Choctaw). To simplify the figure we only show the available capacities simulated using RCP 8.5.

electricity demand and decreased available capacity from thermal generators under climate change drive the requirement for higher installed capacity for the entire fleet. Figure 3.17a shows that in the reference case (which does not account for future climate constraints),

natural gas plants, wind power, and solar power accounted for 69 GW, 24 GW, and 12 GW in 2050, respectively (48%, 17%, and 8% of total installed capacity, respectively). Due to plant decommissioning at the end of their life and high investment costs, coal accounted for just 9 GW (6% of total installed capacity) in 2050 in this reference scenario. These changes in coal-based capacity represent a considerable reduction compared to 2015, when coal accounted for 55 GW (32% of installed capacity, see section 3.2.2).

Including climate change constraints in the planning model changes the composition of the available power plant fleet in 2050, as shown in Figures 3.17b – 3.17c. Climate constraints resulted in capacity deratings in natural gas plants, so the capacity expansion model compensates by building more wind and solar than in the reference scenario. By 2050, assuming RCP 4.5 and RCP 8.5, wind and solar account for 38% – 41% of total capacity relative to 25% in the reference scenario.

The results for solar are worth noting. Solar capacity increased from 12 GW (8% of total capacity) in the reference case to 57 – 65 GW (29% – 33% of total capacity) in the cases with climate change. Unlike wind, solar power plants in the simulations typically have high energy output during the summer (see Figure 3.11), which coincides with high thermal generator deratings due to high air and water temperatures. Therefore, this surplus summertime solar generation helps the system to offset part of the climate-induced losses in thermal capacity. This characteristic of solar generation in summertime makes them more economically attractive when we include summertime reductions in thermal capacity due to climate change.

Finally, although we found that thermal power plants with dry cooling did not experience major reductions in their capacity due to climate change (see Figure 3.16), these plants are more expensive than plants with recirculating cooling. As a result natural gas additions in the simulations are in the form of plants with recirculating cooling.

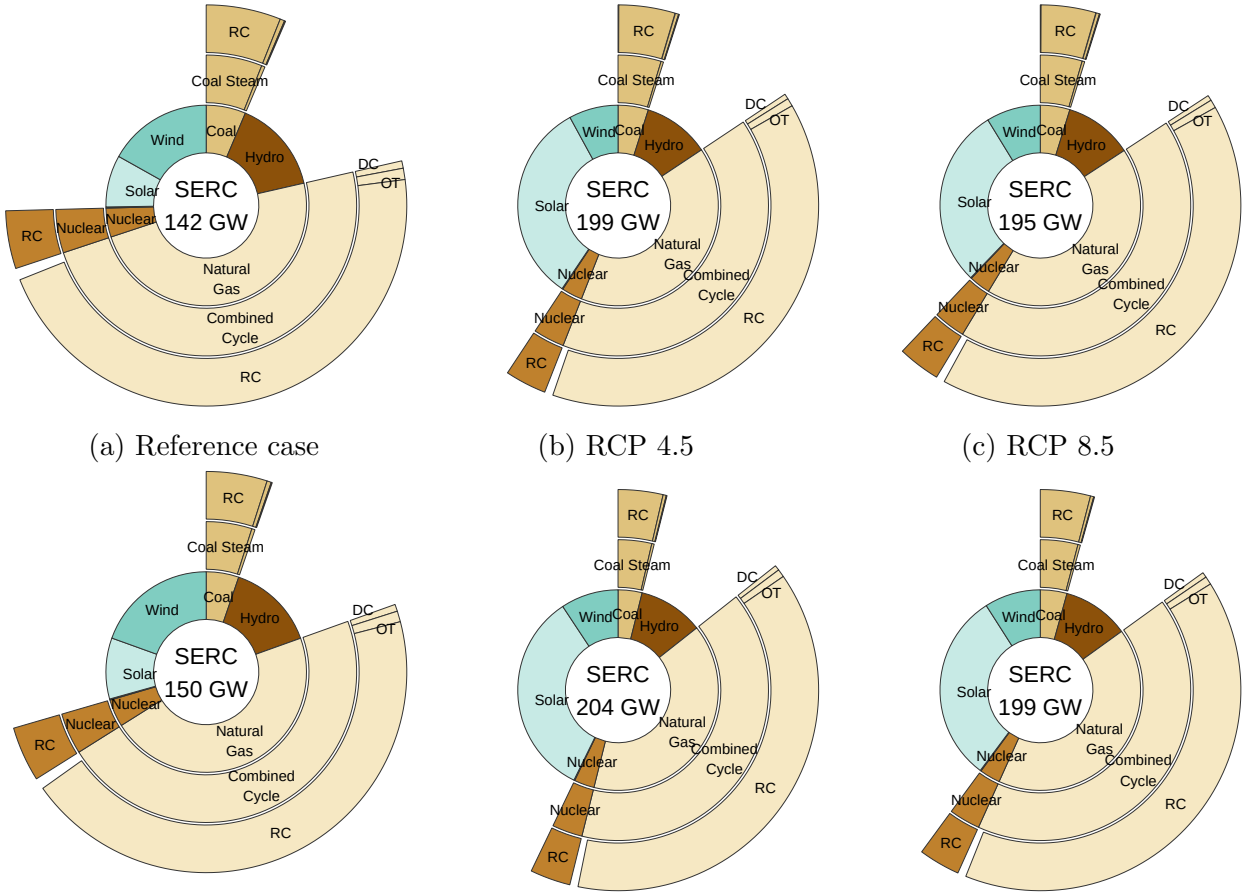

(a) Reference case

(b) RCP 4.5

(c) RCP 8.5

(d) Reference case with CO_2 limits

(e) RCP 4.5 with CO_2 limits

(f) RCP 8.5 with CO_2 limits

Figure 3.17: Final composition of SERC's generator fleet in 2050 for each of the three scenarios (Reference, RCP 4.5, and RCP 8.5). (a) – (c) are simulated without considering any constraints on CO_2 emissions. (d) – (f) are simulated assuming limits on system-wide CO_2 emissions. The numbers in the center of each plot show the total installed capacity in 2050. The inner layer of the pie chart shows the breakdown into the different fuel sources used by the power plants in SERC. The middle layer shows the types of generating technologies – where applicable – used for each type of fuel source. The outer layer presents the cooling technologies used in the respective thermoelectric generators. The codes "OT", "RC", and "DC" stand for, respectively: once-through cooling, recirculating cooling, and dry cooling.

We also simulated scenarios with a 50% reduction in total carbon emissions from power generation in SERC by 2050 compared to 2015. This constraint is consistent with IPCC's mitigation levels needed to reach 2 °C stabilization targets [45]. We assumed that emission caps decrease linearly in the years between 2015 and 2050. Figures 3.17d–3.17f show the results of the simulations of the three climate scenarios considering these CO_2 emission constraints. Results are similar to the ones without carbon emission caps. In the scenarios without carbon emission limits, CO_2 emissions had already decreased substantially because of the scheduled retirement of old coal power plants and the high costs of investing in new coal power plants. However, in order to achieve the 50% target, the CE model had to further invest in renewables in these scenarios. This resulted in a higher total installed capacity and higher participation of renewables.

In the reference case, the total installed capacity increased by 5% compared to the results without carbon constraints. The simulations for the RCP 4.5 and RCP 8.5 scenarios with carbon constraints resulted in capacity requirements approximately 2% higher, compared to the simulations without carbon constraints. Increased capacity requirements are largely the result of increased use of solar and wind power, which account for 40%–42% of the total installed capacity in 2050. Because wind and solar typically have smaller capacity factors, total installed capacity in these cases is greater than the ones without carbon emission limits. Table 3.3 reports the breakdown of the total installed capacity of the generator fleet in 2050 in each scenario simulated. Numbers in parentheses are the percentage of total capacity for each type of power plant.

The differences in the composition of the generator fleet in 2050 translate into changes in the levels of fixed investment costs needed to implement such portfolios. In the reference case, there was an addition of 73 GW of new capacity, most of it from natural gas plants (52%). This represented a total investment in the order of $ 76 billion (USD 2015). In cases including potential effects from climate change, there was an addition of 126 – 130

Table 3.3: Installed capacity of each plant type (in GW) in 2050 for each of the three scenarios (Reference, RCP 4.5, and RCP 8.5)

	With emission limits*			Without emission limits		
	Reference	RCP 4.5	RCP 8.5	Reference	RCP 4.5	RCP 8.5
Coal	7.9 (5%)	7.9 (4%)	8.6 (4%)	9.1 (6%)	9.7 (5%)	9.3 (5%)
Hydro	21.4 (14%)	21.4 (10%)	21.4 (11%)	21.4 (15%)	21.4 (11%)	21.4 (11%)
Natural Gas	69.9 (47%)	80.7 (40%)	83.1 (42%)	69.1 (48%)	80.3 (40%)	83.5 (43%)
Nuclear	6.6 (4%)	6.6 (3%)	6.6 (3%)	6.6 (5%)	6.6 (3%)	6.6 (3%)
Other	0.3 (0%)	0.3 (0%)	0.3 (0%)	0.3 (0%)	0.3 (0%)	0.3 (0%)
Solar	14.8 (10%)	68.3 (33%)	61.3 (31%)	11.9 (8%)	65.0 (33%)	56.6 (29%)
Wind	29.3 (19%)	19.0 (9%)	18.0 (9%)	24.0 (17%)	15.8 (8%)	17.0 (9%)
Total	150.2	204.2	199.3	142.4	199.1	194.7

* CO_2 emissions in 2050 are forced to be 50% of estimated emissions in 2015.

Values in parentheses are percentage of total capacity.

GW, representing a total investment of $ 111 – 113 billion. The increase in expected electricity demand and deratings in the available capacity of thermal power plants increased investment costs by 46% – 48%. Total fixed investment costs also increased in the scenarios with carbon emission constraints. In these scenarios fixed investment costs up to 2050 summed up to $ 82 billion in the reference scenario, and $ 131 – 137 billion in the cases including potential effects from climate change.

There are some caveats in our analysis. First, in our simulations of future electricity demand, we assumed all variables except climate conditions (for example, economic activity, electrification of transportation, and changes in population) remained constant at present levels. We made this strong (and non-realistic) assumption to isolate the impact of climate changes on decisions to invest in new capacity. It was not our goal to predict the future generator fleet. Instead, we examined how planning decisions to expand the generator fleet could change by including climate risks into the decision-making process.

In this analysis, we did not include transmission constraints between the four SERC subregions or energy connections with neighboring regions. The capacity of transmission lines could also be impacted by changes in the climate system [24]. Therefore, including transmission constraints could change some of our results. Including transmission constraints and its climate-induced vulnerabilities should be the focus of future work.

Climate change could also impact solar and wind generation potentials. However, the effects on solar and wind generators are not as clear as in other types of power plants. Past studies have disagreed on the directions of the impacts of climate change on solar and wind energy in the U.S. [24]. Particularly, in the southeast U.S. some studies have found an increase in solar generation potential under climate change scenarios. Incorporating the effects on wind and solar in our modeling framework could be the subject of future extensions of this work.

Also, we only considered as candidate technologies to invest those that are currently mature. For example, we did not consider energy storage (i.e., batteries), fuel cells, next-generation nuclear, among others. Finally, because of the specific characteristics of the power system in the southeast U.S., the results of the case study may not be directly applicable to other regions.

Nevertheless, our results offer insights about the impacts of climate change on the power system that can be useful for stakeholders outside the Southeast. Specifically, our results indicate that including potential climate change effects on electricity demand and power generation in the decision-making process of energy planners is likely to affect the choice of power plants built and the associated investment costs. The specific choice of power plants chosen is likely different in other areas of the U.S. For example, while we found that solar output in the Southeast coincides with times of high capacity deratings in thermoelectric power plants, the same is likely not true in the Midwest, where wind power may be better aligned with deratings. On the other hand, the simulations for the Southeast may offer

insights about the choice of cooling systems in thermoelectric power plants. Our results suggest that natural gas power plants with recirculating systems would suffer deratings under climate change scenarios. This finding is likely consistent in other regions east of the Rocky Mountains, where climate change is likely to results in increased air temperatures and humidity [59]. While power plants with dry cooling systems are less vulnerable in these regions, our simulations suggest these plants are still too expensive to be competitive with other generating technologies.

The results in this paper suggest that low-emission technologies such as nuclear and carbon capture remained uneconomical even with a 50% emissions cap. We did not include potential tax credits in our evaluation of technologies with CCS. These tax credits (such as the Section 45Q Tax Credit in the U.S.) would make thermal projects with CCS more economically attractive and could change the investment decisions in our analysis. Moreover, it is likely that higher carbon constraints required to meet the 1.5-degree climate stabilization target (net-zero emissions by 2050 [45]) would need the deployment of low-carbon technologies that are more expensive than wind and solar power. Such technologies may include advanced nuclear power plants, fossil-based power plants with CCS, but also negative-emission sources like bioenergy with CCS or direct air capture of CO2, which we did not include in this study [45]. Evaluating the vulnerability of these power plants to climate change should be the focus of future work.

3.4 Conclusion

To our knowledge, this study is the first to explicitly and endogenously integrate the combined effects of climate change on electricity demand and available capacity of thermal generators in an analysis of capacity expansion in the U.S. power system. Currently, the U.S. power sector accounts for approximately 28% of greenhouse gas emissions in the coun-

try [107]. Designing a less carbon-intensive power system is a crucial step towards the goal of reducing overall CO_2 emissions. The findings in this paper suggest accounting for climate constraints in the planning process would result in different decisions about the future of the power plant fleet. While we find that including such climate constraints may lead to increased investment requirements, we did not evaluate the operational benefits of planning for climate change. Future work will focus on simulating the operations of the fleet of power plants built in each of the scenarios presented in this paper. Such simulations will allow us to gain a complete understanding of the costs and benefits of planning for climate change.

Chapter 4

Tradeoffs in planning and operation costs due to climate change

4.1 Background

Electric power systems are planned to supply electricity to end users in a reliable and affordable way. When designing the power grid, planning agents must consider numerous long-term and short-term factors with varying degrees of uncertainty in order to attain these goals. Increasingly, the risks to the power sector due to climate change are becoming an important factor in the decision making process of power system planners. According to the Intergovernmental Panel on Climate Change (IPCC), average global temperatures are likely to rise 1.5° C above pre-industrial levels by 2052 [45]. The IPCC also projects a likely increase in meteorological variability, climatic extremes, and droughts. Utilities have already started discussing adaptation strategies to address potential impacts of climate change in their grids [16, 94, 43]. These impacts will likely affect the power system in several ways. On the demand side, for instance, warming temperatures will likely re-

sult in changes in electricity consumption used for to ambient heating and cooling. These changes could result in increased total consumption and peak electricity demand. On the supply side, for example, changes in streamflow could affect hydropower generation. Also, decreased water availability and increased water temperature could reduce the capacity and efficiency of thermal units that use once-through cooling [100]. Additionally, increased air temperature and humidity could reduce the capacity and efficiency of thermal units that use recirculating cooling [100]. Recent events in the US and Europe have already underscored the vulnerabilities of the power system weather extremes. In the summer of 2007, acute drought conditions in the southeast U.S. resulted in the curtailment and shutdown of some nuclear and coal-fired plants within the Tennessee Valley Authority (TVA) system. In France, many nuclear power plants had to reduce operations during a serious drought in 2003 [48]. As the effects from climate change become more prevalent, such events could become even more serious and frequent.

Given these aforementioned risks, a growing body of literature has analyzed how climate change might affect electric power systems [24, 19, 85]. Most studies focused on estimating impacts on individual components of the power system. On the demand side, a majority of the previous work has used top-down econometric models in different spatial and temporal resolutions to estimate changes in electricity demand patterns due to climate change [12, 84, 83, 42, 4, 82, 70, 95, 75, 34, 6]. For example, Auffhammer, Baylis, and Hausman [6] used daily data at the level of load balancing authorities in the continental U.S. to analyze the relationship between average or peak electricity demand and temperature. The authors found moderate and heterogeneous changes in consumption due to climate change, with an average increase of 2.8% by end of century. On the supply side, studies have analyzed how climate change can affect the production of electricity different types of generators [49, 50, 112, 10, 69, 96, 39]. Usually, these studies have focused on assessing reductions in capacity and efficiency of existing individual generators. For instance, Van Vliet et al. [112] estimated that the average useable capacities of 61 thermal plants

in the eastern U.S. could decrease by up to 16% by 2060. Notwithstanding the important insights reached by analyzing these individual factors, it is important to integrate them into a system-wide analysis to better comprehend the risks a power grid faces due to climate change. More recently, some studies have simulated how these climate-related shocks would affect the operation of a power system [76, 77, 97]. However, virtually none of them have integrated their analysis into a comprehensive and coherent configuration that includes how decisions to expand the generator fleet will be impacted by climate change.

In this study, we used a comprehensive and coherent integrated modeling framework to analyze potential tradeoffs in planning and operations costs in the power grid due to climate change. Through this work, we simulated the different climate-change risks in a consistent way [96], by considering the same ensemble of climate models, emission scenarios, and time horizons. We performed a case study of the SERC Reliability corporation, in the Southeast U.S. Figure 4.1 illustrates our modeling framework. We used the downscaled output from twenty different General Circulation Models (GCMs) [93, 2] to generate projections of hourly electricity demand [79]. We also used the output from these climate models as inputs into a chain of hydrological models [56, 55, 115, 73, 116] to generate series of daily river flows and water temperatures, which we then used to estimate hydropower potential under climate change. In addition, we used climate forcings and hydrological variables to estimate capacity deratings for existing and potential thermoelectric power plants under climate change [57, 17, 119]. Moreover, we used U.S. National Renewable Energy Laboratory (NREL) data sets of simulated wind and solar generation profile [109, 30] as upper bounds on wind and solar hourly generation. Then, we integrated all the aforementioned inputs in a capacity expansion model to create future generator fleet configurations under two climate change scenarios (no climate change impacts and assuming climate change impacts). Finally, we used both generator fleet configurations to simulate them under the same two climate change scenarios. This way we were able to compare potential costs and benefits of planning the electricity grid considering climate change haz-

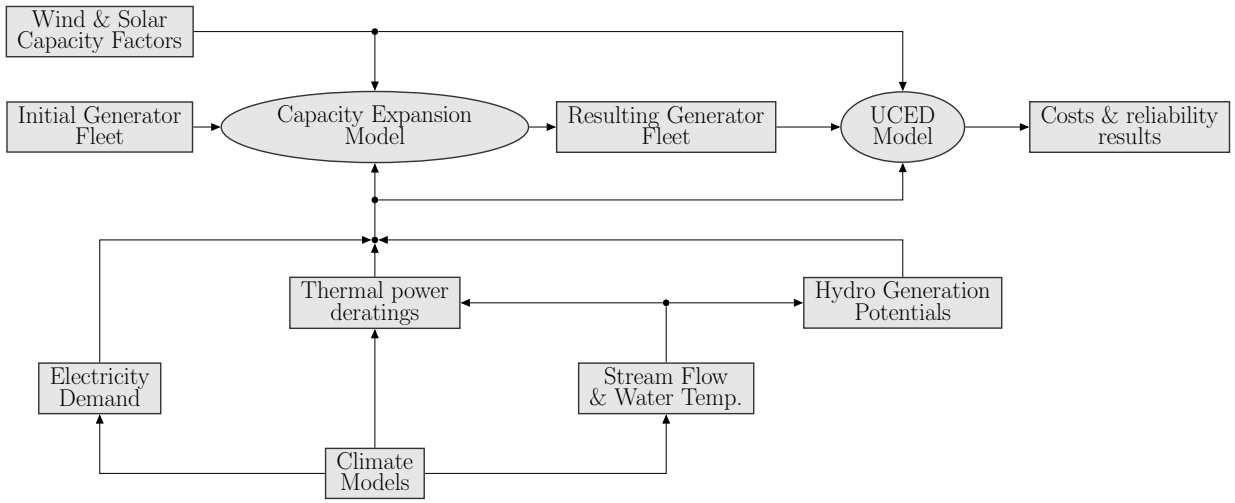

Figure 4.1: Diagram of the modeling framework

ards.

4.2 Data & Methods

4.2.1 Data

To represent historical weather conditions, we used weather data from the University of Idaho Gridded Surface Meteorological Data (gridMET) dataset [1]. This dataset combines desirable spatial attributes of gridded climate data from the PRISM dataset [78, 26] with desirable temporal attributes from the regional reanalysis dataset NLDAS-2 [71] to derive a high-resolution (1/24th degree, ∼4 km) gridded dataset of daily surface meteorological variables. This dataset has been validated by its authors against an extensive network of weather stations. Then, we disaggregated the daily data to hourly values using METSIM (Meteorology Simulator) [13].

To represent future weather conditions under climate change, we used projections of daily air temperature of twenty different Global Circulation Models (GCM) from the Coupled

Model Intercomparison Project 5 (CMIP5) [93], spatially downscaled using the Multivariate Adaptive Constructed Analogs (MACA) method [2]. In addition, we again disaggregated these daily projections to hourly values using METSIM. We selected the output of these climate models under representative concentration pathway RCP8.5. RCP8.5 is usually referred as the "business as usual" emission scenario, since it assumes that carbon emissions will keep increasing at present rates.

To simulate regulated daily river flows and water temperatures in the study region we used a physically-based modeling framework. This process-based modeling approach consists of three models. First, we used a macroscale, spatially distributed hydrological model, the Variable Infiltration Capacity (VIC) model [56] to simulate runoff. Second, the runoff was used as an input into a river routing model, the Model for Scale Adaptive River Transport (MOSART) [55], dynamically coupled to a spatially distributed water management model (WM) [115], to simulate reservoir storage and regulated streamflow. Third, surface meteorological data and simulated hydrologic conditions are used to simulate regulated river temperatures, using a one-dimensional stream temperature model, the River Basin Model (RBM) [116], coupled with a two-layer reservoir thermal stratification module [73]. We ran these models at a grid resolution of 1/8 degree ($\sim$ 12 km) using the climate forcing data from twenty different GCMs from CMIP5 [93], spatially downscaled using the MACA method [2].

We also simulated weather-induced deratings of thermoelectric power plants. We used the Integrated Environmental Control Model (IECM) to estimate typical response curves of thermal generators to changes in weather variables, stream temperatures, and stream flow [57]. These response curves modeled the effects of these weather variables in a power plant's available capacity and water consumption. This way we could map simulated local hourly weather and stream conditions to values of available capacity and water consumption for thermoelectric power plants. For existing thermal power plants with once-through

cooling, we also modeled how the water discharged from the power plants affects stream temperatures using a mass balance equation. We used this estimate to simulate the maximum available capacity of these types of power plants that would not cause water temperatures downstream of the power plant to rise above a certain threshold value. Water quality standards vary by state, but they typically require surface water temperature to remain under 32°C [63]. We used this threshold value in our study.

In order to capture spatial and temporal variability in output among wind and solar farms, we set upper bounds to the hourly generation of wind and solar power plants equal to simulated wind and solar generation profiles from the U.S. National Renewable Energy Laboratory (NREL) [109, 30]. These wind and solar generation databases provide simulated generation profiles for hypothetical plants in the SERC area at 5-minute increments, for 2007–2012 and 2006, respectively. We used 2009 wind generation data, since the overall simulated CF in this year was closer to the average over the complete data set. These databases have historical simulated generation profiles, hence we did not assume impacts of climate change on solar and wind generation. We aggregated generation data to hourly increments by calculating the average generation values for all time steps in each hour. After excluding several solar plants with no generation data, average capacity factors for hypothetical wind and solar plants in SERC in the NREL dataset ranged from 17%–55% and 12%–19%, respectively. Because we did not account for transmission within SERC in our the UCED model, each existing wind and solar unit varied only by capacity and hourly generation profile within each subregion. As such, in order to improve the computational efficiency of the model, we combined existing wind and solar units into single equivalent wind and solar units by summing up their capacities and hourly generation profiles.

To simulate the potential effects of climate change in the available hydro energy at power plants we combined historical data of hydro energy produced by the hydro power plants in the SERC region with the simulations of daily river flows from the VIC and MOSART-

WM models. We assumed that the potential hydro energy available at each power plant is proportional to the regulated stream flow simulated by hydrological models at the plants location. Within the optimization model, the actual generation decision for each hydro generator is limited by both this potential and the installed capacity of the power plant.

4.2.2 Generator fleet cases

We used two configurations of the generator fleet in 2050 in this study. The first was created assuming no effects of climate change on supply and demand. The second was created assuming the effects of climate change on supply and demand described in the previous sections. Both configurations were created by a capacity expansion model integrated within our modeling framework, as described in chapter 3. The fleet configurations were designed using the same same ensemble of climate models and emission scenarios used to simulate effects on supply and demand used in this study.

Figures 4.2a – 4.2b show the two generator fleets used in this analysis. In Figure 4.2a, the capacity expansion decisions were made without including climate induced changes in demand and supply. Electricity demand in this case was simulated using historical weather conditions (1979–2015). We assumed that thermoelectric plants would experience no weather induced capacity deratings. We assumed that generation from individual hydropower plants was the same as the historical average. The resulting fleet has an installed capacity of 142 GW. Wind and solar represent approximately 25% of the fleet. Natural gas power plants total almost half of the total installed capacity in this case.

On the other hand, Figure 4.2b shows the resulting generator fleet when climate change effects in demand and supply are taken into account. We used our estimates of electricity demand, hydro generation potential, and thermoelectric available capacity estimated using projections of meteorological variables from the GCMs under RCP 8.5. In this case,

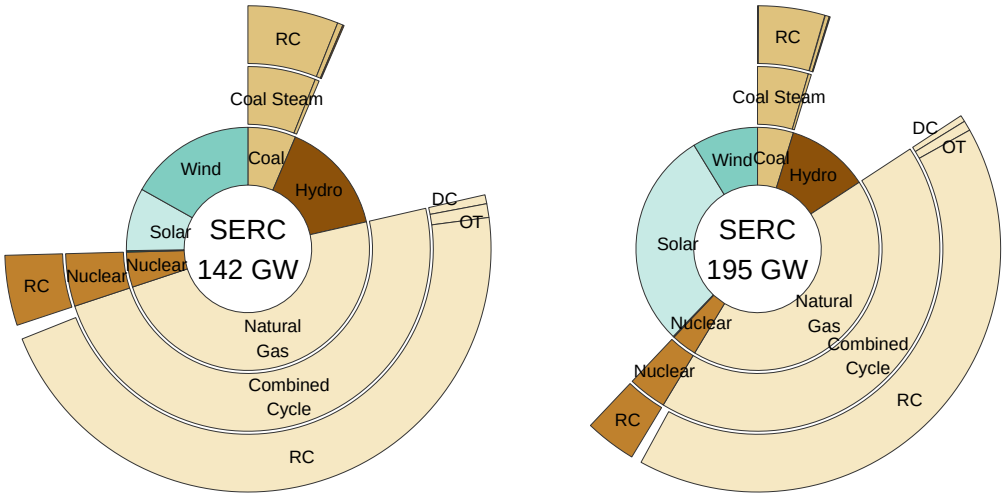

(a) No climate change (b) RCP 8.5

Figure 4.2: Configurations of the generator fleet in 2050

the resulting fleet has an installed capacity of 195 GW (37% higher than in the no climate change case). Wind and solar represent approximately 40% of the fleet. The participation of natural gas power plants is 43%.

4.2.3 Unit commitment model

To analyze the tradeoffs between planning and operational costs under different climate change assumptions, we used a unit commitment and economic dispatch (UCED) [23, 25]. The UCED model optimized electricity generation and reserve provision in order to minimize operational costs while meeting electricity demand and generator-level unit commitment constraints. Minimized operational costs are the sum of variable electricity generation, start-up costs, and estimated cost due to loss of load. We implemented a customized version of this model that included climate induced generation constraints in thermal and hydro generators, and impacts of climate change in electricity demand.

The UCED model ran sequentially for 365 daily simulations of hourly dispatch to build a full 8760-hour simulation of the generation of individual plants. In order to account for

inter-day generator operations, we executed each daily iteration of the UCED model with a 24 hour optimization window plus a 24-hour look-ahead period. The solution of the first 24 hour period determined the initial conditions for the following UCED iteration. To account for variable wind and solar generation, and for generator outages, the UCED model included three operating reserve types: regulation, flexibility, and contigency. These three reserve types are represented as positive reserves, i.e. the system procures capacity for increasing generation in case this is needed. The three types of reserves are modeled as constraints that commit a share of the system's capacity in addition to the generation being allocated to meet actual load. Given current standard operations, only coal steam, oil and gas steam, and NGCC units can provide reserves.

Although our formulation of the UCED model did represent the reserve requirements, for this analysis we turned off these constraints. One of our objectives was to compare how the two generator fleets (built with and without climate change assumptions) would perform under different climate change conditions. A metric of interest in our study was to analyze how loss of load events would change between the different scenarios simulated. In such cases, procured operating reserves could be used to supply generation shortfalls. Therefore, allocating capacity for operating reserves would mask the actual simulated loss of load levels.

In our scenarios of grid operation under climate change, we ran one full annual UCED dispatch simulation for each of the twenty climate model outputs in our dataset. Each of the twenty climate simulations resulted in distinct time series with 8760 values of hourly electricity demand, and 365 values of daily thermal capacity deratings, and hydropower potential. This resulted in twenty different dispatch simulations in each scenario. This way our results took into account the inherent uncertainties in the climate simulations.

We repeated a similar approach in the scenarios of grid operation without climate change effects. In this case, we simulated twenty distinct time series of hourly electricity demand

Table 4.1: Scenario definition

Scenario	Planning stage	Grid operation stage
scenario 1	No climate change effects on demand and supply	No climate change effects on demand and supply
scenario 2	Climate change effects on demand and supply (RCP 8.5)	Climate change efffects on demand and supply (RCP 8.5)
scenario 3	Climate change effects on demand and supply (RCP 8.5)	No climate change effects on demand and supply
scenario 4	No climate change effects on demand and supply	Climate change efffects on demand and supply (RCP 8.5)

using the weather conditions of twenty unique years in our historical dataset. On the supply-side, we assumed that hydro generation potentials were equal to historical averages, and thermal power plants experienced no weather-related capacity deratings.

4.3 Results

To analyze possible tradeoffs between investment and operating costs related to climate change in the electricity sector, we compared cost and reliability metrics of four different scenarios. These four scenarios represent combinations of two grid expansion planning cases and two grid operation cases. Table 4.1 describes the four scenarios considered in this study.

Figure 4.3 compares the total average levelized cost of energy (LCOE) of the four scenarios analyzed. The LCOE is a metric that allows different power sources (or electricity power portfolios) to be compared on a consistent basis. To compute the LCOE, we summed up all fixed and variable costs and divided by the total electricity demand in each scenario. The total LCOE in each scenario is decomposed in five components: capital expenditures (capex) costs, fixed operation and maintenance (fixed O&M) costs, variable O&M costs, fuel costs, and loss of load (LOL) costs. To compute the LCOE component of

the LOL, we used a value of lost load (VoLL) of 5,000 $/MWh (in 2015 USD). This value is based on a study made for ERCOT [60]. It used macroeconomic analysis to provide indicative estimates of foregone economic value when electricity service is disrupted in Texas using assumptions such as state gross domestic product and average rates paid by electricity customers in Texas. Just as a comparison, this value is approximately 50 times higher than the most expensive power plant in our initial fleet.

The total value of the average LCOE on scenarios 1, 2, 3, and 4 is 38.8 $/MWh, 42.5 $/MWh, 42.3 $/MWh, and 150 $/MWh, respectively (in 2015 USD). Both scenarios where the expansion policy is defined assuming no climate change effects (scenarios 1 and 4) resulted in a capex cost of approximately 9 $/MWh. On the other hand, the capacity expansion scenarios assuming climate change effects (scenarios 2 and 3) have a capex cost of approximately 15 $/MWh (66% higher). Variable costs are slightly smaller in the expansion scenarios assuming climate change effects (scenarios 2 and 3). In these cases, the expansion policy builds more wind and solar generators. Therefore, these types of generators represent a greater share of the total energy generated. Wind and solar generators typically have marginal operating costs close to zero, which results in lower overall variable costs. In scenarios 2 and 3 variable costs (fuel + variable O&M) are approximately 22 $/MWh, while in scenarios 1 and 4 variable costs are approximately 24 $/MWh.

The chosen value of lost load used to compute the results in Figure 4.3 led to a large value of the LOL component of the LCOE in scenario 4. This LOL component dominates the resulting total value of the LCOE in scenario 4 (70% of the total LCOE value) and results in the most expensive scenario analyzed. Therefore, the chosen VoLL assumption is crucial to our results. Estimating values of lost load is an important and ongoing topic of study in energy economics [74]. Studies usually rely on one of three ways to estimate VoLL [53]. The first uses consumer surveys and is based on stated preferences [11, 9, 91]. The second way uses cost estimates from previous supply outages [22]. The third alternative is

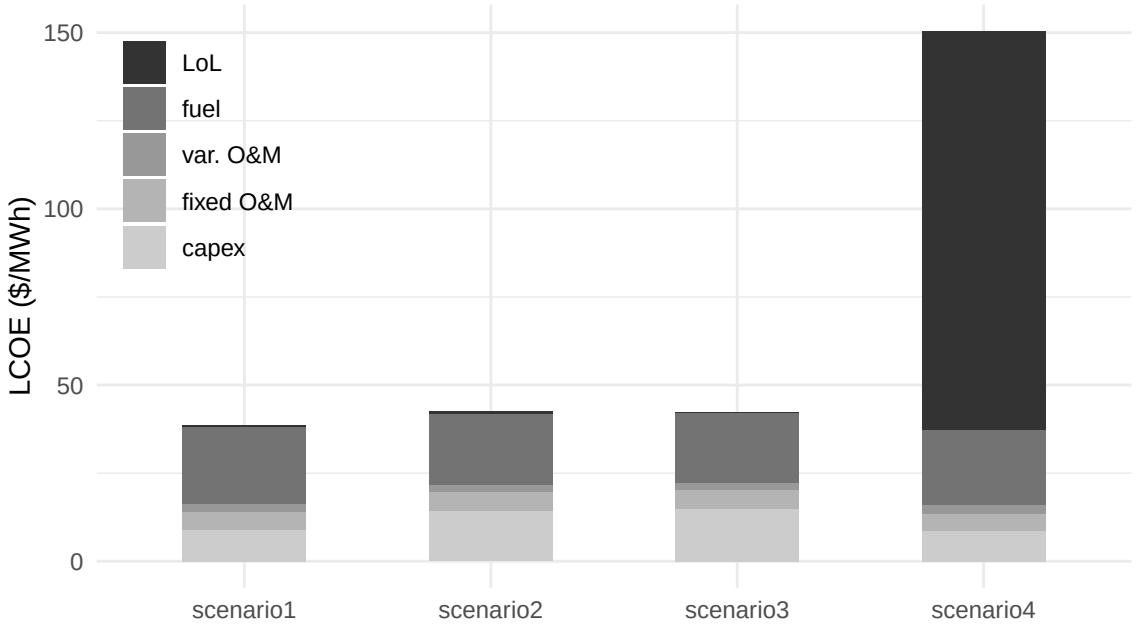

Figure 4.3: Comparison of the levelized cost of energy (LCOE) for the fours scenarios.

based on estimates of macroeconomic production functions [53, 18, 60]. Previous studies have found a wide range of values for VoLL in different regions, from 5,000 $/MWh to 45,000 $/MWh [60]. This variability is due both to methodological differences, and specific characteristics of the regions analyzed. Estimating the value of lost load for the southeast U.S. is beyond the scope of this work. However, we used our results to estimate the implied cost of avoiding this large amount of load loss in scenario 4. This way we could compare it to the estimated values in the literature. We calculated the difference in total costs ($/year) between scenarios 2 and 4 (we excluded from this computation the costs due to loss of load). Then we divided this value by the average amount of LOL (in MWh/year) in scenario 4. According to our results, the cost of avoiding the amount of load loss in scenario 4 would be approximately 197 $/MWh. This value is approximately 4% of the VoLL used in Figure 4.3. This suggests that the cost (in $/MWh) that the system would be paying to avoid the amount of LoL in scenario 4 would be substantially lower than the values of the willingness of consumers to pay to avoid a period without power currently used in the literature.

Figure 4.4 compares the average generation values of each source in each scenario. When we assume climate change conditions in the grid operations (scenarios 2 and 4), total annual electricity consumption is approximately 684 TWh, 3% higher than total electricity consumption in scenarios 1 and 3 (without climate change conditions in the grid operations stage). Most of this increase in consumption is concentrated in the summer season. In the summer, demand in scenarios 2 and 4 is 16% higher than in scenarios 1 and 3. On the other hand, during the winter, electricity consumption is approximately 160 TWh in scenarios 2 and 4 and 166 TWh in scenarios 1 and 3. These results are comparable to the ones found by previous studies that analyzed the impact of climate change on electricity demand in the U.S. ([6, 79])

The combinations of compositions of the generator fleet and grid operating conditions result in different generation patterns in Figure 4.4. In scenarios 2 and 3, 40% of the installed capacity comes wind and solar power plants. However, the generation from wind and solar represents, respectively, 10% and 12% of total generation in scenarios 2 and 3 (summing approximately 145 TWh). Generation from natural gas, on the other hand, accounts for 52% of total generation in scenarios 2 and 3. The share of wind and solar generation is smaller in scenarios 1 and 4. In these scenarios, wind and solar represent 13% and 3% of total generation, respectively.

The generation profiles in the summer are of particular interest. In the summer, natural gas power plants suffer from weather-related capacity deratings in scenarios 2 and 4. In scenario 2, the fleet was planned taking these summertime deratings into account. Therefore, to offset part of this derating, the fleet in scenario 2 has more solar power plants. Solar power plants in the southeast U.S. typically have higher power output in summertime. By having more solar energy available in scenario 2, the system is able to supply virtually all electricity demand. On the other hand, in scenario 4 the design of the generator fleet did not assume natural gas power plants would suffer weather-related deratings.

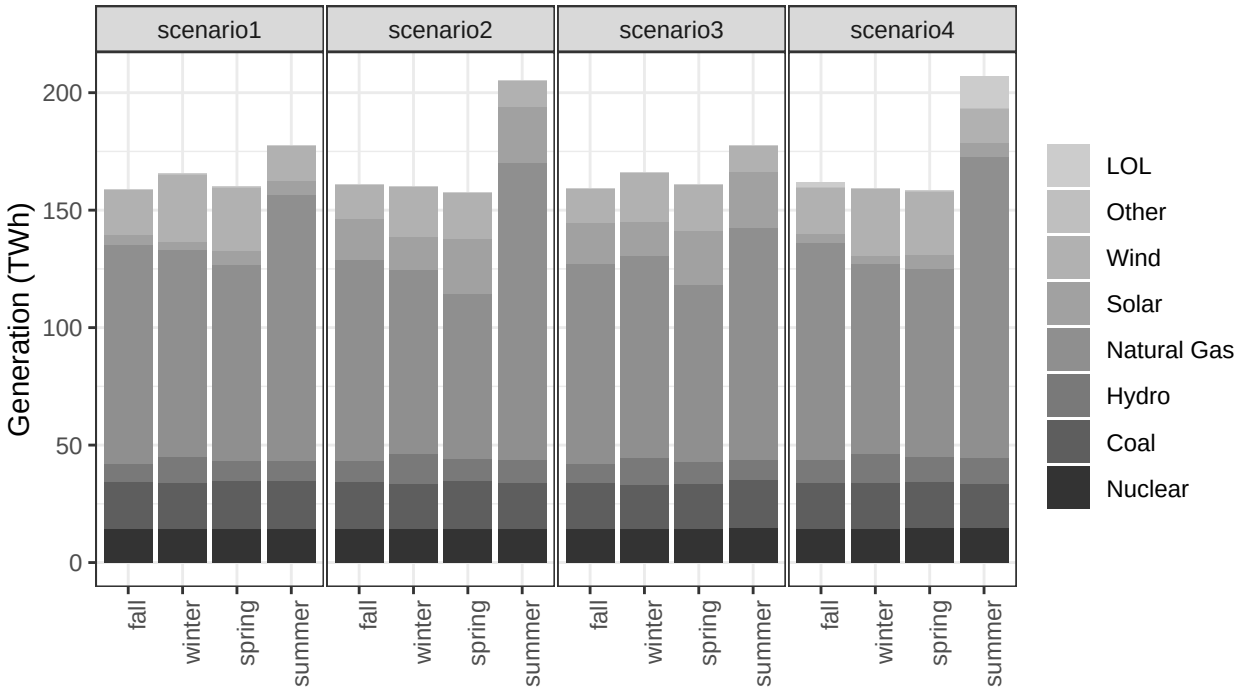

Figure 4.4: Comparison of the generation by source in each season and scenario.

The cost-minimization decisions in the planning stage were to build relatively more natural gas power plants. When these power plants were not able to operate at full capacity during summertime, there was a steep increase in the occurrence of loss of load events. In scenario 4, the system is, on average, unable of delivering 13 TWh of the summertime consumption.

We also analyzed the resulting reliability metrics in our simulations. Figure 4.5 shows the distribution of loss of load probability (LoLP) in each of the four scenarios. These values represent the expected number of hours in the year when a loss of load of any magnitude happened in our simulations. As expected, the scenarios here the capacity expansion policy is planned assuming effects of climate change on supply and demand (scenarios 2 and 3) have low levels of LoLP. In scenario 2, the expansion policy built more capacity than necessary because the policy assumed effects from climate change that did not materialize. This excess capacity results in virtually zero loss of load events. In scenario 3, again the expansion policy assumed effects from climate change. But in this case, the effects as-

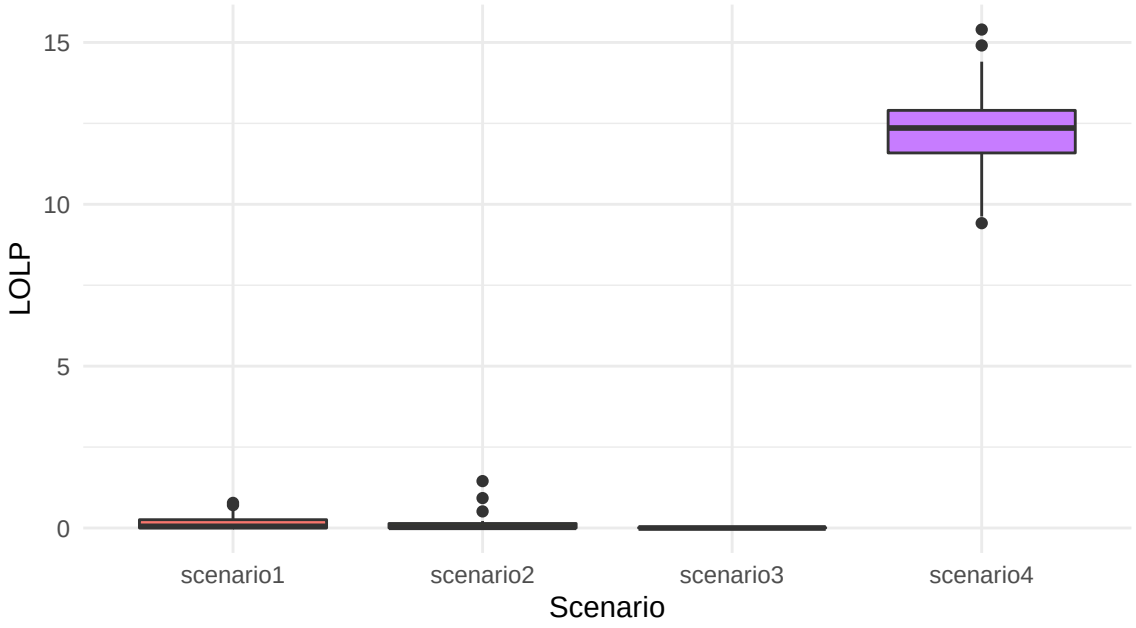

Figure 4.5: Comparison of the loss of load probability (LoLP) in the fours scenarios simulated.

sumed in the planning stage do materialize. This correct expansion policy results in small expected value of loss of load events (0.18%). Similarly, there are low loss of load levels in scenario 1 (0.18%). In this scenario, expansion policy does not include potential effects from climate change and these effects do not materialize in the future. However, scenario 4 has LoLP levels of approximately 12%. This represents that during 12% of the year the system is expected to suffer some kind of load loss. This high value of LoLP is due to two interrelated affects that were not considered in the planning stage of this scenario: the increase in electricity demand related to changes in climate conditions, and the potential reduction in thermal capacity in summertime.

Figure 4.6 compares the kernel densities of the loss of load values in the four scenarios simulated. Areas under each curve are scaled in order to better represent the different average probabilities in each scenario (illustrated in Figure 4.5). As expected, the density plot for scenario 3 show virtually probability zero of any load events. The density plots for scenarios 1, and 2 present similar distributions of LoL. Both distributions have low prob-

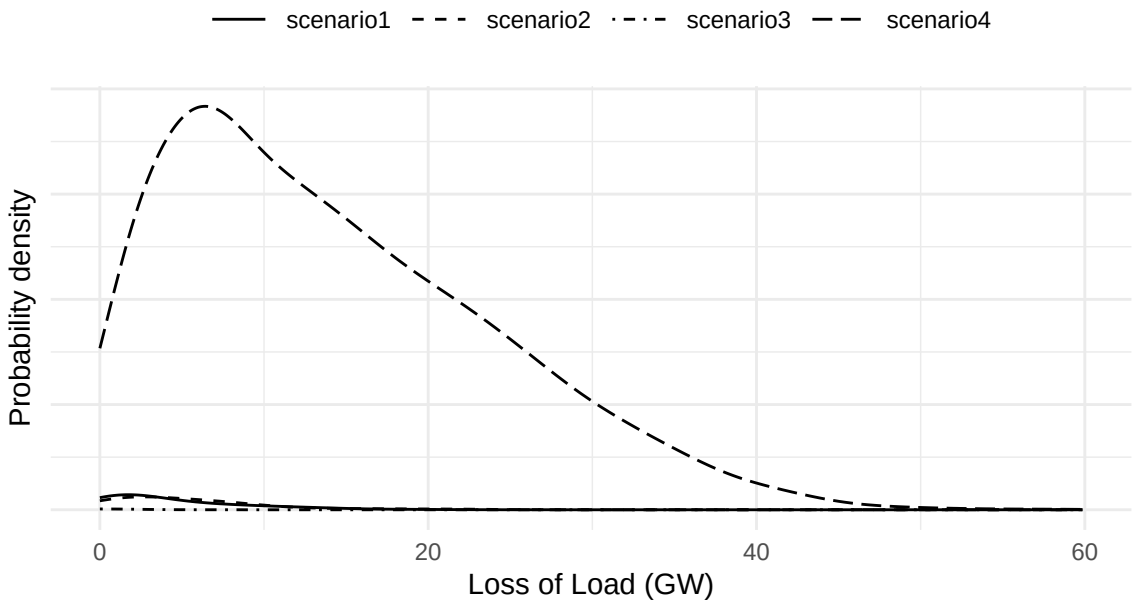

Figure 4.6: Comparison of the kernel densities of loss of load (LoL) in the fours scenarios simulated. Areas under the four curves are scaled in order to represent the different values of the overall probabilities of loss of load.

abilities of any type of shortage event. The average loss of load value in scenarios 1 and 2 is approximately 4.2 GW and 5.2 GW, respectively. On the other hand, scenario 4 (where the expansion policy did not include effects from climate change, but these effects did materialize) shows a wide range of possible values of load loss. The average load loss value is approximately 14 GW. However, there is a 2% probability that simulated load losses in this scenario could surpass 24 GW (17% of the average peak demand value in this scenario).

We also compared the duration of loss of load events in the four scenarios. Figure 4.7 shows the kernel density plots of the loss of load in the four scenarios simulated. In scenarios 1 and 2, average duration of LoL is approximately 3.9 hours and 5.8 hours, respectively. Scenario 3 shows virtually no LoL events. In scenario 4, on the other hand, the average duration of LoL is approximately 11 hours, an increase of 175% compared to scenario 1. Moreover, in scenario 4 the probability that a given LoL event lasts more than 16

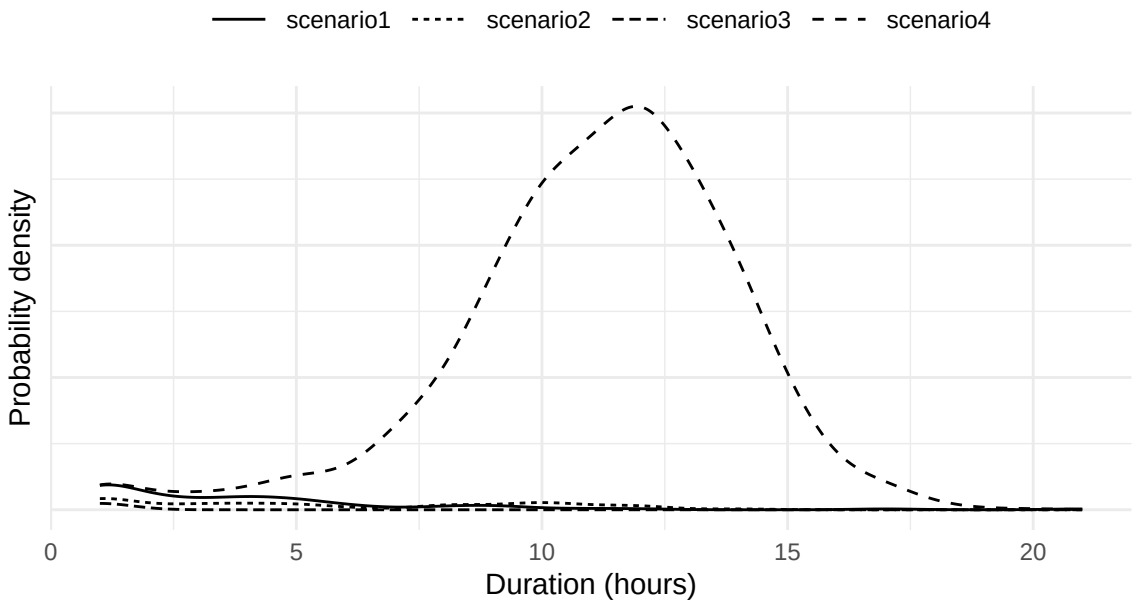

Figure 4.7: Comparison of the kernel densities of the duration of the loss of load (LoL) events in the four scenarios simulated. Areas under the four curves are scaled in order to represent the different values of the overall probabilities of loss of load.

hours is at least 3%.

As commented previously, the high risk of shortages in scenario 4 is driven by two factors that were not taken into account in the planning stage: the increase in electricity demand related to changes in climate conditions, and the potential reduction in thermal capacity in summertime. To better understand how these two factors are affecting the resulting simulations of shortages, we decomposed the simulated values of LoL into thermal deratings and lack of installed capacity. To accomplish this, we used a simplified rule of thumb: shortages are driven first by thermal deratings and then by lack of installed capacity. The rationale for this procedure is: if, by being able to operate thermal power plants at their full capacities, the system would be able to supply all electricity demand, then there would be no need to build more power plants. At the planning stage, agents did build enough capacity, however they did not account for climate-related thermal deratings. On the other hand, if the LoL levels are even greater than the total level of thermal deratings, that

means that planning agents did not build enough capacity to supply the increased demand levels under climate change. Figure 4.8a shows the breakdown of the average LoL (in GW) into the thermal derating and lack of capacity components. Lack of capacity accounts, on average, for approximately 66% of the amount of average LoL. Thermal deratings acount for approximately 34%. The error bars represent the range of variability of each component over the twenty GCMs simulated.

The average values presented in Figure 4.8a do not show the frequency of how these components drive the shortage events. Figure 4.8b shows the joint density plot of the two components. The horizontal axis represents the value of the shortage component caused by thermal deratings, while the value of the shortage component driven by lack of capacity is in the vertical axis. Red colors represent higher frequency events, while blue colors represent lower frequency events. The marginal densities of each component are also illustrated in the plot. While, on average, lack of capacity accounts for the higher share of shortage events, the most frequent events occur when thermal deratings appear to be the main drivers. The mode of the distributions is located at a point where the value of the thermal derating component is approximately 3 GW and the value of the capacity shortfall component is close to zero. Load losses driven by thermal deratings have a maximum value of approximately 7.5 GW. As illustrated in Figure 4.5, simulated load losses in scenario 4 could total over 35 GW in some low probability events. Figure 4.8a shows that these low probability events would be driven mostly by lack of installed capacity.

The results in Figure 4.8a could lead to some insights into possible adaptation strategies to the potential effects of climate change on the power sector. First, we did not include any reserve margin requirements when we simulated our capacity expansion scenarios. As a "rule-of-thumb", power system planners in the U.S. use a percentage of estimated peak demand values (e.g., 15%) as a reserve margin (i.e., amount of installed capacity above estimated peak demand). This reserve margin is intended to allow the system to cope with

values of peak demand higher than the expected ones. In our simulations, a reserve margin requirement could help to mitigate the low probability loss of load events driven by the lack of installed capacity component. Additionally, the more frequent loss of load events driven by thermal deratings could be mitigated by using dry cooling technologies. In our simulations of thermal deratings, natural gas power plants with dry cooling had virtually no weather-driven capacity deratings. Therefore, by retrofitting natural gas power plants to dry cooling, the power grid would not experience the loss of load events driven mostly by thermal deratings. For these cases, retrofitting to dry cooling could be a more cost effective measure than building additional power plants.

There are some caveats in our analysis that should be taken into account when interpreting our results. First, the expansion decisions simulated in our capacity expansion model in the period 2020–2050 are not fully dynamic. These expansion policies are defined assuming static and deterministic input scenarios. This way, all investment decisions in the planning horizon (2020–2050) are defined once (during the planning stage) and do not change. Then we simulate the resulting fleets using different climate conditions. In real life, planning agents would adapt their decisions as they start to observe some of the extreme hazards simulated in scenario 4 (where planning stage does not include climate change effects, but these effects materialize in the grid operations stage). Therefore, scenario 4 is an extreme case that is unlikely to occur. To represent a more realistic investment dynamics in the capacity expansion model, future extensions of this work could use a different approach that inherently included uncertainty and the acquisition of information during the planning stage (e.g., using a real options framework [35]).

Second, both in the planning and grid operating stages, we assumed that future electricity demand would only differ from present values because of changes in climate conditions. Therefore, we assumed that factors such as economic activity, electrification of transportation, and changes in population remained constant at present levels. We made this strong

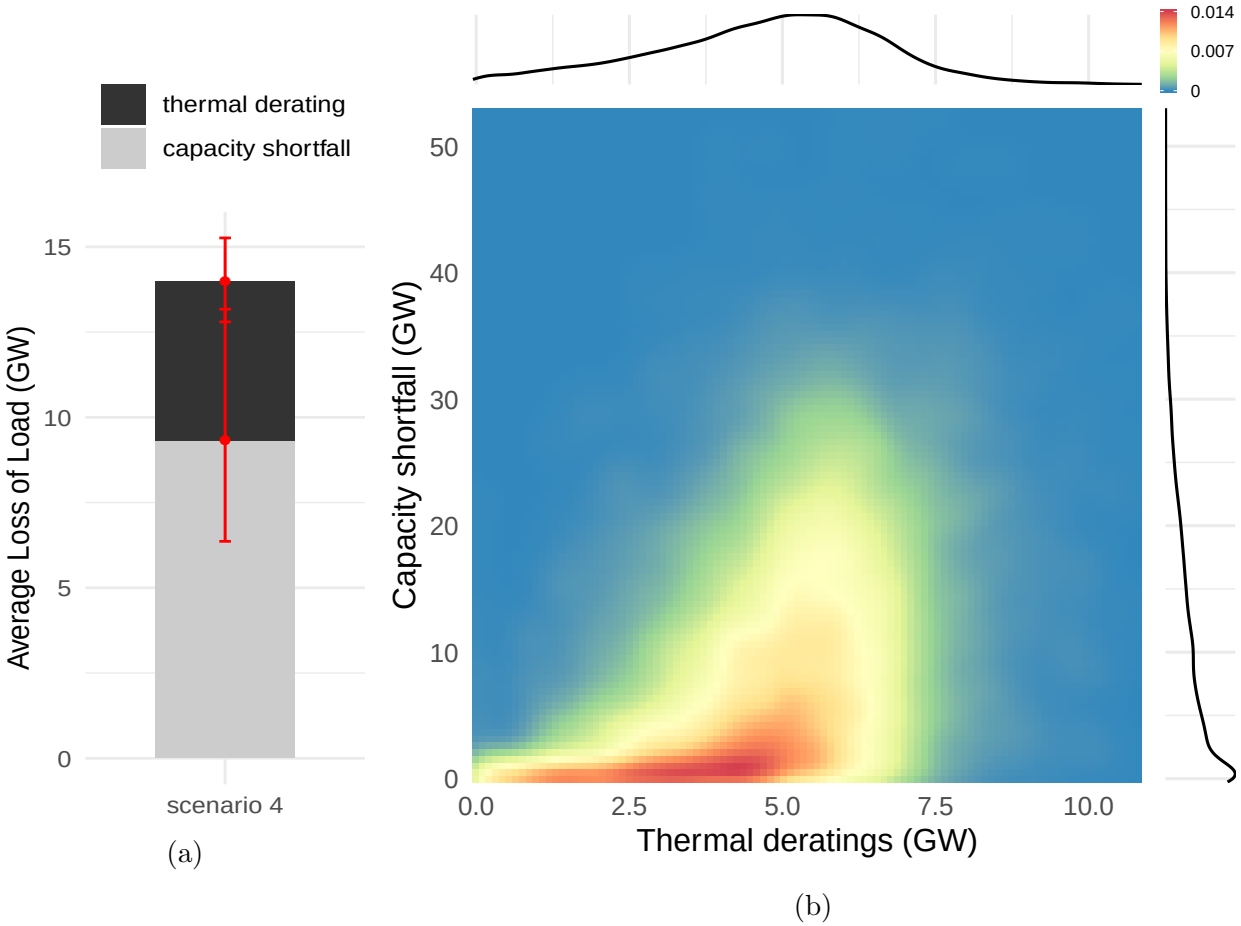

Figure 4.8: Decomposition of the loss of load values in scenario 4. The thermal derating component corresponds to loss of load events that occurred because of the deratings of thermal generators. The capacity shortfall component corresponds to those loss of loads caused by the lack of installed capacity on the system. (a) shows the average value of these components. The red error bars represent the range of values of each component over the twenty GCMs simulated. (b) shows the two-dimensional probability density function of the two components.

(and non-realistic) assumption to isolate a first order impact of climate change on planning and operations costs of the power grid. This way we could analyze the tradeoffs in costs when planning for climate change in the power sector. To get a more detailed assessment of these tradeoffs in costs, future work could merge scenarios of climate, population, and technology change.

Third, our simulations did not include transmission constraints, nor changes in solar and wind generation because of climate change. Transmission capacity is sensitive to ambient air temperature and climate change could result additional transmission restrictions. Climate change could also impact solar and wind generation potentials. However, the effects on solar and wind generators are not as clear as in other types of power plants. Past studies have disagreed on the directions of the impacts of climate change on solar and wind energy in the U.S. [24]. Particularly, in the southeast U.S. some studies have found an increase in solar generation potential under climate change scenarios. Incorporating the effects on transmission, wind, and solar in our modeling framework could be the subject of future extensions of this work.

In spite of these modeling limitations, the results in this paper suggest that climate change could have serious impacts in the power grid that should be taken into account by planning agents. The extreme cost disparity and reliability degradation presented in the results of scenario 4 stress the importance of including the effects of climate change in the planning of the electricity grid. Planning agents usually use standard target levels of reliability metrics to design the expansion of the electricity grid. For example, an acceptable target level of LoLP is 0.1 days/year (or equivalently, 0.03%). The simulations in scenarios 1, 2, and 3 all reach levels of LoLP close to this target. However, scenario 4 results in levels of LoLP of 12%, which would be an unacceptable level of outages. Outages in scenario 4 were also of longer duration (120% longer on average than in scenarios 1 and 2) and of larger magnitude (150% greater than in scenarios 1 and 2).

These high levels of LoLP in scenario 4 resulted in huge costs to the system (150 $/MWh, 260% higher than the other scenarios), mainly due to the implicit costs of loss of load. The additional investments and operating costs needed to avoid the level of loss of load simulated in scenario 4 would be of the order of 200 $/MWh, which is considerably lower than estimated values of the willingness of electricity consumers to pay to avoid loss of load.

4.4 Conclusion

The results presented in this study could inform planning agents in the power sector to come up with adaptation strategies to cope with climate change risks. According to our results, adaptation strategies could include increasing the participation of wind and solar generation in the electricity grid. Solar power, in particular, could help to offset part of the climate related capacity deratings of thermal power plants during summertime. Other adaptation strategies not included in our analysis framework would also be important to make the grid more resilient to the impacts of climate change. For example, in our analysis we assumed that energy efficiency would remain constant at present levels. However, increasing efficiency of ambient cooling methods could also be an important adaptation strategy. It is also interesting to point out that some of these adaptation strategies – such as installing more wind and solar power plants – would also help to mitigate future carbon emissions. This dual characteristic of these strategies (adaptation and mitigation) make them even more attractive. As planning agents look into sustainable pathways for the decarbonization of electricity generation, studies that integrate the different vulnerabilities of the power system to climate change could help decision-makers mitigate reliability and affordability challenges facing the design of the future power grid.

Chapter 5

Conclusion

The impacts of global climate change are already being experienced by communities in the U.S. and other regions of the world [110]. Frequency of high temperature extremes and heavy precipitation events are increasing. Wildfires in the western U.S. are becoming more widespread and the average wildfire season is now longer than decades ago. As these effects become more prevalent, climate change awareness among the general population continues to increase in the U.S. [54]. In such a context, society shall expect policy makers across different areas to implement effective response strategies to face the challenges and hazards caused by the changes in the climate system.

Mitigation strategies will be an essential part of a coherent climate change response policy. According to the Intergovernmental Panel on Climate Change (IPCC), in order to restrict temperature increase to 1.5 °C above pre-industrial levels, society would need to reach and sustain a net zero global anthropogenic CO_2 emissions by 2050 [45]. This would require rapid and far-reaching transformations in energy, land, infrastructure, and industrial systems. In the U.S., the electricity sector is currently responsible for approximately 28% of greenhouse gas emissions [107]. In recent years carbon emission from electricity

generation have decreased because of – among other factors –a continued shift from coal to natural gas, and increased use of renewables. However, in order to the reach the targets recommended by the IPCC, electricity generation will need to change more substantially to zero-emission sources such as nuclear, wind, and solar.

Because of the long-lasting lifecycle of carbon dioxide and other greenhouse gases, past emissions will stay in Earth's atmosphere for decades, if not centuries, to come [45, 80]. This means that society will likely need to implement adaptation strategies to some level of changes in the climate system. Different human and natural systems will experience distinct climate-related risks [110]. Decision makers will need to understand the specific tradeoffs resulting from these climate-risks and how to address them efficiently. The U.S. power sector is specially vulnerable to climate-related risks. Electric grid operations and infrastructure in the U.S. are threatened by variety of climate impacts, including increasing temperatures, heavy rainfall events, wildfires, hurricanes, and storm surge [99]. In order to continue to deliver reliable, affordable, and clean electric power, planning agents will have to adapt their decisions to these new conditions.

This thesis focused on analyzing adaptation strategies in the southeast U.S. power sector to the impacts of climate change. The thesis used an integrated multi-model framework to investigate how the projected changes in climate conditions could impact different and inter-related dimensions of the electricity grid: electricity demand, expansion planning, and grid operations. Integrating all these dimensions in a coherent and comprehensive modeling framework is an important tool to understand the climate-related vulnerabilities the electricity grid faces. Interactions between some of these vulnerabilities could result in compounded risks for the power grid. For example, increases in air temperature could result in an increase in the frequency and magnitude of peak demand events in summertime, at the same time that some thermal generators may experience climate-related capacity deratings. Moreover, these risks could result in changes in the planning decisions, which

could lead to a different composition of the future generator fleet.

In chapter 2, I used an econometric model to analyze how the projected changes in climate conditions could impact intraday electricity demand patterns. I focused this first analysis just at the Tennessee Valley Authority (TVA) region. Our results suggest that climate change could result in an average increase in annual electricity consumption in the TVA region. However, this increase is not uniformly distributed throughout the year. During summer, total electricity consumption could increase on average by 20% while during winter it may decrease on average by 6% by the end of the century.

In chapter 3, I expanded my analysis to the complete SERC region and focused on how climate change would affect the decisions to expand the generator fleet. I expanded the estimates of future hourly electricity demand described in chapter 2 to the complete SERC region. I also simulated decreases in generation of hydro and thermal generators due to climate change. I integrated these simulations in a capacity expansion (CE) model. This CE model is a mixed integer linear programming (MILP) model that we adapted and developed for this study. It finds the composition of the future generator fleet that minimizes costs subject to the estimated effects of climate change. We ran this model under different climate change scenarios from 2020 to 2050. Our results showed that by including these effects due to climate change in the decision making process, the estimated participation of renewables in the generator fleet in 2050 increased from 24% to over 37–40%. Solar power plants could become more economically attractive. This results from the fact that solar energy has higher expected energy output during the summer, a season when thermal generators experience stronger reductions in their available capacity due to higher air and water temperatures.

The results in chapter 3 informed how the effects of climate change would affect decisions to expand the generator fleet. However, each run of the CE model was designed with a deterministic assumption of the effects of climate change in the grid. Therefore, the expan-

sion policy in each scenario was the approximate optimal one for that specific scenario. Investment decisions were defined to satisfy demand requirements at the least cost available. However, one question that the analysis in chapter 3 could not address was how these different expansion policies would perform if a different climate change scenario materialized. What would be the cost tradeoffs of including the climate change assumptions in the planning stage of the electricity grid?

In chapter 4 I used the results from chapter 3 to analyze these issues. I implemented a unit commitment and economic dispatch (UCED) model to investigate the tradeoffs between investing or not in the generator fleet assuming different climate change scenarios. Our results suggested that by not including climate change effects in the planning stage, SERC's power system could experience loss of load levels of 12% and overall energy costs could be 260% higher if climate change conditions do materialize by 2050. Most of this increase in energy cost was because of the costs of loss of load. These high load levels would be driven both by two inter-related factors. Firstly, the expansion policy would underinvest in new capacity in the planning stage because of it would not expect a climate-induced increase in electricity demand. Secondly, the expansion policy did not expect thermal generators to experience capacity deratings during summertime.

The results presented in this thesis underscore the importance of including climate change hazards in the planning stages of power grid. Energy system planners, owners, and operators should prepare for climate change by identifying vulnerabilities, investing in more resilient infrastructure, improving operations, among other adaptation strategies.

The aforementioned results should be interpreted within the limitations of the modeling framework. The modeling configuration used in this thesis linked several different models into an integrated framework in order to represent in more detail different vulnerabilities of the power sector to climate change. Each of these models have different levels of uncertainty that could propagate throughout the simulation and could affect the final results in

different ways. Moreover, in order to better represent power system dynamics and the effects of climate change, I used data in hourly timeframe and high resolution spatial data when possible. While this high resolution data is important to simulate the power system, it can also increase uncertainty of some of the results estimated within my modeling framework. Some of these uncertainties have been explicitly incorporated in this analysis, while other ones have not.

The main example of an uncertainty component explicitly included in this analysis is the variability in the projections of climate variables. To account for this inherent uncertainty, I included the results of twenty different climate simulations and two different emission scenarios (RCPs) in the results. Because the output from the climate models propagates through all other parts of the modeling configuration used in this work, this output can have important effects in the final results. The output from the climate simulations directly affects estimates of electricity demand, availability of thermal generation, and hydro potential.

This can be observed in the simulations of annual electricity consumption (Figure 3.15a) and peak demand (Figure 3.15b). The relative range of annual electricity consumption values is around 5% of the mean values. The relative range of annual peak demand values is approximately 12% of mean peak demand values. This larger variability in peak annual demand values is expected since these are estimates of hourly values of demand. The uncertainty in annual peak demand values is also more critical for some results in this thesis. Peak demand values were directly used in the capacity expansion model to define the amount of new capacity needed to be added in the system. In order to make the results more robust to this variability in the demand estimation, each annual iteration of the capacity expansion model used estimates of electricity demand resulting from three different climate simulations. These three climate simulations represented specific percentiles of the distribution of annual peak demand.

Other sources of uncertainty that were not explicitly included in this analysis could also impact demand values. In this analysis I assumed that future electricity demand would only change in response to changes in air temperature conditions. This was a deliberate assumption, since our goal was to isolate how the changes in climate projected by the GCMs would affect the demand for electricity. However, as discussed in chapter 2, changes in weather patterns will certainly not be the only factor that will affect future electricity demand. Other important factors will also affect future electricity demand and could have an impact on total values of electricity demand larger than the simulated effects of climate change presented in this work. A few examples of these factors are: population changes, efficiency gains in electricity end use, and an increase in electrification of energy end uses.

There is considerable uncertainty of how some of these factors will interact with changes in the climate system and their final combined impact on electricity demand. The National Renewable Energy Laboratory (NREL) projects a reference scenario where nationwide electricity consumption could increase by 24% by 2050 [64] (these projections do not include climate change related impacts). However, under scenarios of higher electrification of energy end uses electricity consumption could increase 49% (medium electrification scenario) and 71% (high electrification scenario) by 2050 [64]. Most of this variation is because of differences in the assumptions of the amount of electrification in the transportation sector. These changes in the electrification of transportation could also impact intraday electricity consumption patterns discussed in chapter 2 because of vehicle charging behavior. The effects of vehicle charging behaviors in the intraday load curve are still uncertain. These uncertain effects could impact some of the results presented in this thesis. For example, an increase in "off-peak" hours electric vehicle charging could result in changes in the optimal generation mix results presented in chapter 3.

While these socio-economic effects in electricity demand were not explicitly analyzed in this work, it could be valuable to include them in a more detailed analysis. Possible feed-

back effects between climate change and these socio-economic factors could change some of the results presented in this thesis. The modeling framework presented in this thesis could be extended to include specific socio-economic scenarios in the simulation of future electricity demand.

Another limitation of this analysis was the definition of the set of future candidate technologies to invest in the capacity expansion model in chapter 3. I only considered as candidate technologies to invest those that are at a current mature development state. For example, I did not include energy storage (i.e., batteries), fuel cells, next-generation nuclear, among others. Including these additional technologies would be straightforward in our modeling framework, as long as there is reliable data available. Adding additional candidate technologies could change the tradeoff costs discussed in chapters 3 and 4.

The simulations in chapters 3 and 4 did not include transmission constraints, nor changes in solar and wind generation because of climate change. Transmission capacity is sensitive to ambient air temperature and climate change could result additional transmission restrictions. Climate change could also impact solar and wind generation potentials. However, the effects on solar and wind generators are not as clear as in other types of power plants. Past studies have disagreed on the directions of the impacts of climate change on solar and wind energy in the U.S. [24]. Particularly, in the southeast U.S. some studies have found an increase in solar generation potential under climate change scenarios. Incorporating the effects on transmission, wind, and solar in our modeling framework could be the subject of future extensions of this work.

Finally, this analysis focused on the southeast U.S. While climate change will affect the power sector in all regions in the U.S., impacts will vary by region. Different regions have specific vulnerabilities. These vulnerabilities depend on changes to regional climates and the types of energy systems in each region. Therefore, the conclusions presented in this thesis should not be extended to other areas in the U.S. However, the modeling framework

presented in this thesis can easily be extended to other regions of the country.

Climate change and extreme weather pose a serious threat to the U.S. power system. In order to design an electricity grid that is resilient to the impacts of climate change, planning agents must understand the specific vulnerabilities of electricity grid to the changes in the climate condition. Vulnerabilities in different parts of the power system could interact with one another and result in compounding risks. Therefore, it is important to perform system-wide integrated analysis such as the one performed in this thesis in order to inform the decisions of planning agents in the power sector. Such informed planning decisions will be essential to build a 21st grid that is able to supply electricity to end users in a reliable and affordable way.

Bibliography

[1] John T. Abatzoglou. "Development of gridded surface meteorological data for ecological applications and modelling". In: *International Journal of Climatology* 33.1 (Jan. 2013), pp. 121–131. ISSN: 08998418. DOI: 10.1002/joc.3413. URL: http://doi.wiley.com/10.1002/joc.3413.

[2] John T. Abatzoglou and Timothy J. Brown. "A comparison of statistical downscaling methods suited for wildfire applications". In: *International Journal of Climatology* 32.5 (Apr. 2012), pp. 772–780. ISSN: 08998418. DOI: 10.1002/joc.2312. URL: http://doi.wiley.com/10.1002/joc.2312.

[3] Melissa R. Allen et al. "Impacts of climate change on sub-regional electricity demand and distribution in the southern United States". In: *Nature Energy* 1.8 (2016). ISSN: 20587546. DOI: 10.1038/nenergy.2016.103. URL: www.nature.com/natureenergy.

[4] Anthony D. Amato et al. "Regional energy demand responses to climate change: Methodology and application to the commonwealth of massachusetts". In: *Climatic Change* 71.1-2 (2005), pp. 175–201. ISSN: 01650009. DOI: 10.1007/s10584-005-5931-2.

[5] Anin Aroonruengsawat and Maximilian Auffhammer. "Impacts of Climate Change on Residential Electricity Consumption: Evidence from Billing Data". In: *The Economics of Climate Change: Adaptations Past and Present*. Ed. by Gary D Libecap

and Richard H Steckel. University of Chicago Press, May 2011, pp. 311–342. DOI: 10.7208/chicago/9780226479903.001.0001. URL: http://www.nber.org/chapters/c11991.

[6] Maximilian Auffhammer, Patrick Baylis, and Catherine H. Hausman. "Climate change is projected to have severe impacts on the frequency and intensity of peak electricity demand across the United States". In: *Proceedings of the National Academy of Sciences* 114.8 (2017), pp. 1886–1891. ISSN: 0027-8424. DOI: 10.1073/pnas.1613193114. URL: https://www.pnas.org/content/pnas/114/8/1886.full.pdf.

[7] Maximilian Auffhammer et al. "Using weather data and climate model output in economic analyses of climate change". English. In: *Review of Environmental Economics and Policy* 7.2 (2013), pp. 181–198. ISSN: 17506816. DOI: 10.1093/reep/ret016. URL: https://academic.oup.com/reep/article-lookup/doi/10.1093/reep/ret016.

[8] Kristen Averyt et al. *Freshwater Use by U.S. Power Plants: Electricity's Thirst for a Precious Resource*. Tech. rep. Union of Concerned Scientists, 2011. URL: https://www.ucsusa.org/clean%7B%5C_%7Denergy/our-energy-choices/energy-and-water-use/freshwater-use-by-us-power-plants.html.

[9] P J Balducci et al. *Electrical Power Interruption Cost Estimates for Individual Industries, Sectors, and U.S. Economy*. Tech. rep. Richland, WA: Pacific Northwest National Laboratory (PNNL), Feb. 2002. DOI: 10.2172/926127. URL: http://www.osti.gov/servlets/purl/926127-BH7Ndx/.

[10] Matthew D. Bartos and Mikhail V. Chester. "Impacts of climate change on electric power supply in the Western United States". In: *Nature Climate Change* 5.8 (Aug. 2015), pp. 748–752. ISSN: 17586798. DOI: 10.1038/nclimate2648. URL: http://www.nature.com/articles/nclimate2648.

[11] Michael Beenstock, Ephraim Goldin, and Yoel Haitovsky. "Response bias in a conjoint analysis of power outages". In: *Energy Economics* 20.2-6 (Apr. 1998), pp. 135–156. ISSN: 01409883. DOI: 10.1016/s0140-9883(97)00017-0.

[12] David B. Belzer, Michael J. Scott, and Ronald D. Sands. "Climate change impacts on U.S. commercial building energy consumption: An analysis using sample survey data". In: *Energy Sources* 18.2 (1996), pp. 177–201. ISSN: 00908312. DOI: 10.1080/00908319608908758.

[13] Andrew Bennett et al. *METSIM: Meteorology Simulator (Version 2.0.0)*. 2019. URL: http://doi.org/10.5281/zenodo.3247806.

[14] Seth Blumsack, Constantine Samaras, and Paul Hines. *Long-term electric system investments to support Plug-in Hybrid Electric Vehicles*. 2008. DOI: 10.1109/PES.2008.4596906. URL: http://ieeexplore.ieee.org/document/4596906/.

[15] Theodore J. Bohn et al. "Global evaluation of MTCLIM and related algorithms for forcing of ecological and hydrological models". English. In: *Agricultural and Forest Meteorology* 176 (2013), pp. 38–49. ISSN: 01681923. DOI: 10.1016/j.agrformet.2013.03.003. URL: http://linkinghub.elsevier.com/retrieve/pii/S0168192313000579.

[16] Bonneville Power Administration. *BPA prepares for a changing climate*. 2014. URL: https://www.bpa.gov/news/newsroom/Pages/BPA-prepares-for-a-changing-climate.aspx.

[17] Carnegie Mellon University. *Integrated Environmental Control Model (IECM)*. Pittsburgh, PA, 2018. URL: http://cmu.edu/epp/iecm/index.html.

[18] Rui Castro, Sérgio Faias, and Jorge Esteves. "The cost of electricity interruptions in Portugal: Valuing lost load by applying the production-function approach". In: *Utilities Policy* 40 (June 2016), pp. 48–57. ISSN: 09571787. DOI: 10.1016/j.jup.2016.04.003.

[19] Shankar N. Chandramowli and Frank A. Felder. "Impact of climate change on electricity systems and markets - A review of models and forecasts". English. In: *Sustainable Energy Technologies and Assessments* 5 (2014), pp. 62–74. ISSN: 22131388. DOI: 10.1016/j.seta.2013.11.003. URL: http://linkinghub.elsevier.com/retrieve/pii/S2213138813000805.

[20] Vaibhav Chaturvedi et al. "Long term building energy demand for India: Disaggregating end use energy services in an integrated assessment modeling framework". English. In: *Energy Policy* 64 (Jan. 2014), pp. 226–242. ISSN: 03014215. DOI: 10.1016/j.enpol.2012.11.021. URL: http://linkinghub.elsevier.com/retrieve/pii/S030142151200986X.

[21] Leon Clarke et al. "Effects of long-term climate change on global building energy expenditures". English. In: *Energy Economics* 72 (2018), pp. 667–677. ISSN: 01409883. DOI: 10.1016/j.eneco.2018.01.003. URL: https://linkinghub.elsevier.com/retrieve/pii/S0140988318300112.

[22] Jane L. Corwin and William T Miles. *Impact Assessment of the 1977 New York City Blackout*. Tech. rep. Washington, DC (United States): Washington Procurement Operations Office, July 1977, pp. 1–155. DOI: 10.2172/6584645. URL: http://www.osti.gov/servlets/purl/6584645/.

[23] Michael T. Craig, Paulina Jaramillo, and Bri Mathias Hodge. "Carbon dioxide emissions effects of grid-scale electricity storage in a decarbonizing power system". In: *Environmental Research Letters* 13.1 (Jan. 2018), p. 014004. ISSN: 17489326. DOI: 10.1088/1748-9326/aa9a78. URL: http://stacks.iop.org/1748-9326/13/i=1/a=014004?key=crossref.d76684669dfe1d7287c7907ff6e3e771.

[24] Michael T. Craig et al. "A review of the potential impacts of climate change on bulk power system planning and operations in the United States". In: *Renewable and Sustainable Energy Reviews* 98 (Dec. 2018), pp. 255–267. ISSN: 18790690. DOI:

10.1016/j.rser.2018.09.022. URL: https://www.sciencedirect.com/science/article/pii/S1364032118306701.

[25] Michael T. Craig et al. "Effects on power system operations of potential changes in wind and solar generation potential under climate change". In: *Environmental Research Letters* 14.3 (Mar. 2019). ISSN: 17489326. DOI: 10.1088/1748-9326/aaf93b.

[26] Christopher Daly et al. "Physiographically sensitive mapping of climatological temperature and precipitation across the conterminous United States". English. In: *International Journal of Climatology* 28.15 (2008), pp. 2031–2064. ISSN: 10970088. DOI: 10.1002/joc.1688. URL: https://rmets.onlinelibrary.wiley.com/doi/full/10.1002/joc.1688.

[27] Melissa Dell, Benjamin F. Jones, and Benjamin A. Olken. " What Do We Learn from the Weather? The New Climate-Economy Literature ? " In: *Journal of Economic Literature* 52.3 (Sept. 2014), pp. 740–798. ISSN: 0022-0515. DOI: 10.1257/jel.52.3.740. URL: http://pubs.aeaweb.org/doi/abs/10.1257/jel.52.3.740.

[28] Tyler A. DeNooyer et al. "Integrating water resources and power generation: The energy-water nexus in Illinois". In: *Applied Energy* 162 (Jan. 2016), pp. 363–371. ISSN: 03062619. DOI: 10.1016/j.apenergy.2015.10.071. URL: https://www.sciencedirect.com/science/article/pii/S0306261915012982.

[29] James A. Dirks et al. "Impacts of climate change on energy consumption and peak demand in buildings: A detailed regional approach". English. In: *Energy* 79.C (2015), pp. 20–32. ISSN: 03605442. DOI: 10.1016/j.energy.2014.08.081. URL: http://linkinghub.elsevier.com/retrieve/pii/S0360544214010469.

[30] Caroline Draxl et al. "The Wind Integration National Dataset (WIND) Toolkit". In: *Applied Energy* 151 (Aug. 2015), pp. 355–366. ISSN: 0306-2619. DOI: 10.1016/

J.APENERGY.2015.03.121. URL: https://www.sciencedirect.com/science/article/pii/S0306261915004237?via%7B%5C%%7D3Dihub.

[31] Energy Information Administration. *Form EIA-923 Detailed Data with Previous Form Data (EIA-906/920)*. 2017. URL: https://www.eia.gov/electricity/data/eia923/.

[32] Jiyong Eom et al. "China's building energy demand: Long-term implications from a detailed assessment". English. In: *Energy* 46.1 (2012), pp. 405–419. ISSN: 03605442. DOI: 10.1016/j.energy.2012.08.009. URL: http://linkinghub.elsevier.com/retrieve/pii/S0360544212006214.

[33] Federal Energy Regulatory Commission. *Form No. 714 - Annual Electric Balancing Authority Area and Planning Area Report*. 2016. URL: http://www.ferc.gov/docs-filing/forms/form-714/data.asp.

[34] Guido Franco and Alan H. Sanstad. "Climate change and electricity demand in California". In: *Climatic Change* 87.1 SUPPL (2007), pp. 139–151. ISSN: 01650009. DOI: 10.1007/s10584-007-9364-y.

[35] Graeme Guthrie. "Real options analysis of climate-change adaptation: investment flexibility and extreme weather events". In: *Climatic Change* 156.1-2 (Sept. 2019), pp. 231–253. ISSN: 15731480. DOI: 10.1007/s10584-019-02529-z.

[36] Stanton W. Hadley and Alexandra A. Tsvetkova. "Potential Impacts of Plug-in Hybrid Electric Vehicles on Regional Power Generation". English. In: *Electricity Journal* 22.10 (Dec. 2009), pp. 56–68. ISSN: 10406190. DOI: 10.1016/j.tej.2009.10.011. URL: http://linkinghub.elsevier.com/retrieve/pii/S104061900900267X.

[37] Stanton W. Hadley et al. "Responses of energy use to climate change: A climate modeling study". English. In: *Geophysical Research Letters* 33.17 (2006), p. 270. ISSN: 00948276. DOI: 10.1029/2006GL026652. URL: http://doi.wiley.com/10.1029/2006GL026652.

[38] Shem Heiple and David J. Sailor. "Using building energy simulation and geospatial modeling techniques to determine high resolution building sector energy consumption profiles". English. In: *Energy and Buildings* 40.8 (2008), pp. 1426–1436. ISSN: 03787788. DOI: 10.1016/j.enbuild.2008.01.005. URL: http://linkinghub.elsevier.com/retrieve/pii/S0378778808000200.

[39] Candise L. Henry and Lincoln F. Pratson. "Differentiating the Effects of Climate Change-Induced Temperature and Streamflow Changes on the Vulnerability of Once-Through Thermoelectric Power Plants". In: *Environmental Science & Technology* (2019). ISSN: 0013-936X. DOI: 10.1021/acs.est.8b05718. URL: https://pubs.acs.org/sharingguidelines.

[40] Eric S. Hittinger and Inês M. L. Azevedo. "Bulk Energy Storage Increases United States Electricity System Emissions". In: *Environmental Science & Technology* 49.5 (Mar. 2015), pp. 3203–3210. ISSN: 0013-936X. DOI: 10.1021/es505027p. URL: https://pubs.acs.org/doi/10.1021/es505027p.

[41] J Scott Holladay and Rebecca J Davis. *Energy Intensity and Electricity Consumption in Tennessee*. Tech. rep. 2016. URL: http://bakercenter.utk.edu/wp-content/uploads/2016/03/PolicyBrief-2-16-Holladay-Final.pdf.

[42] Ching Lai Hor, Simon J. Watson, and Shanti Majithia. "Analyzing the impact of weather variables on monthly electricity demand". English. In: *IEEE Transactions on Power Systems* 20.4 (2005), pp. 2078–2085. ISSN: 08858950. DOI: 10.1109/TPWRS.2005.857397. URL: http://ieeexplore.ieee.org/lpdocs/epic03/wrapper.htm?arnumber=1525139.

[43] Hydro-Québec. *Sustainability Report 2018*. Tech. rep. 2018. URL: http://www.hydroquebec.com/data/documents-donnees/pdf/sustainability-report.pdf.

[44] IPCC. *Climate Change 2014: Synthesis Report. Contribution of Working Groups I, II and III to the Fifth Assessment Report of the Intergovernmental Panel on Cli-*

mate Change. Tech. rep. 2014. URL: http://www.ipcc.ch/pdf/assessment-report/ar5/syr/AR5_SYR_FINAL_SPM.pdf.

[45] IPCC. "Summary for Policymakers". In: *Global warming of 1.5 C. An IPCC Special Report on the impacts of global warming of 1.5 C above pre industrial levels and related global greenhouse gas emission pathways, in the context of strengthening the global response to the threat of climate change,* ed. by Valérie Masson-Delmotte et al. Geneva, Switzerland, 2018, 32 pp. URL: https://report.ipcc.ch/sr15/pdf/sr15%7B%5C_%7Dspm%7B%5C_%7Dfinal.pdf.

[46] Morna Isaac and Detlef P. van Vuuren. "Modeling global residential sector energy demand for heating and air conditioning in the context of climate change". In: *Energy Policy* 37.2 (2009), pp. 507–521. ISSN: 03014215. DOI: 10.1016/j.enpol.2008.09.051.

[47] IWGSCC. *Social Cost of Carbon for Regulatory Impact Analysis Under Executive Order 12866*. Tech. rep. 2010, p. 53. URL: https://www.epa.gov/sites/production/files/2016-12/documents/scc%7B%5C_%7Dtsd%7B%5C_%7D2010.pdf.

[48] T. A. Kimmell and J. A. Veil. *Impact of drought on U.S. steam electric power plant cooling water intakes and related water resource management issues*. Tech. rep. Argonne, IL: Argonne National Laboratory (ANL), Apr. 2009. DOI: 10.2172/951252. URL: http://www.osti.gov/servlets/purl/951252-CV8mWm/.

[49] Hagen Koch and Stefan Vögele. "Dynamic modelling of water demand, water availability and adaptation strategies for power plants to global change". In: *Ecological Economics* 68.7 (May 2009), pp. 2031–2039. ISSN: 09218009. DOI: 10.1016/j.ecolecon.2009.02.015. URL: https://www.sciencedirect.com/science/article/pii/S0921800909000639?via%7B%5C%%7D3Dihub.

[50] Hagen Koch et al. "Trends in water demand and water availability for power plants-scenario analyses for the German capital Berlin". In: *Climatic Change* 110.3-4 (Feb.

2012), pp. 879–899. ISSN: 01650009. DOI: 10.1007/s10584-011-0110-0. URL: http://link.springer.com/10.1007/s10584-011-0110-0.

[51] US National Renewable Energy Laboratory. *2018 Annual Technology Baseline*. Golden, CO: National Renewable Energy Laboratory, 2018. URL: https://atb.nrel.gov/.

[52] Maryse Labriet et al. "Worldwide impacts of climate change on energy for heating and cooling". English. In: *Mitigation and Adaptation Strategies for Global Change* 20.7 (Oct. 2013), pp. 1111–1136. ISSN: 13812386. DOI: 10.1007/s11027-013-9522-7. URL: http://link.springer.com/10.1007/s11027-013-9522-7.

[53] Eimear Leahy and Richard S.J. Tol. "An estimate of the value of lost load for Ireland". In: *Energy Policy* 39.3 (Mar. 2011), pp. 1514–1520. ISSN: 03014215. DOI: 10.1016/j.enpol.2010.12.025.

[54] Anthony Leiserowitz et al. *Climate change in the American mind: December 2018*. Tech. rep. New Haven, CT: Yale University and George Mason University, 2018. URL: https://climatecommunication.yale.edu/publications/climate-change-in-the-american-mind-december-2018/.

[55] Hongyi Li et al. "A Physically Based Runoff Routing Model for Land Surface and Earth System Models". In: *Journal of Hydrometeorology* 14.3 (June 2013), pp. 808–828. ISSN: 1525-755X. DOI: 10.1175/jhm-d-12-015.1. URL: http://journals.ametsoc.org/doi/abs/10.1175/JHM-D-12-015.1.

[56] Xu Liang et al. "A simple hydrologically based model of land surface water and energy fluxes for general circulation models". In: *Journal of Geophysical Research* 99.D7 (July 1994), p. 14415. ISSN: 0148-0227. DOI: 10.1029/94jd00483. URL: http://doi.wiley.com/10.1029/94JD00483.

[57] Aviva Loew. "Tradeoffs in energy, water use, and cost at thermoelectric power plants". English. PhD thesis. 2018, p. 155. ISBN: 9780438533042. DOI: 10.1107/s01087681

99006072/na00905sup6.fcf. URL: https://search.proquest.com/docview/2123082025?accountid=9902.

[58] Aviva Loew, Paulina Jaramillo, and Haibo Zhai. "Marginal costs of water savings from cooling system retrofits: A case study for Texas power plants". In: *Environmental Research Letters* 11.10 (Oct. 2016), p. 104004. ISSN: 17489326. DOI: 10.1088/1748-9326/11/10/104004. URL: http://stacks.iop.org/1748-9326/11/i=10/a=104004?key=crossref.b52ecf967b1c0e1276c76c01383db077.

[59] Aviva Loew et al. "Fossil Fuel-fired Power Plant Operations Under A Changing Climate". In: *Climatic Change* (Oct. 2019). Manuscript submitted for publication.

[60] London Economics International LLC. *Estimating the value of lost load*. Tech. rep. 2013, pp. 3–76. URL: www.londoneconomics.com.

[61] Roger Lueken, Jay Apt, and Fallaw Sowell. "Robust resource adequacy planning in the face of coal retirements". English. In: *Energy Policy* 88 (2016), pp. 371–388. ISSN: 03014215. DOI: 10.1016/j.enpol.2015.10.025. URL: http://linkinghub.elsevier.com/retrieve/pii/S0301421515301543.

[62] J. Macknick et al. "Operational water consumption and withdrawal factors for electricity generating technologies: A review of existing literature". In: *Environmental Research Letters* 7.4 (Dec. 2012), p. 045802. ISSN: 17489326. DOI: 10.1088/1748-9326/7/4/045802. URL: http://stacks.iop.org/1748-9326/7/i=4/a=045802?key=crossref.6f4ebd5836ab24141e19d95fd1e65709.

[63] N. Madden, A. Lewis, and M. Davis. "Thermal effluent from the power sector: An analysis of once-through cooling system impacts on surface water temperature". In: *Environmental Research Letters* 8.3 (Sept. 2013), p. 035006. ISSN: 17489326. DOI: 10.1088/1748-9326/8/3/035006. URL: http://stacks.iop.org/1748-9326/8/i=3/a=035006?key=crossref.d2aef1361a05ed203ffe916c5f56e827.

[64] Trieu Mai et al. *Electrification Futures Study: Scenarios of Electric Technology Adoption and Power Consumption for the United States*. Tech. rep. Golden, CO: National Renewable Energy Laboratory, 2018. URL: https://www.nrel.gov/docs/fy18osti/71500.pdf..

[65] Johanna L. Mathieu et al. "Quantifying changes in building electricity use, with application to demand response". In: *IEEE Transactions on Smart Grid* 2.3 (2011), pp. 507–518. ISSN: 19493053. DOI: 10.1109/TSG.2011.2145010. URL: http://ieeexplore.ieee.org/document/5772947/.

[66] James McCall, Jordan Macknick, and Daniel Hillman. *Water-Related Power Plant Curtailments: An Overview of Incidents and Contributing Factors*. Tech. rep. 2016. DOI: 10.2172/1338176. URL: http://www.osti.gov/servlets/purl/1338176/.

[67] James McFarland et al. "Impacts of rising air temperatures and emissions mitigation on electricity demand and supply in the United States: a multi-model comparison". English. In: *Climatic Change* 131.1 (July 2015), pp. 111–125. ISSN: 15731480. DOI: 10.1007/s10584-015-1380-8. URL: http://link.springer.com/10.1007/s10584-015-1380-8.

[68] Jerry M. Melillo, Terese (T.C.) Richmond, and Gary W. Yohe, eds. *Climate Change Impacts in the United States: The Third National Climate Assessment*. 2014, 841 pp. ISBN: 9780160924026. DOI: 10.7930/J0Z31WJ2.

[69] Ariel Miara et al. "Climate and water resource change impacts and adaptation potential for US power supply". English. In: *Nature Climate Change* 7.11 (2017), pp. 793–798. ISSN: 17586798. DOI: 10.1038/nclimate3417. URL: https://www.nature.com/articles/nclimate3417.

[70] S. Mirasgedis et al. "Modeling framework for estimating impacts of climate change on electricity demand at regional level: Case of Greece". English. In: *Energy Conversion and Management* 48.5 (2007), pp. 1737–1750. ISSN: 01968904. DOI: 10.

1016/j.enconman.2006.10.022. URL: http://linkinghub.elsevier.com/retrieve/pii/S0196890406003414.

[71] Kenneth E. Mitchell. "The multi-institution North American Land Data Assimilation System (NLDAS): Utilizing multiple GCIP products and partners in a continental distributed hydrological modeling system". In: *Journal of Geophysical Research* 109.D7 (2004), p. 7449. ISSN: 0148-0227. DOI: 10.1029/2003jd003823.

[72] Whitney K. Newey and Kenneth D. West. "A Simple, Positive Semi-Definite, Heteroskedasticity and Autocorrelation Consistent Covariance Matrix". In: *Econometrica* 55.3 (2006), p. 703. ISSN: 00129682. DOI: 10.2307/1913610. URL: http://www.jstor.org/stable/1913610.

[73] Ryan J. Niemeyer et al. "A Thermally Stratified Reservoir Module for Large-Scale Distributed Stream Temperature Models With Application in the Tennessee River Basin". In: *Water Resources Research* 54.10 (Oct. 2018), pp. 8103–8119. ISSN: 19447973. DOI: 10.1029/2018WR022615. URL: https://onlinelibrary.wiley.com/doi/abs/10.1029/2018WR022615.

[74] Marten Ovaere et al. "How detailed value of lost load data impact power system reliability decisions". In: *Energy Policy* 132 (Sept. 2019), pp. 1064–1075. ISSN: 03014215. DOI: 10.1016/j.enpol.2019.06.058.

[75] Suchao Parkpoom and Gareth P. Harrison. "Analyzing the impact of climate change on future electricity demand in Thailand". English. In: *IEEE Transactions on Power Systems* 23.3 (2008), pp. 1441–1448. ISSN: 08858950. DOI: 10.1109/TPWRS.2008.922254. URL: http://ieeexplore.ieee.org/articleDetails.jsp?arnumber=4493403.

[76] Raphael Payet-Burin et al. "Optimization of regional water - power systems under cooling constraints and climate change". In: *Energy* 155 (July 2018), pp. 484–494. ISSN: 03605442. DOI: 10.1016/j.energy.2018.05.043. URL: https://www.

sciencedirect.com/science/article/pii/S0360544218308636?via%7B%5C%%7D3Dihub.

[77] Jakob Peter. "How does climate change affect electricity system planning and optimal allocation of variable renewable energy?" In: *Applied Energy* 252 (Oct. 2019), p. 113397. ISSN: 03062619. DOI: 10.1016/j.apenergy.2019.113397. URL: https://www.sciencedirect.com/science/article/pii/S0306261919310712?via%7B%5C%%7D3Dihub.

[78] PRISM Climate Group. *PRISM Climate Data*. 2016. URL: http://www.prism.oregonstate.edu/.

[79] Francisco Ralston Fonseca et al. "Seasonal effects of climate change on intra-day electricity demand patterns". English. In: *Climatic Change* 33.1 (2019), pp. 1–17. ISSN: 1573-1480. DOI: 10.1007/s10584-019-02413-w. URL: https://doi.org/10.1007/s10584-019-02413-w.

[80] Burton Richter. "Climate modeling". In: *Beyond Smoke and Mirrors: Climate Change and Energy in the 21st Century*. Cambridge University Press, 2010, pp. 16–26. DOI: 10.1017/CBO9780511802638.004.

[81] David Roberts. *After rising for 100 years, electricity demand is flat. Utilities are freaking out.* 2018. URL: https://www.vox.com/energy-and-environment/2018/2/27/17052488/electricity-demand-utilities%7B%5C%%7D0Ahttp://files/880/electricity-demand-utilities.html.

[82] Matthias Ruth and Ai Chen Lin. "Regional energy demand and adaptations to climate change: Methodology and application to the state of Maryland, USA". In: *Energy Policy* 34.17 (2006), pp. 2820–2833. ISSN: 03014215. DOI: 10.1016/j.enpol.2005.04.016.

[83] D. J. Sailor and A. A. Pavlova. "Air conditioning market saturation and long-term response of residential cooling energy demand to climate change". English. In: *En-*

ergy 28.9 (2003), pp. 941–951. ISSN: 03605442. DOI: 10.1016/S0360-5442(03)00033-1. URL: http://linkinghub.elsevier.com/retrieve/pii/S0360544203000331.

[84] David J. Sailor and J. Ricardo Muñoz. "Sensitivity of electricity and natural gas consumption to climate in the U.S.A. - Methodology and results for eight states". In: *Energy* 22.10 (1997), pp. 987–998. ISSN: 03605442. DOI: 10.1016/S0360-5442(97)00034-0.

[85] Roberto Schaeffer et al. "Energy sector vulnerability to climate change: A review". English. In: *Energy* 38.1 (2012), pp. 1–12. ISSN: 03605442. DOI: 10.1016/j.energy.2011.11.056. URL: http://linkinghub.elsevier.com/retrieve/pii/S0360544211007870.

[86] Michael J. Scott, Laura E. Wrench, and Donald L. Hadley. "Effects of climate change on commercial building energy demand". In: *Energy Sources* 16.3 (1994), pp. 317–332. ISSN: 15210510. DOI: 10.1080/00908319408909081.

[87] Kyle Siler-Evans, Inês Lima Azevedo, and M. Granger Morgan. "Marginal emissions factors for the U.S. electricity system". In: *Environmental Science and Technology* 46.9 (May 2012), pp. 4742–4748. ISSN: 0013936X. DOI: 10.1021/es300145v.

[88] Kyle Siler-Evans et al. "Regional variations in the health, environmental, and climate benefits of wind and solar generation". In: *Proceedings of the National Academy of Sciences* 110.29 (July 2013), pp. 11768–11773. ISSN: 0027-8424. DOI: 10.1073/pnas.1221978110.

[89] DSIRE(Database of State Incentives for Renewables & Efficiency). *Business Energy Investment Tax Credit (ITC)*. 2018. URL: http://programs.dsireusa.org/system/program/detail/658 (visited on 12/12/2018).

[90] Nicholas Stern. "Economics, Ethics and Climate Change". In: *The Economics of Climate Change: The Stern Review*. Cambridge University Press, 2007, pp. 25–45. DOI: 10.1017/CBO9780511817434.006.

[91] Michael J Sullivan, Josh Schellenberg, and Marshall Macdonald Blundell. *Updated Value of Service Reliability Estimates for Electric Utility Customers in the United States*. Tech. rep. Berkeley, CA (United States): Lawrence Berkeley National Laboratory (LBNL), Jan. 2015. DOI: 10.2172/1172643. URL: http://www.osti.gov/servlets/purl/1172643/.

[92] Mili-Ann M. Tamayao et al. "Regional Variability and Uncertainty of Electric Vehicle Life Cycle CO2 Emissions across the United States". In: *Environmental Science & Technology* 49.14 (July 2015), pp. 8844–8855. ISSN: 0013-936X. DOI: 10.1021/acs.est.5b00815. URL: https://pubs.acs.org/doi/10.1021/acs.est.5b00815.

[93] Karl E. Taylor, Ronald J. Stouffer, and Gerald A. Meehl. "An overview of CMIP5 and the experiment design". English. In: *Bulletin of the American Meteorological Society* 93.4 (2012), pp. 485–498. ISSN: 00030007. DOI: 10.1175/BAMS-D-11-00094.1. URL: http://journals.ametsoc.org/doi/abs/10.1175/BAMS-D-11-00094.1.

[94] Tennesse Valley Authority. *Climate Change Adaptation Action Plan*. Tech. rep. 2016. URL: https://www.tva.gov/file%7B%5C_%7Dsource/TVA/Site%20Content/About%20TVA/Guidelines%20and%20Reports/Sustainability%20Plans%20and%20Performance/pdf/tva%7B%5C_%7Dclimate%7B%5C_%7Dadaptation%7B%5C_%7Dplan%7B%5C_%7D2016%7B%5C_%7D%7B%5C_%7Dfinal.pdf.

[95] Marcus J. Thatcher. "Modelling changes to electricity demand load duration curves as a consequence of predicted climate change for Australia". In: *Energy* 32.9 (2007), pp. 1647–1659. ISSN: 03605442. DOI: 10.1016/j.energy.2006.12.005.

[96] I. Tobin et al. "Vulnerabilities and resilience of European power generation to 1.5 °C, 2 °C and 3 °C warming". In: *Environmental Research Letters* 13.4 (Apr. 2018), p. 044024. ISSN: 17489326. DOI: 10.1088/1748-9326/aab211. URL: http://stacks.iop.org/1748-9326/13/i=4/a=044024?key=crossref.7132b6b600e244c44cef30e5d9da6a42.

[97] S. W.D. Turner et al. "Compound climate events transform electrical power shortfall risk in the Pacific Northwest". In: *Nature Communications* 10.1 (Dec. 2019), p. 8. ISSN: 20411723. DOI: 10.1038/s41467-018-07894-4. URL: http://www.nature.com/articles/s41467-018-07894-4.

[98] U.S. Energy Information Administration (EIA). *Hydroelectric generators are among the United States' oldest power plants*. 2017. URL: https://www.eia.gov/todayinenergy/detail.php?id=30312 (visited on 05/16/2019).

[99] US Department of Energy. *Climate Change and the Electricity Sector: Guide for Climate Change Resilience Planning*. Tech. rep. Sept. 2016. URL: https://www.energy.gov/sites/prod/files/2016/10/f33/Climate%20Change%20and%20the%20Electricity%20Sector%20Guide%20for%20Climate%20Change%20Resilience%20Planning%20September%202016%7B%5C_%7D0.pdf.

[100] US Department of Energy. *Climate Change and the U.S. Energy Sector: Regional Vulnerabilities and Resilience Solutions*. Tech. rep. 2015, p. 193. URL: http://energy.gov/sites/prod/files/2015/10/f27/Regional%7B%5C_%7DClimate%7B%5C_%7DVulnerabilities%7B%5C_%7Dand%7B%5C_%7DResilience%7B%5C_%7DSolutions%7B%5C_%7D0.pdf.

[101] US Department of Energy. *Hydropower Vision. A New Chapter for America's 1st Renewable Electricity Source*. Tech. rep. 2016, pp. 1–348. DOI: DOE/GO-102016-4869. URL: https://www.energy.gov/sites/prod/files/2016/10/f33/Hydropower-Vision-Full-Report-10212016.pdf.

[102] US Energy Information Administration. *Electric Power Annual 2017*. Tech. rep. 2018. URL: https://www.eia.gov/electricity/annual/archive/pdf/03482017.pdf.

[103] US Energy Information Administration. *Winter residential electricity consumption expected to increase from last winter*. 2016. URL: https://www.eia.gov/todayinenergy/detail.php?id=29112 (visited on 12/17/2019).

[104] US Energy Information Administration (EIA). *Form EIA-860 detailed data with previous form data (EIA-860A/860B)*. 2019. URL: https://www.eia.gov/electricity/data/eia860/ (visited on 07/22/2019).

[105] US Environmental Protection Agency (EPA). *Documentation for EPA's Power Sector Modeling Platform v6: Using the Integrated Planning Model*. 2018. URL: https://www.epa.gov/sites/production/files/2018-05/documents/epa%7B%5C_%7Dplatform%7B%5C_%7Dv6%7B%5C_%7Ddocumentation%7B%5C_%7D-%7B%5C_%7Dall%7B%5C_%7Dchapters%7B%5C_%7Dv15%7B%5C_%7Dmay%7B%5C_%7D31%7B%5C_%7D10-30%7B%5C_%7Dam.pdf.

[106] US Environmental Protection Agency (EPA). *Emissions & Generation Resource Integrated Database*. English. 2016. URL: https://www.epa.gov/energy/emissions-generation-resource-integrated-database-egrid.

[107] US Environmental Protection Agency (EPA). *Inventory of U.S. Greenhouse Gas Emissions and Sinks: 1990 – 2017*. Tech. rep. 2019. URL: https://www.epa.gov/ghgemissions/inventory-us-greenhouse-gas-emissions-and-sinks.

[108] US Environmental Protection Agency (EPA). *National Electric Energy Data System (NEEDS) v6*. URL: https://www.epa.gov/airmarkets/national-electric-energy-data-system-needs-v6 (visited on 07/22/2019).

[109] US National Renewable Energy Laboratory. *Solar Power Data for Integration Studies*. 2010. URL: https://www.nrel.gov/grid/solar-power-data.html (visited on 07/15/2019).

[110] USGCRP. *Impacts, Risks, and Adaptation in the United States: Fourth National Climate Assessment, Volume II*. Ed. by David R. Reidmiller et al. Washington, DC, USA: U.S. Global Change Research Program, 2018, p. 1515. DOI: 10.7930/NCA4.2018. URL: nca2018.globalchange.gov.

[111] Michelle T.H. Van Vliet et al. "Impacts of recent drought and warm years on water resources and electricity supply worldwide". In: *Environmental Research Letters* 11.12 (Dec. 2016), p. 124021. ISSN: 17489326. DOI: 10.1088/1748-9326/11/12/124021. URL: http://stacks.iop.org/1748-9326/11/i=12/a=124021?key=crossref.fe8bf630221dcb9684ebf68a1a51870c.

[112] Michelle T.H. Van Vliet et al. "Vulnerability of US and European electricity supply to climate change". In: *Nature Climate Change* 2.9 (Sept. 2012), pp. 676–681. ISSN: 1758678X. DOI: 10.1038/nclimate1546. URL: http://www.nature.com/articles/nclimate1546.

[113] Aranya Venkatesh et al. "Implications of Near-Term Coal Power Plant Retirement for SO ¡sub¿2¡/sub¿ and NO ¡sub¿X¡/sub¿ and Life Cycle GHG Emissions". In: *Environmental Science & Technology* 46.18 (Sept. 2012), pp. 9838–9845. ISSN: 0013-936X. DOI: 10.1021/es3023539. URL: https://pubs.acs.org/doi/abs/10.1021/es3023539.

[114] M. T.H. van Vliet et al. "Multi-model assessment of global hydropower and cooling water discharge potential under climate change". In: *Global Environmental Change* 40 (Sept. 2016), pp. 156–170. ISSN: 09593780. DOI: 10.1016/j.gloenvcha.2016.07.007. URL: https://www.sciencedirect.com/science/article/pii/S0959378016301236?via%7B%5C%%7D3Dihub.

[115] N. Voisin et al. "One-Way coupling of an integrated assessment model and a water resources model: Evaluation and implications of future changes over the US Midwest". In: *Hydrology and Earth System Sciences* 17.11 (2013), pp. 4555–4575. ISSN: 10275606. DOI: 10.5194/hess-17-4555-2013. URL: www.hydrol-earth-syst-sci.net/17/4555/2013/.

[116] John R. Yearsley. "A semi-Lagrangian water temperature model for advection-dominated river systems". In: *Water Resources Research* 45.12 (Dec. 2009). ISSN: 00431397. DOI: 10.1029/2008WR007629. URL: http://doi.wiley.com/10.1029/2008WR007629.

[117] Sha Yu et al. "Scenarios of building energy demand for China with a detailed regional representation". English. In: *Energy* 67 (Apr. 2014), pp. 284–297. ISSN: 03605442. DOI: 10.1016/j.energy.2013.12.072. URL: http://linkinghub.elsevier.com/retrieve/pii/S036054421400005X.

[118] Haibo Zhai and Edward S. Rubin. "Performance and cost of wet and dry cooling systems for pulverized coal power plants with and without carbon capture and storage". In: *Energy Policy* 38.10 (2010), pp. 5653–5660. ISSN: 03014215. DOI: 10.1016/j.enpol.2010.05.013. URL: www.elsevier.com/locate/enpol.

[119] Haibo Zhai, Edward S. Rubin, and Peter L. Versteeg. "Water use at pulverized coal power plants with postcombustion carbon capture and storage". English. In: *Environmental Science and Technology* 45.6 (2011), pp. 2479–2485. ISSN: 0013936X. DOI: 10.1021/es1034443. URL: http://pubs.acs.org/doi/abs/10.1021/es1034443.

[120] Yuyu Zhou, Jiyong Eom, and Leon Clarke. "The effect of global climate change, population distribution, and climate mitigation on building energy use in the U.S. and China". English. In: *Climatic Change* 119.3-4 (Aug. 2013), pp. 979–992. ISSN:

01650009. DOI: 10.1007/s10584-013-0772-x. URL: http://link.springer.com/10.1007/s10584-013-0772-x.

Appendix A

List of General Circulation Models

The section presents details of the different General Climate Models (GCM) used in this study. Table A.1 shows twenty different models used in our study. We obtained the output of GCMs from the Coupled Model Intercomparison Project 5 [93], spatially downscaled using the Multivariate Adaptive Constructed Analogs (MACA) method [2]. In addition, these projections were also disaggregated to hourly values using the Mountain Microclimate Simulation Model (MTCLIM) [15].

The following plots show the average seasonal air temperature simulated by each climate model in each period used in our study. They show how different models differ on their predictions of air temperature on our study region. We can see that in the summer there are a couple of models that consistently predict higher air temperatures than the rest of the climate models.

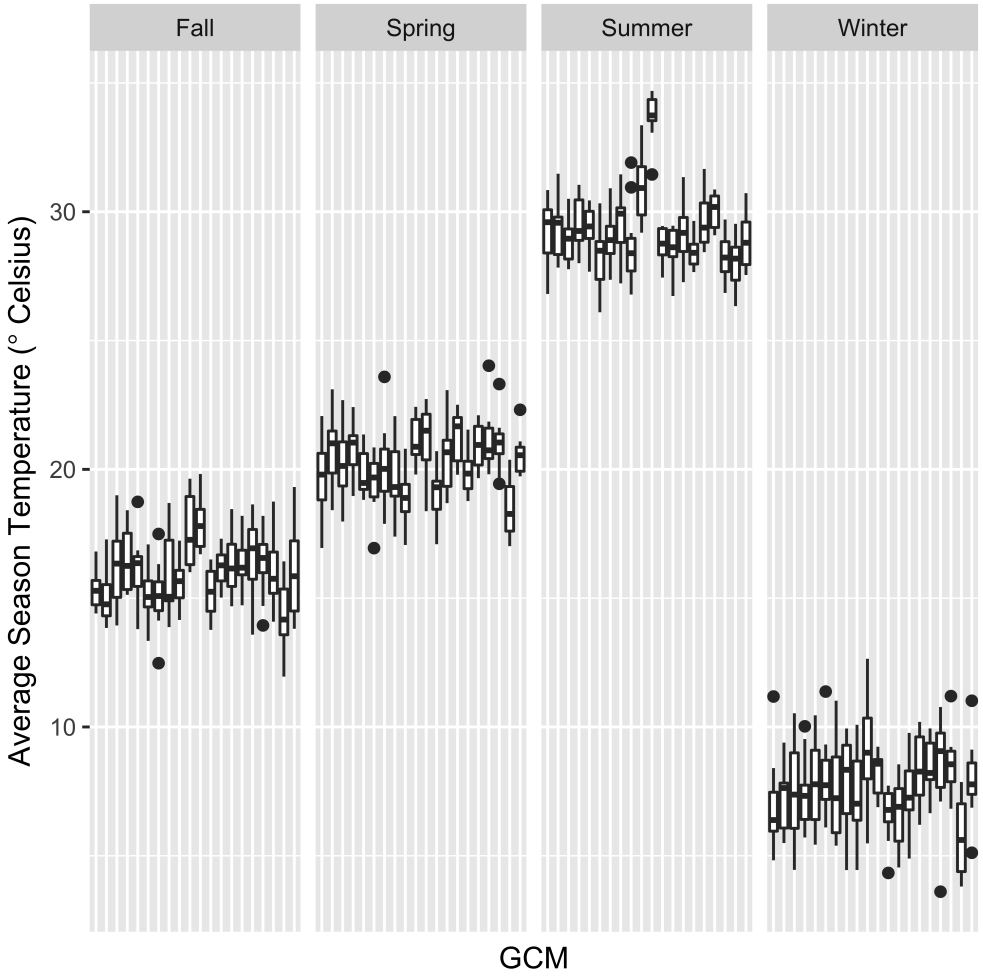

Figure A.1: Average seasonal air temperature simulated by each climate model in the period 2055-2065

Table A.1: List of GCMs used in this study

Modeling Center	Model	Institution
BCC	BCC-CSM1.1 BCC-CSM1.1(m)	Beijing Climate Center, China Meteorological Administration
CCCma	CanESM2	Canadian Centre for Climate Modelling and Analysis
CNRM-CERFACS	CNRM-CM5	Centre National de Recherches Meteorologiques / Centre Europeen de Recherche et Formation Avancees en Calcul Scientifique
CSIRO-QCCCE	CSIRO-Mk3.6.0	Commonwealth Scientific and Industrial Research Organisation in collaboration with the Queensland Climate Change Centre of Excellence
GCESS	BNU-ESM	College of Global Change and Earth System Science, Beijing Normal University
INM	INM-CM4	Institute for Numerical Mathematics
IPSL	IPSL-CM5A-LR IPSL-CM5A-MR IPSL-CM5B-LR	Institut Pierre-Simon Laplace
MIROC	MIROC5	Atmosphere and Ocean Research Institute (The University of Tokyo), National Institute for Environmental Studies, and Japan Agency for Marine-Earth Science and Technology
MIROC	MIROC-ESM MIROC-ESM-CHEM	Japan Agency for Marine-Earth Science and Technology, Atmosphere and Ocean Research Institute (The University of Tokyo), and National Institute for Environmental Studies
MRI	MRI-CGCM3	Meteorological Research Institute
NCAR	CCSM4	National Center for Atmospheric Research
NCC	NorESM1-M	Norwegian Climate Centre
NOAA GFDL	GFDL-ESM2G GFDL-ESM2M	Geophysical Fluid Dynamics Laboratory
MOHC (additional realizations by INPE)	HadGEM2-ES365 HadGEM2-CC365	Met Office Hadley Centre (additional HadGEM2-ES realizations contributed by Instituto Nacional de Pesquisas Espaciais)

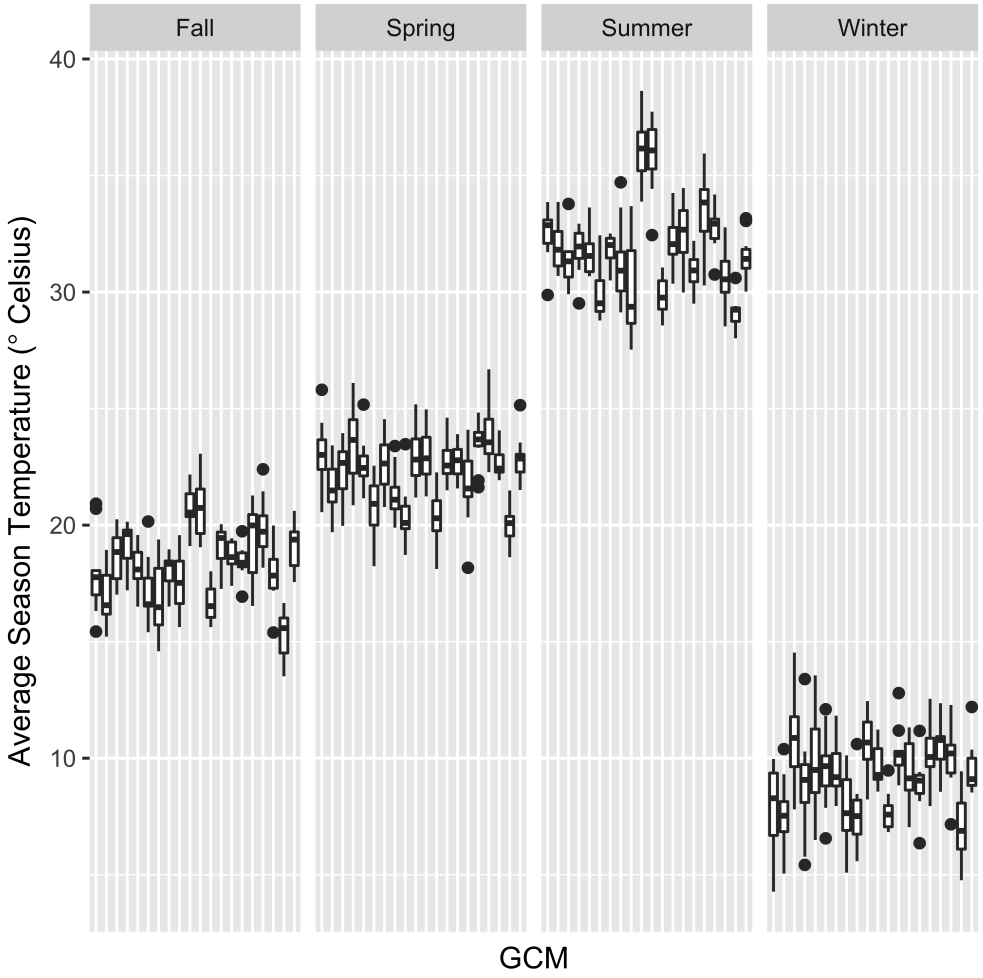

Figure A.2: Average seasonal air temperature simulated by each climate model in the period 2089-2099

Appendix B

Piecewise linear model

The relationship between hourly electricity demand and air temperature is modeled using a piecewise linear model. An important aspect of this method is that it preserves continuity at the breakpoints of the estimated piecewise linear function. Figure B.1 shows a simple example of an arbitrary piecewise linear function with two break points.

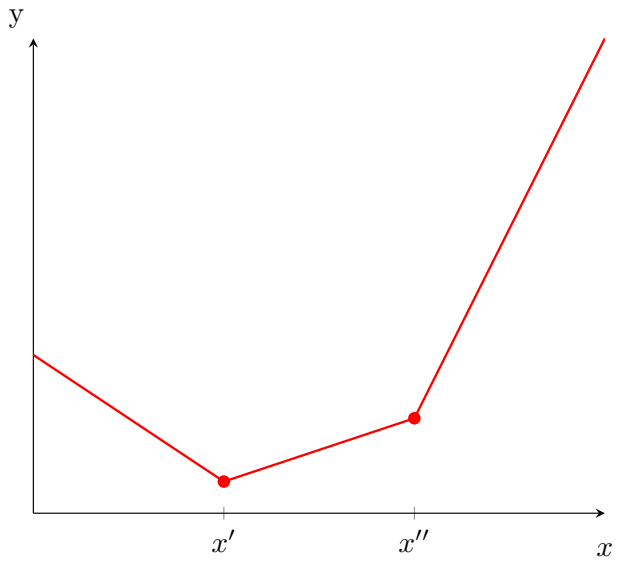

Figure B.1: Example of a piece wise linear function with two break points (x' and x'')

Equation B.1 shows the expression that we use to model this function. In our case, the

parameters β_0, δ_1, δ_2 and δ_3 are estimated using our data. $\mathbb{1}_{x>a}$ represents the indicator function and is defined as being equal to 1 when $x > a$ and zero otherwise.

$$\begin{aligned} y = \beta_0 + \delta_1 \min\{x, x'\} + \delta_2 \min\{x - x', x'' - x'\}\mathbb{1}_{x>x'} \\ + \delta_3 \min\{x - x''\}\mathbb{1}_{x>x''} \end{aligned} \tag{B.1}$$

We can see this formulation preserves continuity on the break points by analyzing one of the cases. If $x \leq x'$, then we have $y_1 = \beta_0 + \delta_1 x$. On the other hand, if $x' < x < x''$, then $y_2 = \beta_0 + \delta_1 x' + \delta_2(x - x') = (\beta_0 + \delta_1 x' - \delta_2 x') + \delta_2 x$.

Now, if we have $x \to x'^{-}$, then $y = y_1 \to \beta_0 + \delta_1 x'$. On the other hand, if $x \to x'^{+}$ then $y = y_2 \to (\beta_0 + \delta_1 x' - \delta_2 x') + \delta_2 x' = \beta_0 + \delta_1 x'$. Since both limits converge to the same value, we have preserved continuity at the breakpoint x'.

To estimate the parameters of the piecewise linear function, the air temperature variable T is decomposed into N different temperature components $T_j^c(T)$, where $j \in \{1, \ldots, N\}$ in the same manner as done in [65]. The process of decomposing the temperature into these components starts by first dividing the range of temperature values into N temperature intervals. Let B_k be the bounds of the the intervals where $k = 1, \ldots, N-1$. Then each temperature value T is decomposed using the following process:

1. If $T > B_1$, then $T_j^c(T) = B_1$. Otherwise, $T_j^c(T) = T$ and $T_j^c(T) = 0 \quad \forall\ j = 2, \ldots, N$ and the process ends.

2. For $n = 2, \ldots, N-2$, if $T > B_n$, then $T_j^c(T) = B_n - B_{n-1}$. Otherwise, $T_j^c(T) = T - B_{n-1}$ and $T_j^c(T) = 0 \quad \forall\ j = n+1, \ldots, N$ and the process ends.

3. If $T > B_{N-1}$, then $T_{N-1}^c(T) = B_{N-1} - B_{N-2}$ and $T_N^c(T) = T - B_{N-1}$

Table B.1 presents a simple numerical example of the decomposition of different tempera-

ture values.

Table B.1: Example of computation of temperature components with bounds $B_i = 10 \times i$ $i = 1, \ldots, 5$ (in arbitrary temperature units)

T	T_1^c	T_2^c	T_3^c	T_4^c	T_5^c	T_6^c
2	2	0	0	0	0	0
18	10	8	0	0	0	0
32	10	10	10	2	0	0
47	10	10	10	10	7	0
58	10	10	10	10	10	8

Appendix C

Estimated coefficients of the linear model

Table C.1 presents the estimated slopes of the piecewise linear function in each of the chosen temperature bins. Standard errors are estimated using Newey-West standard errors [72] that account for up to 14 days of serial correlation in the residuals. We tested several different values for the lag parameter (L) in the Newey-West estimator. We chose a value of $L = 336$ hours (14 days) as longer values of L did not change the standard errors significantly.

Table C.1: Estimated slopes of the piecewise linear function

Temperature Bin $[°C]$	Coefficient Value $[\frac{MW}{°C}]$	SE	p-value
$<= -30°C$	2	0.2	< 0.001
$(-30°C, 0°C]$	-596	22.1	< 0.001
$(0°C, 10°C]$	-372	11.1	< 0.001
$(10°C, 20°C]$	-60	11.3	< 0.001
$(20°C, 30°C]$	537	13.9	< 0.001
$> 30°C$	874	39.2	< 0.001
$R^2 = 0.853$			
$R^2_{adj} = 0.853$			

Appendix D

Definition of the capacity expansion scenarios

We simulated a total of six different cases encompassing two different dimensions of our problem: the climate change scenario considered, and SERC's CO_2 emission limit scenario.

Reference case (no climate change effects):

The reference case emulated the decisions of energy planners when they do not take into account the potential effects of climate change on future electricity demand and on the available capacity of thermoelectric power plants. It is supposed to be the baseline case, against which the two other cases will be compared to in order to assess the potential effects of climate change in the decisions to expand the capacity of the generator fleet.

In this reference case, we did not simulate any type of curtailments on thermoelectric power plants, which is typically the standard procedure in most capacity expansion simulations. The available capacity of these thermoelectric plants is always the same (equal to the name-

plate capacity).

The definition of the electricity demand projection was more cumbersome. Ideally, we would have used a static annual electricity demand profile that would represent a typical current electricity demand under present climate conditions (without the effects of climate change). Because we were simulating one calendar year each time (in intervals of five years), using present historical values of electricity demand would have resulted on possible selection issues. The year selected could have been a typically warm (or cold) year, which would impact the demand values we would have used on the whole simulation horizon. Also averaging several years into one single annual electricity demand profile would end up over smoothing our time series of electricity demand. Moreover, there is the issue that since our future projections with climate change are created by a regression model, there will always be differences between the historical values and the simulated ones. Ideally, we would like to use our regression model to *backcast* the electricity demand under present conditions, so that both time series are directly comparable.

In order to use the regression model to simulate present electricity demand, we needed typical weather variables to use as explanatory variables. This again will have the same issues as the ones described in the previous paragraph. Using weather variables from a single historical year will result in possible selection bias issues. Averaging several years will over smooth our time series of air temperature (and other weather variables).

To overcome these issues, we used our historical data set (1979–2015) and our econometric model to simulate hourly demand for all years in this data set. As explained in section 3.2.4, we assumed that the annual fixed-effect parameter is fixed at the value estimated for 2015. This way the only factor changing in our simulation were the climate conditions. For each year in our historical dataset we estimated the system wide hourly peak demand value, resulting in a distribution of estimated peak demand values. We used this distribution as a representation of SERC's electricity demand under present weather conditions.

To account for the inter-annual variability in weather, we chose the three years in our simulated distribution of historical peak demand values that represented the 20%, 50%, and 80% quantile values of this distribution. We selected peak demand as a descriptive metric because the electricity grid tends to be designed for maximum load days [6].

This way we tried to minimize some of the issues described above. First, by considering over thirty years of weather conditions, we had a good representation of present weather conditions. Second, since we chose three years representing three different quantiles, our decision model took into account not a single year, but three different years that represented both years with high demand and low demand. This way, it was able to take this variability into account and perform a trade-off between fixed investment costs and variable generation costs.

Milder climate change effects (RCP 4.5):

In the "milder" climate change scenario we used our estimates of electricity demand, hydro generation potential, and thermoelectric available capacity estimated using projections of meteorological variables from the GCMs under RCP 4.5. Similarly to the issues described in reference case, in the climate change case the choice of a specific GCM could lead to problems in our simulation. Because we were simulating one calendar year each time (in intervals of five years), using the output of the same GCM every year could result in possible selection and representation issues. The inter-annual variability of the GCMs could end up hiding changes in the climate signal. For example, one year with mild temperatures (which would result in low electricity demand values) could be due to this natural variability and not because the climate is getting milder. A better representation of simulated climate conditions in one of the annual steps of our simulation is to consider the distribution of the output of all twenty GCMs in that year. However, including all GCMs

in the optimization problem would result in a model that could too big to be computationally solved. To overcome these issues, we performed a procedure analogous to the one described for the reference case. In each year of our simulation, we estimated the system wide hourly peak demand value for each of the twenty GCMS, resulting in a distribution of estimated peak demand values. Next, we chose the output of three among the twenty GCMs that represented the 20%, 50%, and 80% quantile values of the distribution of system-wide peak demand. This way we could minimize the effect in our analysis of the intrinsic inter-annual variability among the different GCMs (which could occur if we chose the outputs of a specific GCM over the complete simulation horizon) without resulting in an optimization problem that was too big to be solved..

Stronger climate change effects (RCP 8.5):

In the "stronger" climate change scenario we used our estimates of electricity demand, hydro generation potential, and thermoelectric available capacity estimated using projections of meteorological variables from the GCMs under RCP 8.5. We repeated the procedure detailed in the "milder" scenario. In each year of our simulation, we chose the output of three among the twenty GCMs that represented the 20%, 50%, and 80% quantile values of the distribution of system-wide peak demand under RCP 8.5.

Appendix E

Detailed formulation of the capacity expansion model

We implemented the capacity expansion model in the General Algebraic Modeling System (GAMS) Version 24.4 and solved it using CPLEX Version 12. In this section, we present the detailed formulation of the capacity expansion model.

We ran the CE model in five year increments between 2015 and 2050. In each annual iteration, the model selected what plant types to build in order to minimize the total annualized system cost. This cost is represented by the sum of annualized fixed investment costs and variable operating costs of the final generator fleet. Specifically, the model had the choice to build wind, solar, coal steam, coal steam with carbon capture and sequestration (CCS), combined cycle natural gas, combined cycle natural gas with CCS, and nuclear. New coal and natural gas plants could use recirculating cooling or dry cooling systems. Our analysis did not include hydro power plants as a candidate technology. Investment in hydro power plant has been minimal in the last few decades [98] and available resources for new hydro plants in this area are limited [99]. We could not include all grid cells as

potential sites for building thermal power plants, because doing so would result in a computationally intractable model. Therefore, we chose approximately 45 sites in each region. These 45 sites are approximately uniformly distributed inside each region. They were chosen in order to maximize the spatial representation of each region and to maintain the size of our problem within feasible dimensions.

In the cases including the effects of climate change we ran our optimization model considering the climate projections of three different GCMs. In each year of our capacity expansion simulation, we used the output of three among the twenty GCMs that represented in the 20%, 50%, and 80% quantile values of the distribution of system-wide peak demand. This way we did not use the output of the same GCMs every year. Investment decisions in each year were done in order to satisfy the operating constraints taking into account the realization of the climate conditions represented by all three GCMs. By doing this, our results were more robust to the intrinsic variability within the different climate models. We performed a similar procedure with the reference case, but we chose the 20%, 50%, and 80% quantile values from our historical data set (1979–2015).

For computational tractability, we ran each annual iteration of the CE model in hourly intervals for a set of seven representative contiguous days per season. These representative periods in each season were chosen such that they minimized the Root Mean Squared Error (RMSE) with respect to the total simulated hourly demand for each season. Additionally we also included a set of two so called *special days* in our analysis. The first special day is the calendar day when peak annual net demand occurs. The second is the calendar day with the highest levels of system wide curtailments on existing thermal generators. This way each annual time step in our CE simulation considered $4 \times 7 \times 24 + 2 \times 24 = 720$ hourly periods for each of the three GCM projections included. An instance of this model with these parameters presented over 4 million variables and over 4 million constraints.

Table E.1: Decision Variables of the CE model

Variable	Definition
$n_{c,j}^{(c)}$	number of new thermal generators of type j in the class that CAN be curtailed (the (c) superscript) built in CELL c
$n_{z,j}^{(\bar{c})}$	number of new thermal generators of type j in the class that CANNOT be curtailed (the $(\bar{c})$ superscript) built in ZONE z
$n_{z,j}^{(r)}$	number of new generators of type j in the class RENEWABLE (the (r) superscript) built in ZONE z
$p_{g,c,j,t}^{(c)}$	electricity generation (GWh) in scenario g at time t of new generators of type j in the class that CAN be curtailed (the (c) superscript) built in CELL c
$p_{g,z,j,t}^{(\bar{c})}$	electricity generation (GWh) in scenario g at time t of new generators of type j in the class that CANNOT be curtailed (the $(\bar{c})$ superscript) built in ZONE z
$p_{g,z,j,t}^{(r)}$	electricity generation (GWh) in scenario g at time t of new generators of type j in the class RENEWABLE (the (r) superscript) built in ZONE z
$p_{g,i,t}$	electricity generation (GWh) in scenario g at time t of existing generator of index i
$\text{flow}_{g,\ell,t}$	flow on line ℓ (GW) in hour t and scenario g
$s_{g,i,t}$	electricity stored (in GWh) in scenario g at time t of existing pumped hydro generator $i \in \mathcal{I}^{(ph)}$
$c_{g,i,t}$	electricity charged (in GWh) in scenario g at time t of existing pumped hydro generator $i \in \mathcal{I}^{(ph)}$

Definition of the symbols

Tables E.1 – E.4 present the definitions of the symbols used in the capacity expansion model.

Objective Function

The objective function Equation E.1 computes the total sum of annual fixed and variable costs of the final generator fleet. The first line in Equation E.1 computes the total annual fixed costs (capital expenses and fixed O&M) for new thermal power plants that can be curtailed. The second line computes the total annual fixed costs for new thermal power

Table E.2: Sets of the CE model

Set	Definition
$\mathcal{B}$	set of user-defined time blocks. These are needed for computational purposes. $\mathcal{B}$ = {peak-hours, winter, summer, spring, fall, special periods}
$\mathcal{I}$	set of existing generators in the fleet.
$\mathcal{I}(z)$	subset of existing generators that are located in zone z. $\mathcal{I}(z) \subseteq \mathcal{I}$
$\mathcal{I}^{(w)}$	subset of existing wind generators in the fleet. $\mathcal{I}^{(w)} \subseteq \mathcal{I}$
$\mathcal{I}^{(s)}$	subset of existing solar generators in the fleet. $\mathcal{I}^{(s)} \subseteq \mathcal{I}$
$\mathcal{I}^{(h)}$	subset of existing hydro generators in the fleet. $\mathcal{I}^{(h)} \subseteq \mathcal{I}$
$\mathcal{I}^{(ph)}$	subset of existing pumped hydro generators in the fleet. $\mathcal{I}^{(ph)} \subseteq \mathcal{I}$
$\mathcal{I}^{(\cdot)}(z)$	subset of wind or solar generators that are located in zone z. $\mathcal{I}^{(\cdot)}(z) \subseteq \mathcal{I}(z)$
$\mathcal{C}$	set of grid cells that new techs can be placed in.
$\mathcal{C}(z)$	subset of grid cells that new techs can be placed in that are located in zone z. $\mathcal{C}(z) \subseteq \mathcal{C}$
$\mathcal{J}$	set of candidate plant types for new construction
$\mathcal{J}^{(c)}$	subset of plant types for new construction that can be curtailed. $\mathcal{J}^{(c)} \subseteq \mathcal{J}$
$\mathcal{J}^{(\bar{c})}$	subset of plant types for new construction that CANNOT be curtailed. $\mathcal{J}^{(\bar{c})} \subseteq \mathcal{J}$
$\mathcal{J}^{(r)}$	subset of plant types for new construction that are renewable. $\mathcal{J}^{(r)} \subseteq \mathcal{J}$
$\mathcal{L}$	set with transmission lines between load zones
$\mathcal{Z}$	set with user defined load zones
$\mathcal{G}$	set with climate model scenarios

Table E.3: Parameters of the CE model

Parameter	Definition
$P^{MAX}_{g,c,j,t}$	Maximum electricity generation capacity, accounting for deratings, of plant type $j \in \mathcal{J}^{(c)}$ at cell grid c at time t and in scenario g (GWh)
P^{NP}_{j}	Nameplate electricity generation capacity of plant type $j \in \mathcal{J}$ (GWh)
$P^{MAX}_{g,i,t}$	Maximum electricity generation capacity, accounting for deratings, of existing generator i (non solar and non wind) at time t and in scenario g (GWh)
$P^{MAX}_{solar,t}$	Maximum electricity generation by all existing solar generators at time t (GWh)
$P^{MAX}_{wind,t}$	Maximum electricity generation by all existing wind generators at time t (GWh)
$P^{(H)}_{g,i,m,y}$	Maximum hydropower potential of hydro generator i at month m, year y, and scenario g (GWh)
$\overline{\text{flow}}_{\ell}$	Capacity of transmission line ℓ (GW)
FOM_j	Annual fixed operation and maintenance costs of plant type j (\$/GW)
$CAPEX_j$	Capital expenses of new plant of type j (\$/GW)
$OC_{(\cdot)}$	Operating cost of plant type j or of existing plant i (\$/GWh)
$FC_{(\cdot)}$	Fuel cost of plant type j or of existing plant i (\$/MMBTU)
$HR_{(\cdot)}$	Heat rate of plant type j or of existing plant i (MMBTU/GWh)
M	Planning reserve margin as fraction (%) of demand
Q	Discount rate
D_j	lifetime (years) of candidate plant of type j
S^{MAX}_{i}	maximum storage capacity (in GWh) of pumped hydro generator $i \in \mathcal{I}^{(ph)}$
η_i	charging rate efficiency (as % of installed capacity) of pumped hydro generator $i \in \mathcal{I}^{(ph)}$

Table E.4: Indices of the CE model

Indices	Definition
b	Time blocks representing peak-hours, winter, summer, spring, fall, special periods. $b \in \mathcal{B}$
c	grid cells that new techs can be placed in. $c \in \mathcal{C}$
ℓ	Transmission Lines. $\ell \in \mathcal{L}$
i	existing generators in fleet. $i \in \mathcal{I}$
z	sub regions of SERC. $z \in \mathcal{Z}$
g	climate model scenario. $g \in \mathcal{G}$

plants that can not be curtailed. The third line computes the total annual fixed costs for new renewable power plants. Finally, the fourth line in Equation E.1 computes the total annual variable costs (fuel costs and variable O&M) for all power plants in the final generator fleet (both new and existing).

$$
\begin{aligned}
TC = & \sum_{c \in \mathcal{C}} \sum_{j \in \mathcal{J}^{(c)}} n_{c,j}^{(c)} \times P_j^{NP} \times (FOM_j + CAPEX_j \times CRF_j) \\
& + \sum_{z \in \mathcal{Z}} \sum_{j \in \mathcal{J}^{(\bar{c})}} n_{z,j}^{(\bar{c})} \times P_j^{NP} \times (FOM_j + CAPEX_j \times CRF_j) \\
& + \sum_{z \in \mathcal{Z}} \sum_{j \in \mathcal{J}^{(r)}} n_{z,j}^{(r)} \times P_j^{NP} \times (FOM_j + CAPEX_j \times CRF_j) \\
& + \frac{1}{|\mathcal{G}|} \sum_{g \in \mathcal{G}} \Bigg[\sum_{b} \Bigg(W_b \sum_{t_b \in T_b} \Bigg(\sum_{c \in \mathcal{C}} \sum_{j \in \mathcal{J}^{(c)}} p_{g,c,j,t_b}^{(c)} \times OC_{j,t_b} + \sum_{z \in \mathcal{Z}} \sum_{j \in \mathcal{J}^{(\bar{c})}} p_{g,z,j,t}^{(\bar{c})} \times OC_{j,t_b} \\
& \qquad + \sum_{z \in \mathcal{Z}} \sum_{j \in \mathcal{J}^{(r)}} p_{g,z,j,t_b}^{(r)} \times OC_{j,t_b} + \sum_{i \in \mathcal{I}} p_{g,i,t_b} \times OC_{i,t_b} \Bigg) \Bigg) \Bigg]
\end{aligned}
\tag{E.1}
$$

CRF_j is the capital recovery ratio of each technology j and is defined as:

$$
CRF_j = \frac{Q}{1 - (1/(1+Q)^{D_j})} \tag{E.2}
$$

The variable operating cost OC (in \$/MWh) for new and existing generators is equal to:

$$
OC_j = VOM_j + HR_j \times FC_j \qquad \forall\, j \in \mathcal{J} \qquad \text{(new generators)} \tag{E.3}
$$

$$
OC_i = VOM_i + HR_i \times FC_i \qquad \forall\, i \in \mathcal{I} \qquad \text{(existing generators)} \tag{E.4}
$$

Supply vs Demand constraint

The supply vs demand constraint in Equation E.5 forces dispatched generation in every hour of our simulation period to be the same as projected demand.

$$\begin{aligned} P^{D}_{g,t,z} = &\sum_{i \in \mathcal{I}(z)} p_{g,i,t} + \sum_{c \in \mathcal{C}(z)} \sum_{j \in \mathcal{J}^{(c)}} p^{(c)}_{g,c,j,t_b} + \sum_{j \in \mathcal{J}^{(\bar{c})}} p^{(\bar{c})}_{g,z,j,t_b} + \sum_{j \in \mathcal{J}^{(r)}} p^{(r)}_{g,z,j,t_b} \\ &+ \sum_{\ell:\text{end}(\ell)=z} \text{flow}_{g,\ell,t} - \sum_{\ell:\text{begin}(\ell)=z} \text{flow}_{g,\ell,t} \qquad \forall\ g, t, z \end{aligned} \tag{E.5}$$

Reserve margin constraint

The reserve margin constraint in Equation E.6 represents the common behavior of energy planning agents of adding a reserve margin above projected hourly peak demand value in order to account for generator failures, greater than expected demand values and other risks. In this case, the reserve margin constraint takes into account simulated curtailments from thermal generators and the typical generation from renewables at the projected peak demand hour. We apply this reserve margin constraint for each zone in our analysis.

$$\begin{aligned} (1+M) \times P^{D}_{g^{(p)},t^{(p)},z} \leq &\sum_{c \in \mathcal{C}} \sum_{j \in \mathcal{J}^{(c)}} P^{MAX}_{g^{(p)},c,j,t^{(p)}} \times n^{(c)}_{c,j} + \sum_{j \in \mathcal{J}^{(r)}} P^{MAX}_{g^{(p)},z,j,t^{(p)}} \times n^{(r)}_{z,j} \times CF_{j,t^{(p)}} \\ &+ \sum_{i \in \mathcal{I}(z) \setminus \{\mathcal{I}^{(w)}(z) \cup \mathcal{I}^{(s)}(z)\}} P^{MAX}_{g^{(p)},i,t^{(p)}} + P^{MAX}_{\text{solar},z,t^{(p)}} + P^{MAX}_{\text{wind},z,t^{(p)}} \end{aligned} \tag{E.6}$$

where $g^{(p)}$ and $t^{(p)}$ are, respectively, the climate model simulation and the hour in the year that peak demand value occurs for zone z ($z \in \mathcal{Z}$).

Maximum generation constraints

Equation E.7 – E.8 show the upper bound in hourly generation by existing solar and wind generators, respectively. Existing solar and wind generators are aggregated in each load zone z.

$$\sum_{i \in \mathcal{I}^{(s)}(z)} p_{g,i,t} \leq P^{MAX}_{\text{solar},z,t} \quad \forall\ g, z, t \tag{E.7}$$

$$\sum_{i \in \mathcal{I}^{(w)}(z)} p_{g,i,t} \leq P^{MAX}_{\text{wind},z,t} \quad \forall\ g, z, t \tag{E.8}$$

Equations E.9 represents the upper bound in hourly generation by existing non renewable generators.

$$p_{g,i,t} \leq P^{MAX}_{g,i,t} \quad \forall\ g, t \text{ and } \forall\ i \in \mathcal{I} \setminus \{\mathcal{I}^{(w)} \cup \mathcal{I}^{(s)}\} \tag{E.9}$$

Equations E.10 – E.12 represent the upper bound in hourly generation by new thermal generators, new thermal generators that are not curtailed, and new renewable generators, respectively.

$$p^{(c)}_{g,c,j,t} \leq P^{MAX}_{g,c,j,t} \times n^{(c)}_{c,j} \quad \forall\ g, c, t \text{ and } \forall\ j \in \mathcal{J}^{(c)} \tag{E.10}$$

$$p_{g,z,j,t}^{(\bar{c})} \leq P_{z,j,t}^{MAX} \times n_{z,j}^{(\bar{c})} \quad \forall\ g, z, t \text{ and } \forall\ j \in \mathcal{J}^{(\bar{c})} \tag{E.11}$$

$$p_{g,z,j,t}^{(r)} \leq n_{z,j}^{(r)} \times P_{j}^{NP} \times CF_{j,t} \quad \forall\ g, z, t \text{ and } \forall\ j \in \mathcal{J}^{(r)} \tag{E.12}$$

Hydro energy constraint

Equation E.13 represents the seasonal upper bounds on hydro energy generation for each individual hydro plant.

$$W_b \times \sum_{t \in b} p_{g,i,t} \leq \sum_{m,y \in b} P_{i,m,y}^{(H)} \quad \forall\ g, b \in \mathcal{B} \text{ and } \forall\ i \in \mathcal{I}^{(h)} \tag{E.13}$$

Pumped hydro generation constraints

The set of equations in Equation E.14 represent the dynamics of a pumped hydro power plant $i \in \mathcal{I}^{(ph)}$. The first inequality limits the hourly generation to the state of charge of the power plant. The second equation couples the state of charge at time t with state of charge in the previous period. The third inequality limits the amount of energy (in GWh) that can be stored to S_i^{MAX}. The last inequality limits the rate of charge (in GWh/h) in

time t

$$\begin{aligned}
&p_{g,i,t} < s_{g,i,t-1} && \forall\ g,t \text{ and } \forall\ i \in \mathcal{I}^{(ph)} \\
&s_{g,i,t} = s_{g,i,t-1} - p_{g,i,t} + c_{g,i,t} && \forall\ g,t \text{ and } \forall\ i \in \mathcal{I}^{(ph)} \\
&s_{g,i,t} < S_i^{MAX} && \forall\ g,t \text{ and } \forall\ i \in \mathcal{I}^{(ph)} \\
&c_{g,i,t} < \eta_i \times P_i^{MAX} && \forall\ g,t \text{ and } \forall\ i \in \mathcal{I}^{(ph)}
\end{aligned} \tag{E.14}$$

Transmission constraint

Equation E.15 represents the limits in transmission of electricity between the load zones.

$$0 \leq \text{flow}_{g,\ell,t} \leq \overline{\text{flow}}_\ell \quad \forall\ g,\ell,t \tag{E.15}$$

Carbon Emissions

Equation E.16 represents the limit on system wide annual carbon emission.

$$\frac{1}{|\mathcal{G}|}\sum_{g\in\mathcal{G}}\Bigg[\sum_{b}\Bigg(W_b\sum_{t_b\in T_b}\Bigg(\sum_{c\in\mathcal{C}}\sum_{j\in\mathcal{J}^{(c)}}p^{(c)}_{c,j,t_b}\times OC_{j,t_b}+\sum_{z\in\mathcal{Z}}\sum_{j\in\mathcal{J}^{(\bar{c})}}p^{(\bar{c})}_{z,j,t}\times OC_{j,t_b} + \sum_{z\in\mathcal{Z}}\sum_{j\in\mathcal{J}^{(r)}}p^{(r)}_{z,j,t_b}\times OC_{j,t_b}+\sum_{i\in\mathcal{I}}p_{i,t_b}\times OC_{i,t_b}\Bigg)\Bigg)\Bigg] \leq \text{CO}_{2lim} \tag{E.16}$$

Appendix F

Additional results of the capacity expansion model

Figure F.1 shows the resulting added capacity in each of the three cases (reference case, RCP 4.5, and RCP 8.5) and in each of the years simulated. Decisions are grouped by each of the four SERC subregions considered in our analysis. Because we did not impose transmission constraints between the four regions in this analysis, there are some years (specially in 2040 for the RCP 4.5 case) when the model decides to overbuild in one specific region.

Figure F.2 shows the simulated generation values of different types of power plants in 2050. All three cases were simulated without considering any constraints on CO_2 emissions. In the reference case, thermal, wind, and solar represent, respectively, 78%, 14%, and 3% of total generation. In both cases with climate change effects, thermal, wind, and solar represent, respectively, 73%, 10%, and 12% of total generation.

Figures F.3 and F.4 show, respectively, resulting added capacity and simulated generation values of different types of power plants in 2050. All three cases were simulated assuming

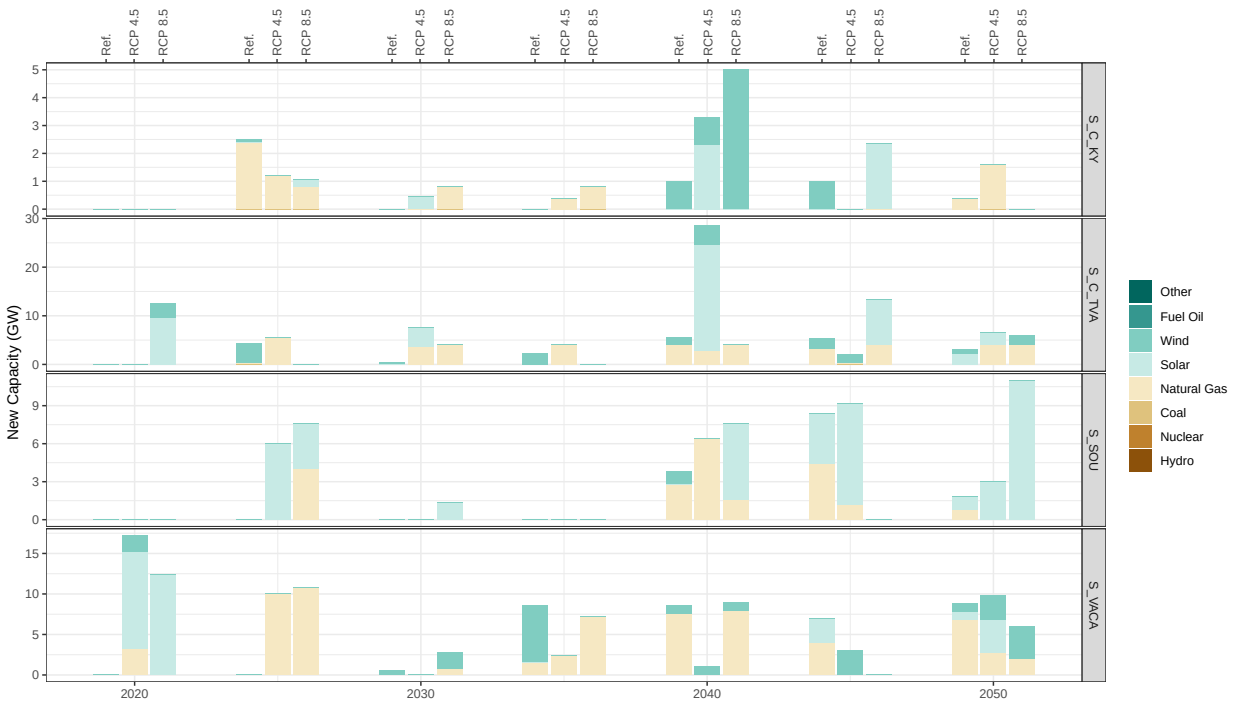

Figure F.1: New capacity added in each step of the capacity expansion simulation. Results are shown for each of the three scenarios (Reference, RCP 4.5, and RCP 8.5) and each of the four sub regions considered in SERC. All three cases are simulated without considering any constraints on CO_2 emissions.

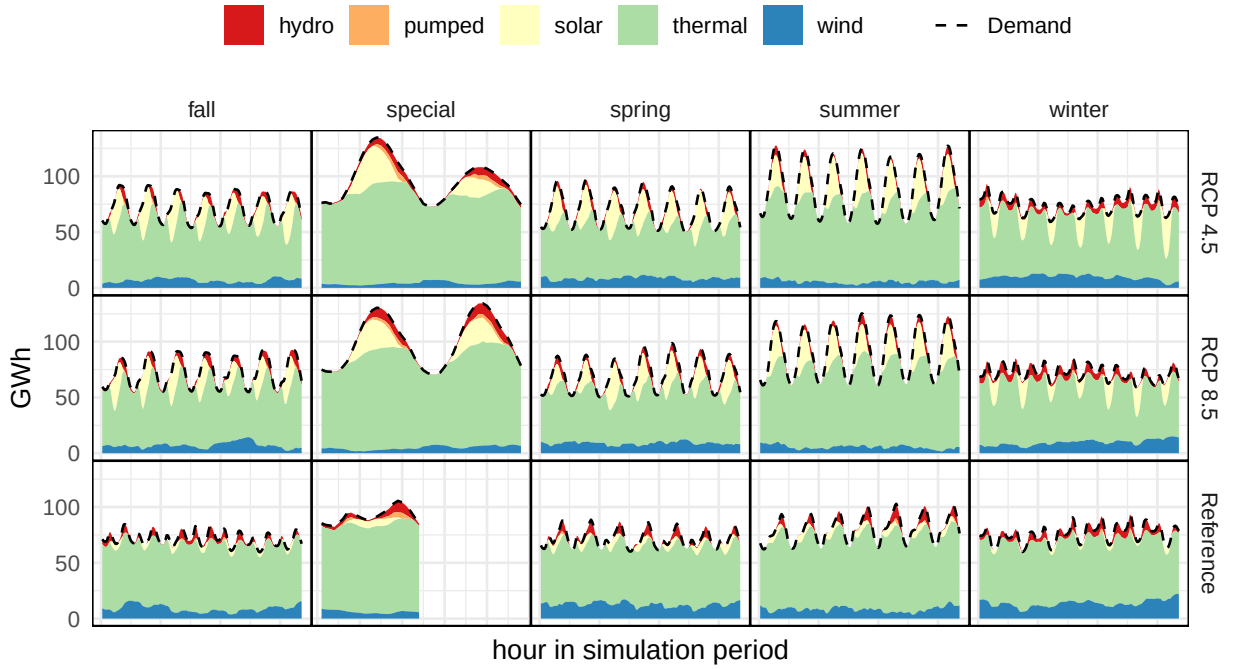

Figure F.2: Simulated generation (in GWh) of different types of power plants in 2050. All three cases were simulated without considering any constraints on CO_2 emissions.

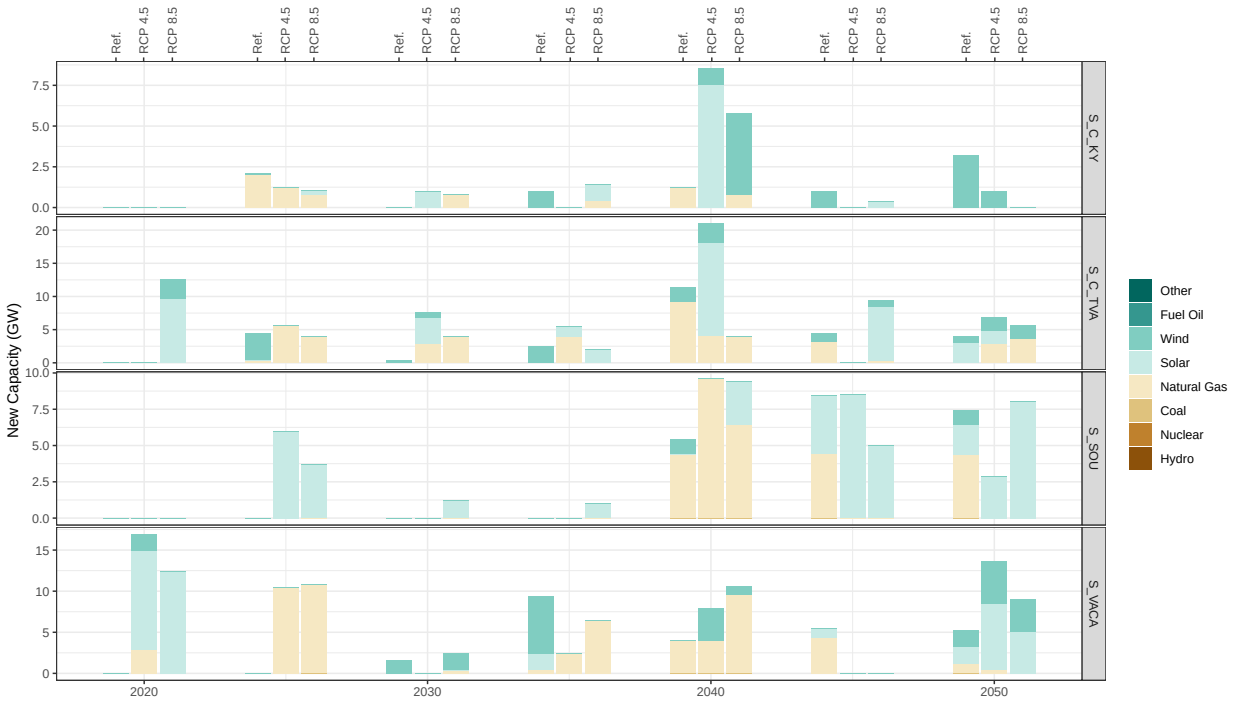

Figure F.3: New capacity added in each step of the capacity expansion simulation. Results are shown for each of the three scenarios (Reference, RCP 4.5, and RCP 8.5) and each of the four sub regions considered in SERC. All three cases are simulated assuming limits on system wide CO_2 emissions. CO_2 emissions in 2050 are forced to be 50% of estimated emissions in 2015.

limits on system wide CO_2 emissions. CO_2 emissions in 2050 are forced to be 50% of estimated emissions in 2015. In the reference case, thermal, wind, and solar represent, respectively, 75%, 17%, and 4% of total generation. In both cases with climate change effects, thermal, wind, and solar represent, respectively, 71%, 10%, and 13% of total generation.

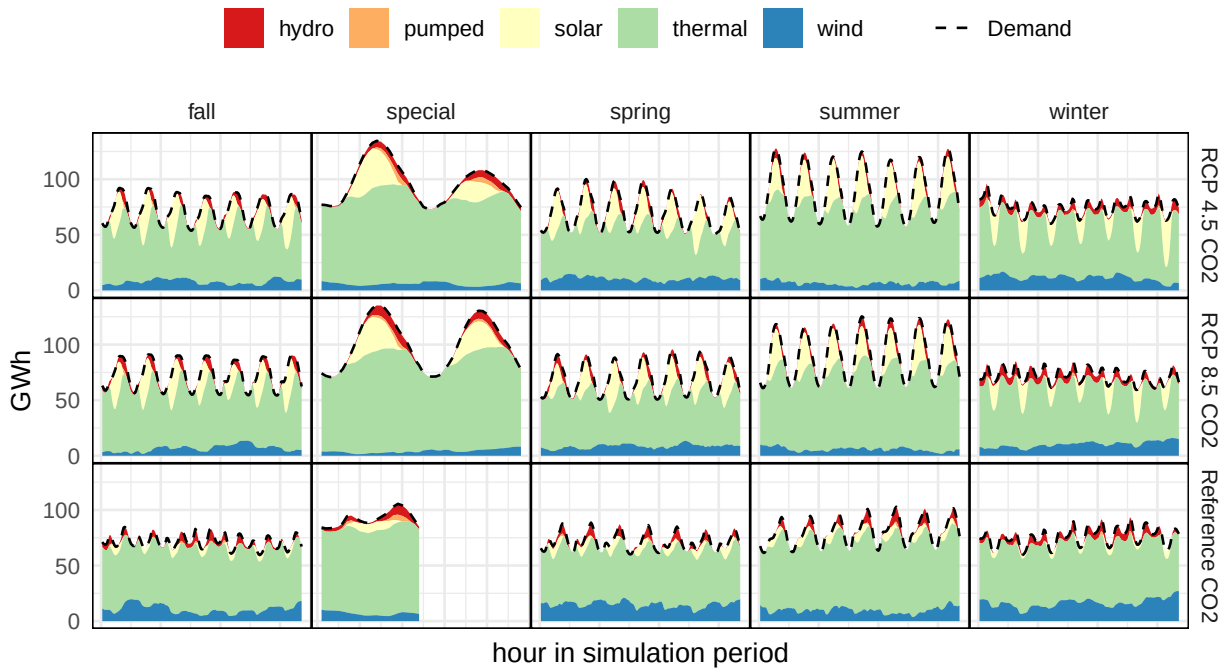

Figure F.4: Simulated generation (in GWh) of different types of power plants in 2050. All three cases were simulated simulated assuming limits on system wide CO_2 emissions. CO_2 emissions in 2050 are forced to be 50% of estimated emissions in 2015.

Appendix G

Detailed formulation of the unit commitment and economic dispatch model

We implemented the unit commitment and economic dispatch (UCED) model in the General Algebraic Modeling System (GAMS) Version 24.4 and solved it using CPLEX Version 12. In this section, we present the detailed formulation of the UCED model.

Definitions

Tables G.1 – G.4 present the definitions of the symbols used in the capacity expansion model.

Table G.1: Sets of the UCED model

Set	**Definition**
T	simulation time horizon (set of hours)
$\mathcal{I}$	set of generators in the fleet.
$\mathcal{I}(z)$	set of generators in the fleet located in zone z.
$\mathcal{I}_s(z)$	set of solar generators in the fleet in zone z $\mathcal{I}_s(z) \subseteq \mathcal{I}(z)$
$\mathcal{I}_w(z)$	set of wind generators in the fleet in zone z $\mathcal{I}_w(z) \subseteq \mathcal{I}(z)$
$\mathcal{I}^{(h)}$	set of hydropower generators in the fleet $\mathcal{I}^{(h)} \subseteq \mathcal{I}$
$\mathcal{I}^{(ph)}$	set of pumped storage generators in the fleet $\mathcal{I}^{(ph)} \subseteq \mathcal{I}$
$\mathcal{L}$	set with transmission lines between load zones
$\mathcal{Z}$	set with user defined load zones

Table G.2: Decision Variables of the UCED model

Variable	**Definition**
$g_{i,t}$	Electricity generation above minimum stable load by generator i at time t (MWh)
$nse_{z,t}$	Non-served energy at time t at zone z (MWh)
$p_{i,t}$	Electricity generation by generator i at time t (MWh)
$r_{i,t}$	Bi-directional regulation reserves provided by generator i at time t (MWh)
$s_{i,t}$	Spinning reserves provided by generator i at time t (MW)
$f_{i,t}$	Flexibility reserves provided by generator i at time t (MW)
$u_{i,t}$	Binary variable indicating on/off state of generator i at time t, where 1 indicates on $\{0,1\}$
$v_{i,t}$	Binary variable indicating generator i turns on at time t $\{0,1\}$
$w_{i,t}$	Binary variable indicating generator i turns off at time t $\{0,1\}$
$\text{flow}_{\ell,t}$	flow on line ℓ (GW) in hour t
$c_{i,t}$	electricity charged (in MWh) at time t of existing pumped hydro generator $i \in \mathcal{I}^{(ph)}$
$z_{i,t}$	electricity stored (in MWh) at time t of existing pumped hydro generator $i \in \mathcal{I}^{(ph)}$

Table G.3: Parameters of the UCED model

Parameter	**Definition**
$CNSE$	Cost of non-served energy ($/MWh)
G_i	Electricity generation above minimum load by generator i in last hour of prior optimization period (MWh)
K	Number of hours before which a generator can turn on in the current optimization horizon, based on when it shut off in the last optimization period and its MDT
MDT_i	Minimum down time for generator i, which indicates the number of hours that must elapse before a generator can turn on once it shuts off (hours)
$OC_{i,t}$	Operating cost of generator i at time t ($/MWh)
P_i	Electricity generation by generator i in the last period of the prior optimization horizon (MWh)
$P_{z,t}^{D}$	Electricity demand in zone z at time t (MWh)
$P_{i,t}^{MAX}$	Maximum electricity generation capacity of generator i at time t (MWh)
$P_{z,t}^{MAX,SOLAR}$	Maximum electricity generation by all solar generators in zone z at time t (MWh)
$P_{z,t}^{MAX,WIND}$	Maximum electricity generation by all wind generators in zone z at time t (MWh)
P_i^{hydro}	Maximum daily hydropower potential of generator $i \in \mathcal{I}^{(h)}$ (MWh)
P_i^{MIN}	Minimum stable load of generator i (MWh)
$R_{z,t}$	Required bi-directional regulation reserves at time t and zone z (MWh)
$S_{z,t}$	Required spinning reserves at time t and zone z (MWh)
$F_{z,t}$	Required flexibility reserves at time t and zone z (MWh)
RE_i	Generator i eligible (1) or not (0) to provide regulation reserves
SE_i	Generator eligible (1) or not (0) to provide spinning reserves
FE_i	Generator eligible (1) or not (0) to provide flexibility reserves
RR	Scalar that translates hourly ramp limit to ramp limit over regulation reserve timeframe
RS	Scalar that translates hourly ramp limit to ramp limit over spinning reserve timeframe
RF	Scalar that translates hourly ramp limit to ramp limit over flexibility reserve timeframe
RL_i	Hourly ramp limit of generator i (MWh)
SU_i	Start-up cost for generator i ($)
U_i	On/off state of generator i in the last period of the prior optimization horizon {0,1}
Z_i^{MAX}	maximum storage capacity (in MWh) of pumped hydro generator $i \in \mathcal{I}^{(ph)}$

Table G.4: Indices of the UCED model

Indices	Definition
t	time (hour) $t \in T$
ℓ	Transmission Lines. $\ell \in \mathcal{L}$
i	generators in fleet. $i \in \mathcal{I}$
z	sub regions of SERC. $z \in \mathcal{Z}$

Objective Function

The UCED model minimizes total operational costs (TC), or the sum of electricity generation, start-up, and non-served energy costs

$$TC = \sum_{i \in \mathcal{I}, t \in T} [p_{i,t} \times OC_{i,t} + v_{i,t} \times SU_i] + \sum_{t \in T, z \in \mathcal{Z}} nse_{z,t} \times CNSE \tag{G.1}$$

System-wide Electricity Demand and Reserve Requirement Constraints

Electricity generation plus non-served energy must equal system-wide demand in zone and each time period:

$$P^D_{t,z} = \sum_{i \in \mathcal{I}(z)} p_{i,t} + \sum_{\ell:\text{end}(\ell)=z} \text{flow}_{\ell,t} - \sum_{\ell:\text{begin}(\ell)=z} \text{flow}_{\ell,t} + nse_{z,t} \tag{G.2}$$

Provided spinning (s), regulation (r), and flexibility reserves (f) must equal or exceed required spinning (S), regulation (R), and flexibility (F) reserve requirements, respectively,

in each zone and each time period:

$$\begin{aligned}
\sum_{i \in \mathcal{I}(z)} s_{i,t} &\geq S_{z,t} \quad \forall\ t \in T,\ z \in \mathcal{Z} \\
\sum_{i \in \mathcal{I}(z)} r_{i,t} &\geq R_{z,t} \quad \forall\ t \in T,\ z \in \mathcal{Z} \\
\sum_{i \in \mathcal{I}(z)} f_{i,t} &\geq F_{z,t} \quad \forall\ t \in T,\ z \in \mathcal{Z}
\end{aligned} \tag{G.3}$$

Generator-Specific Generation and Reserve Constraints

Electricity generation is represented by two variables, total generation ($p_{i,t}$ in MWh]) and generation above minimum stable load ($g_{i,t}$ in MWh):

$$\begin{aligned}
p_{i,t} &= P_i^{MIN} \times u_{i,t} + g_{i,t} \\
g_{i,t} &\leq \left(P_{i,t}^{MAX} - P_i^{MIN}\right) \times u_{i,t}
\end{aligned} \tag{G.4}$$

Aggregate electricity generation by wind and solar generators must be less than or equal to aggregate wind ($P_{z,t}^{MAX,WIND}$ in MWh) and solar ($P_{z,t}^{MAX,SOLAR}$ in MWh) generation profiles:

$$\sum_{i \in \mathcal{I}_s(z)} p_{i,t} \leq P_{z,t}^{MAX,SOLAR} \quad \forall\ t \in T, z \in \mathcal{Z} \tag{G.5}$$

$$\sum_{i \in \mathcal{I}_w(z)} p_{i,t} \leq P_{z,t}^{MAX,WIND} \quad \forall\ t \in T, z \in \mathcal{Z} \tag{G.6}$$

The sum of hourly electricity generation by hydro generators must be less than or equal to total estimated hydropower potential over the simulation period (P_i^{hydro} in MWh):

$$\sum_{t \in T} p_{i,t} \leq P_i^{hydro} \quad i \in \mathcal{I}^{(h)} \tag{G.7}$$

Electricity generation plus provided reserves cannot exceed maximum capacity of each generator:

$$p_{i,t} + r_{i,t} + s_{i,t} + f_{i,t} \leq P_{i,t}^{MAX} \quad \forall\ i \in \mathcal{I} \tag{G.8}$$

Generators must be online and eligible to provide reserves, and cannot provide reserves in excess of their ramp limit over the reserve timeframe:

$$s_{i,t} \leq SE_i \times RL_i \times RS \times u_{i,t} \quad \forall\ i \in \mathcal{I}, t \in T \tag{G.9}$$

$$r_{i,t} \leq RE_i \times RL_i \times RR \times u_{i,t} \quad \forall\ i \in \mathcal{I}, t \in T \tag{G.10}$$

$$f_{i,t} \leq FE_i \times RL_i \times RF \times u_{i,t} \quad \forall\ i \in \mathcal{I}, t \in T \tag{G.11}$$

Ramp Constraints

Up and down ramp constraints limit changes in electricity generation above minimum stable load plus accounting for spinning and regulation reserves:

$$(g_{i,t} + s_{i,t} + r_{i,t}) - g_{i,t-1} \leq RL_i \quad \forall\ i \in \mathcal{I}, t \in T \tag{G.12}$$

$$g_{i,t-1} - (g_{i,t} + r_{i,t}) \leq RL_i \quad \forall\ i \in \mathcal{I}, t \in T \tag{G.13}$$

For $t = 1$, we define $g_{i,t-1} = G_i$. In the first UCED run, $G_i = 0$.

Unit Commitment Constraints

A generator is on or off depending on turn on and turn off decisions

$$u_{i,t} = u_{i,t-1} + v_{i,t} - w_{i,t} \quad \forall\ i \in \mathcal{I}, t \in T \tag{G.14}$$

For $t = 1$, we define $u_{i,t-1} = U_i$. In the first UCED run, $U_i = 0$. Generators cannot turn on until they reach their minimum down time (MDT):

$$1 - u_{i,t} \geq w_{i,t-(MDT_i-1)} + w_{i,t-(MDT_i-2)} + \ldots + w_{i,t} \quad \forall\ i \in \mathcal{I}, t > K_i \tag{G.15}$$

To account for shut downs in the prior optimization window, carried hours of minimum down time from the prior UC run (K_i) are enforced:

$$u_{i,t} \geq 0 \quad \forall\ i \in \mathcal{I}, t \leq K_i \tag{G.16}$$

Pumped hydro generation constraints

The set of equations in Equation G.17 represent the dynamics of a pumped hydro power plant $i \in \mathcal{I}^{(ph)}$. The first inequality limits the hourly generation to the state of charge of the power plant. The second equation couples the state of charge at time t with state of charge in the previous period. The third inequality limits the amount of energy (in MWh) that can be stored to Z_i^{MAX}. The last inequality limits the rate of charge (in MWh/h) in time t

$$\begin{aligned} p_{i,t} &< z_{i,t-1} && \forall t \text{ and } \forall\ i \in \mathcal{I}^{(ph)} \\ z_{i,t} &= z_{i,t-1} - p_{i,t} + c_{i,t} && \forall\ i \in \mathcal{I}^{(ph)} \\ z_{i,t} &< Z_i^{MAX} && \forall\ i \in \mathcal{I}^{(ph)} \\ c_{i,t} &< \eta_i \times P_i^{MAX} && \forall\ i \in \mathcal{I}^{(ph)} \end{aligned} \tag{G.17}$$

Transmission Constraint

Transfers of electricity in each transmission line are limited by the line's capacity

$$0 \leq \text{flow}_{\ell,t} \leq \overline{\text{flow}}_{\ell} \quad \forall\ \ell, t \tag{G.18}$$